HUMAN HEALTH RISKS ASSOCIATED WITH FAILURE OF PROPOSED TREATMENT NORTH HOLLYWOOD WEST WELL FIELD

(Step 5 of 97-005 Evaluation)

Prepared for

California State Water Resources Control Board, Division of Drinking Water

Prepared on Behalf of

Los Angeles Department of Water & Power

Water Quality Division, Groundwater Remediation Group

Prepared by

Owner's Agent Team led by Hazen and Sawyer (Hazen) with primary input from Worley and Arcadis

December 2020

EXECUTIVE SUMMARY

The Division of Drinking Water (DDW) 97-005 evaluation process consists of 11 steps for assessing proposals, establishing appropriate permit conditions, and approving the use of an extremely impaired drinking water source. This report documents Step 5 of the 97-005 evaluation process, i.e., "Human Health Risks Associated with Failure of Proposed Treatment" for the Los Angeles Department of Water and Power's (LADWP's) owned and operated North Hollywood West (NHW) Well Field.

As groundwater in the vicinity of the NHW Well Field is impaired by contamination, LADWP is required to demonstrate compliance with the California State Water Resources Control Board (SWRCB), DDW 97-005 Process Memo for Extremely Impaired Sources (DDW Process Memo 97-005) (DDW, 2015). DDW considers a source to be "extremely impaired" if it meets two or more of 10 DDW-developed criteria. Based on available water quality data, groundwater in the vicinity of the NHW Well Field meets up to four criteria as described in the Raw Water Quality Characterization (RWQC) report for the NHW Well Field (Step 2 of 97-005 Evaluation). **It is imperative that the precursors Step 2 (Raw Water Quality Characterization) and Step 4 (Effective Treatment and Monitoring) reports are read prior to, or in conjunction with this report, "*as each step lies upon the findings and conclusions of the prior step*" (DDW, 2015).**

LADWP, pursuant to the Comprehensive Environmental Response, Compensation, and Liability Act of 1980 (CERCLA) and the National Oil and Hazardous Substances Pollution Contingency Plan (NCP), has selected the NHW Interim Remedial Action (IRA) to address hazardous substances dissolved in groundwater entering the NHW Well Field under active pumping conditions. LADWP's selected IRA includes, among other things, a groundwater pump and treatment system intended to reduce the toxicity, mobility, and volume of contaminated groundwater through treatment and help restore the beneficial uses of groundwater in the vicinity of the NHW Well Field. The NHW IRA involves extracting and treating impacted groundwater from up to five wells (i.e., three Remediation Wells with a design that allows expansion to enable treatment of five Remediation Wells to avoid the need for new or amended permitting in the event that a future response action involves pumping two additional remediation wells and conveying water from those wells to the NHW treatment plant, following compliance with the NCP). The treated water will be used as a source of potable water supply. The associated planned treatment facility is referred to as the North Hollywood West Wellhead Treatment (NHWWT). Further information regarding the NHW IRA is documented in the NHW Well Field RWQC report (Step 2 of 97-005 Evaluation).

In accordance with the DDW Process Memo 97-005, LADWP have evaluated the probability of NHWWT failure and assessed the potential health risk associated with such a failure, as described herein.

The evaluation of failure, which included an assessment of each NHWWT component mode of failure, concluded that the sand separators, cartridge filters, and granular activated carbon (GAC) contactors do not affect the treatment performance and therefore do not pose a health risk to the public under a failure scenario. Failure of these components would result in increased maintenance activities. Peroxide feed and ultra violet (UV) reactor failure would pose a limited and brief increase in risk to the public. However, online monitoring and a four-hour window of operator troubleshooting of the equipment would limit potential of high exposure.

Human health risk calculations using the approach described in the DDW Process Memo 97-005, which includes the use of maximum calculated constituents of concern (COPCs) concentrations in untreated NHWWT effluent, indicate that, even in the event of total NHWWT failure, incremental cancer and non-

cancer risks are small and within accepted risk limits. Multiple failures spanning several years, presented as a worst-case scenario and are not expected to reasonably occur, showed cancer risk below de minimis (1E-06), and the non-cancer hazard (i.e., the ratio of the maximum estimated arrival concentrations of COPCs to non-cancer PHGs) are below the DDW threshold value of 1.0. Additionally, exposure to microbial organisms is not considered to pose a risk of disease in the event of a treatment failure, based on comparison to the California maximum contaminant level (MCL).

This report satisfies the applicable requirement outlined in the DDW Process Memo 97-005 for Step 5 of the 97-005 evaluation process, i.e., “Human Health Risks Associated with Failure of Proposed Treatment”.

TABLE OF CONTENTS

Figures within Text

Tables within Text

Appendices

List of Acronyms and Abbreviations

Acronym/Abbreviation	Term
1,1-DCE	1,1-Dichloroethene
%	Percent
µ	micron
µg	microgram
µg/L	microgram(s) per Liter
AL	Action Level
AOP	Advanced Oxidation Process
CalEPA	California Environmental Protection Agency
CERCLA	Comprehensive Environmental Response, Compensation, and Liability Act of 1980
cis-1,2-DCE	cis-1,2-Dichloroethene
COPCs	Constituents of Potential Concern
DDW	Division of Drinking Water
DLR	Detection Limit for Reporting
DPH	Department of Public Health
DTSC	Department of Toxic Substances Control
EBCT	Empty Bed Contact Time
EPA	United States Environmental Protection Agency
ft	Feet
GAC	Granular Activated Carbon
gpm	Gallon per Minute
HPL	Hewitt Pit Landfill
HHRA	Human Health Risk Assessment
HI	Health Index
HQ	Hazard Quotient
hrs.	Hours
IRA	Interim Response Action
IRAD	Interim Remedial Action Decision
LADWP	Los Angeles Department of Water and Power
MCL	Maximum Contaminant Level
NH	North Hollywood
NHW	North Hollywood West

Acronym/Abbreviation	Term
NHWWT	North Hollywood West Wellhead Treatment
NL	Notification Level
OEHHA	Office of Environmental Health Hazard Assessment
PCE	Tetrachloroethene
PDCs	Power Distribution Cabinets
PHG	California Public Health Goal
PLC	Programmable Logic Controller
RAOs	Remedial Action Objectives
RfD	Reference Dose
RI/FS	Remedial Investigation/Feasibility Study
RSC	Relative Source Contribution
RSL	Regional Screening Level
RWQC	Raw Water Quality Characterization
RWQCB	Regional Water Quality Control Board
SA/CA	Source Assessment / Contaminant Assessment
SFB	San Fernando Basin
SWRCB	State Water Resources Control Board
TARP	Tucson Airport Remediation Project
TCE	Trichloroethene
Temp	Temperature
THQ	Target Hazard Quotient
UV	Ultraviolet
VOC	Volatile Organic Compound
WTP	Water Treatment Plant

1 INTRODUCTION

The Division of Drinking Water (DDW) 97-005 evaluation process consists of 11 steps for assessing proposals, establishing appropriate permit conditions, and approving the use of an extremely impaired drinking water source. The 11 step 97-005 evaluation process is illustrated in Figure 1-1. This report documents Step 5 of the 97-005 evaluation process, i.e., "Human Health Risks Associated with Failure of Proposed Treatment" for the Los Angeles Department of Water and Power's (LADWP's) owned and operated North Hollywood West (NHW) Well Field. The location of the NHW Well Field is shown in Figure 1-2.

It is imperative that the precursor Step 2 (Raw Water Quality Characterization) and Step 4 (Effective Treatment and Monitoring) reports are read prior to, or in conjunction with this report, "*as each step lies upon the findings and conclusions of the prior step*" (DDW, 2015).

1.1 Purpose

The purpose of Step 5 of the 97-005 evaluation process is to evaluate the potential human health risks posed by failure of the planned treatment facility (Section 1.3).

1.2 Scope of Work

In accordance with the DDW Process Memo 97-005, the following scope of work was performed and are described herein:

- Probability of treatment failure evaluation which incorporates the assessment of likely treatment failure modes and rate of failure, described in Section 2.
- Assessment of potential human health risks associated treatment failure (Section 3) which considers:
    - The duration of exposure to contaminated drinking water, considering the proposed frequency of monitoring, and the time it takes for the plant operator to receive the monitoring results;
    - The human health risks associated with such exposure over the course of the failure scenario; and
    - Potential cumulative risks due to multiple failures.

1.3 Background

Due to the degree of groundwater impairment by contamination in the vicinity of the NHW Well Field, LADWP is required to demonstrate compliance with the California State Water Resources Control Board (SWRCB), DDW 97-005 Process Memo for Extremely Impaired Sources (DDW Process Memo 97-005) (DDW, 2015). DDW considers a source to be "extremely impaired" if it meets two or more of 10 DDW-developed criteria. Based on available water quality data, groundwater in the vicinity of the NHW Well Field meets up to four criteria as described in the Raw Water Quality Characterization (RWQC) report for the NHW Well Field (Step 2 of 97-005 Evaluation).

LADWP, pursuant to the Comprehensive Environmental Response, Compensation, and Liability Act of 1980 (CERCLA) and the National Oil and Hazardous Substances Pollution Contingency Plan (NCP), has selected the NHW Interim Remedial Action (IRA) to address hazardous substances dissolved in groundwater entering the NHW Well Field under active pumping conditions. LADWP's selected IRA

includes, among other things, a groundwater pump and treatment system intended to reduce the toxicity, mobility, and volume of contaminated groundwater through treatment and help restore the beneficial uses of groundwater in the vicinity of the NHW Well Field. The NHW IRA involves, among other things, extracting and treating impacted groundwater from up to five wells (i.e., three Remediation Wells with a design that allows expansion to enable treatment of five Remediation Wells to avoid the need for new or amended permitting in the event that a future response action involves pumping two additional remediation wells and conveying water from those wells to the NHW treatment plant, following compliance with the NCP). The treated water will be used as a source of potable water supply. The associated planned treatment facility is referred to as North Hollywood West Wellhead Treatment (NHWWT), the approximate footprint of the facility is shown in Figure 1-2. Further information regarding the NHW IRA is documented in the NHW Well Field RWQC report (Step 2 of 97-005 Evaluation).

1.4 Document Organization

This report is organized into the following sections:

Section 1 - Introduction: This section provides the introductory and background information, purpose of evaluation, regulatory requirements and organization of the document.

Section 2 - Evaluation of the Risks of Failure: Provides a summary of the evaluation of risks of failure for the NHWWT.

Section 3 - Assessment of Potential Human Health Risks: Documents the evaluation of potential health risks associated with failure of the NHWWT.

Section 4 - Conclusions: Summarizes the outcomes of the evaluation of human health risks associated with potential failure of the NHWWT.

Section 5 - References: Information sources referenced in this report are provided in this section.

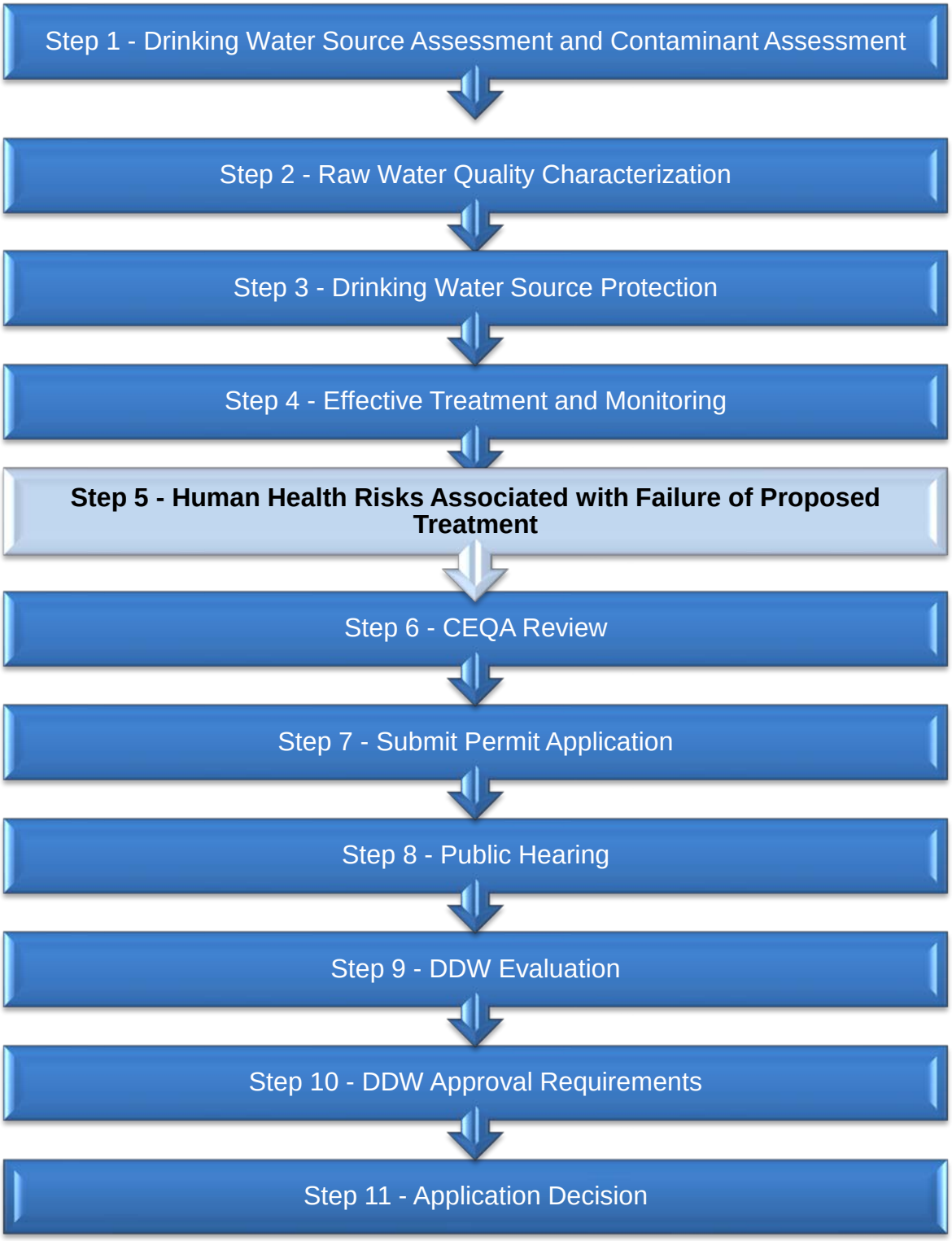

Figure 1-1 DDW Eleven-Step 97-005 Evaluation Process for an Extremely Impaired Drinking Water Source

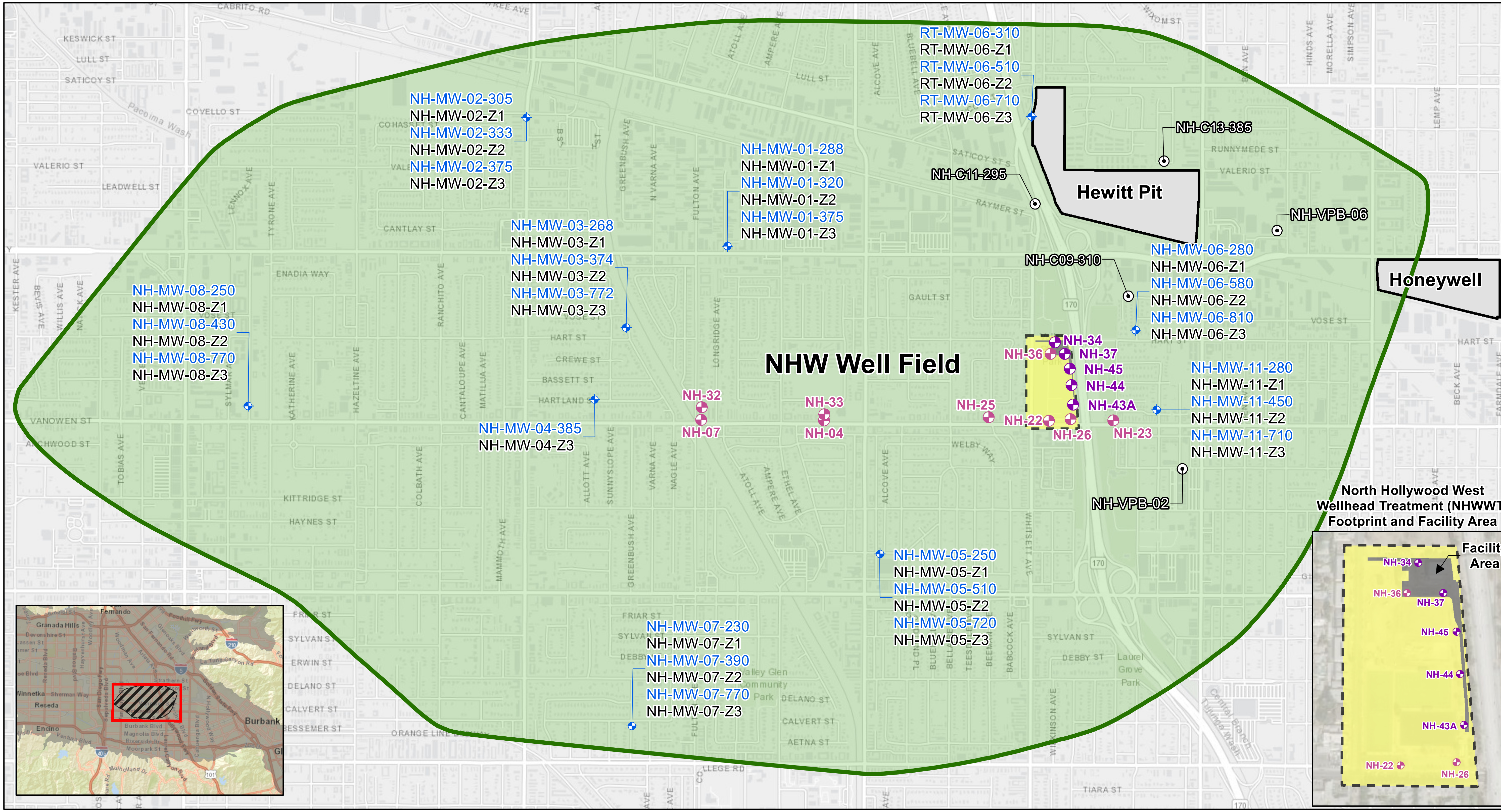

N
W E
S
0 1,750
Feet

Sources: Esri, HERE, Garmin, USGS, Intermap, INCREMENT P, NRCan, Esri Japan, METI, Esri China (Hong Kong), Esri Korea, Esri (Thailand), NGCC, (c) OpenStreetMap contributors, and the GIS User Community

Note:
Features shown on this figure are approximate and should be used for indicative purposes
GSIS Monitoring Wells are from NH-MW-05 to NH-MW-11

Legend

- USEPA MONITORING WELLS
- REMEDIATION WELLS
- NHW PRODUCTION WELLS
- GSIS MONITORING WELLS
- NH-MW-08-270 Well ID (Former)
- NH-MW-08-Z1 LADWP Well ID
- NHW STUDY AREA BOUNDARY (10 YR CAPTURE ZONE)

LA DWP Los Angeles Department of Water & Power

Hazen ARCADIS Advisian

NORTH HOLLYWOOD WEST (NHW) WELL FIELD STUDY AREA

SWL	SB	10/30/2020
308038-13235 302 DDW 97-005		1-2

2 EVALUATION OF THE RISKS OF FAILURE

In this section, the proposed treatment system was evaluated in terms of its probability to fail. Likely treatment failure modes were also evaluated.

2.1 Probability of Failure and System Monitoring

In accordance with DDW Process Memo 97-005, an evaluation of the risks of failure and its frequency of failure was completed for the proposed system. For facilities with multiple treatment technologies, as in the NHWWT case, the failure mode and its health effects for each of the processes are discussed.

The NHWWT process comprises pre-treatment that includes sand separators and cartridge filters followed by Ultraviolet Advanced Oxidation Process (UV AOP); using hydrogen peroxide and UV light) and granular activated carbon (GAC) for hydrogen peroxide quenching. Figure 2-1 presents a process flow diagram for the NHWWT facility. Each of the components are described in subsequent subsections.

The rate of failure was estimated based on experience and data for treatment technologies and similarly engineered projects. The estimation for the frequency of failure was based on the Tucson Water's Tucson Airport Remediation Project (TARP) facility, located in Arizona, which has similar treatment process as the proposed NHWWT. The Tucson Water TARP facility comprises cartridge filters with UV AOP and GAC vessels for hydrogen peroxide quenching. The Tucson Water TARP water treatment plant has been in operation for over 5 years. An interview was conducted to review operational experience and equipment failure rates. The following sections summarize the potential failures in each treatment component.

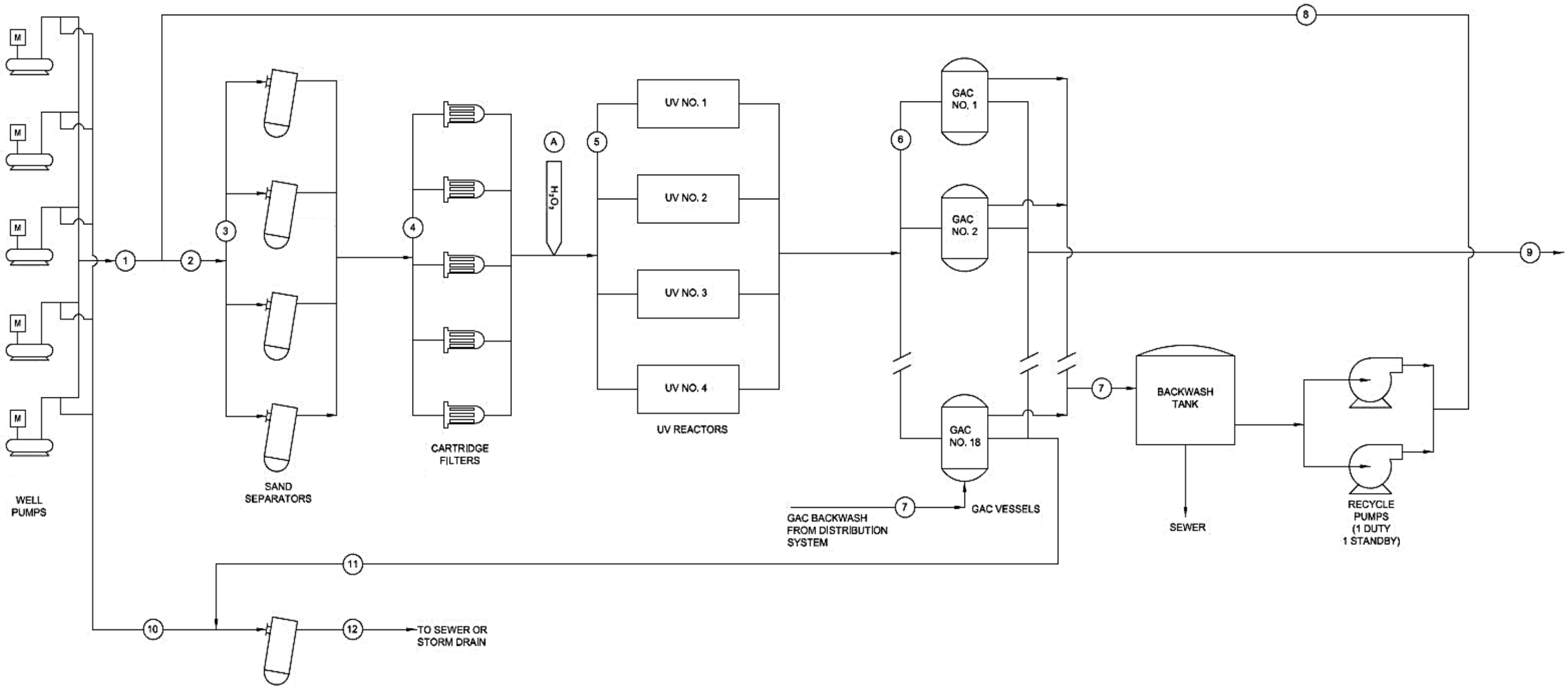

Figure 2-1 NHWWT Flow Diagram

2.1.1 Pre-Treatment

The pre-treatment system comprises four sand separators and five cartridge filters. The sand separators remove sediment or debris from the groundwater. The influent water is pumped into the top of the sand separator where centrifugal forces separate the large particles outward toward the walls of the chamber and settle at the bottom. Purging of the sand separator is performed periodically to remove accumulation of sediments.

The cartridge filters are the second step of pre-treatment, where smaller and lighter particles passing through the sand separator are removed. The cartridge filters contain filter elements within a steel vessel. The water passes through the filters, which separate the smaller particulates. Replacement of the filters is necessary once the filters are clogged or the head loss has increased above the design conditions.

2.1.1.1 Sand Separator

If one of the sand separators fails, then one-quarter (1/4) of flow passes with no large particle removal. The failure would increase the differential pressure across the cartridge filter at a faster rate. The system will alert the operators for filter replacement based on the monitored differential pressure. If the pressure is too high, the likelihood of a filter puncture is increased allowing large particles to flow through the system. The treatment in this scenario is not affected by the failure of a sand separator and therefore has no anticipated increase in health risks. Failure would only result in increased operational activity.

2.1.1.2 Cartridge Filter

Failure of one cartridge filter will result in one-fifth (1/5) of the flow passing with no fine particle removal. This can cause increased GAC head loss, which may require an increase in the backwashing frequency. This poses no health risk to the public since the treatment is not affected by the failure scenario. Similar to the sand separator, the loss of a cartridge filter only increases operational activity.

2.1.2 UV AOP

The UV AOP system comprises a peroxide system and UV reactors. UV reactors photolyze hydrogen peroxide to generate hydroxyl radicals that oxidize the contaminants being treated. The hydrogen peroxide storage and feed system consist of two 9,000-gallon storage tanks with the capacity to hold a full truck of chemical delivery. Hose metering pumps in duty/standby configuration are used to feed hydrogen peroxide. The peroxide is measured by hydrogen peroxide residual analyzer upstream of the UV reactors.

The system consists of four UV reactors (three duty and one redundant train) for treatment. The system's maximum flow capacity is 12,750 gallons per minute (gpm). Each UV train includes isolation valves, a magnetic flow meter, and one UV reactor. The UV reactors include power distribution cabinets (PDCs) and programmable logic controllers (PLCs) for adjusting lamp power and the number of lamps energized. Each UV train has one UV chamber, with 8 UV sections for each chamber. Each UV section has 24 lamps (192 total lamps per reactor).

2.1.2.1 Peroxide Feed System

One potential failure is a loss of the hydrogen peroxide dose, resulting in a lower hydroxyl radical formation and possibly under-treatment of the water. An alarm will be generated if a peroxide residual is below the target. Failure of the hydrogen peroxide feed system could result in limited volatile organic compound (VOC) reduction through UV photolysis and limited treatment of 1,4-dioxane and VOCs through the UV system. However, the downstream GAC system would act as a secondary barrier for VOC removal. 1,4-dioxane removal through GAC is not expected.

2.1.2.2 UV Reactor

UV reactor failure was explored in two scenarios: (1) single lamp and (2) all lamp failure. The single lamp failure would result in 1/192 reduction of UV intensity where the power and the peroxide dose would automatically be adjusted by the system programming. The system's response would generate a lamp failure alarm. This failure scenario causes no health effect to the public due to the system being capable of automatically adjusting to maintain treatment setpoints.

The second scenario of all lamps failing in a UV reactor (e.g., failure due to an electrical failure). This translates into treatment of one-third (1/3) or one-fourth (1/4) of the flow, depending on the number of online UV reactor trains, of the flow to pass through the system without treatment until the system is shut down. The UV reactor controls will automatically isolate the faulted UV train. The system, similar to the first scenario, would alarm for a lamp failure. The health effects posed to the public through this scenario would include brief exposure to 1,4-dioxane. GAC has the ability to act as a secondary barrier for the VOCs.

Treatment of 1,4-dioxane and VOCs is mitigated by UV AOP process. Bench tests were conducted in order to support the technical evaluation of the UV AOP with site specific treatment goals. The testing also compared two lamp technologies: LPHO (low-pressure high output) and MP (medium pressure). The LPHO showed higher efficiency and was able to achieve the target 1.9-log reduction of 1,4-dioxane while simultaneously reducing VOC concentrations. For further information, the North Hollywood West Treatability Testing Bench-Scale Report is provided in Appendix A.

2.1.3 GAC

Excess hydrogen peroxide is required upstream of the UV reactor to generate hydroxyl radicals for treatment, and the hydrogen peroxide is not completely photolyzed by the UV light. GAC is used for quenching (i.e., removing) the residual hydrogen peroxide. Hydrogen peroxide catalytically reacts with the GAC media that breaks down the hydrogen peroxide into oxygen and water. Up to Eighteen (18) GAC vessels will be operated in parallel with an Empty Bed Contact Time (EBCT) of 5 minutes. The system includes a hydrogen peroxide analyzer downstream of GAC, and an alarm will be generated if hydrogen peroxide is detected after GAC treatment. If hydrogen peroxide breakthrough occurs, the GAC media will be changed out.

Failure of GAC would translate into hydrogen peroxide breakthrough, and residual hydrogen peroxide exerts a chlorine demand. Chlorine dosing downstream of the plant for disinfection would act as a peroxide quenching agent, resulting in increased chlorine usage and loss of residual, which can be increased after the water reaches the North Hollywood Pump Station. GAC performance failure does not pose a direct health effect on the public since treatment of 1,4-dioxane and VOCs is not affected when UV AOP is operational.

2.1.4 Analyzers

Online monitoring equipment is used to assess performance of the NHWWT Facility. Table 2-1 summarizes the analyzers and their purpose:

Table 2-1 NHWWT Facility Analyzers and Associated Purposes

Location Description	Instrument	Parameter(s) Tested	Purpose
UV Building Analyzer Wall	RealTech UV254	UVT	Measures UV transmittance (UVT), the amount of UV light that can pass through a water sample. A lower UVT will require the UV reactors to operate at a higher UV output.
UV Building Analyzer Wall	Nitrate Analyzer	Nitrate	Monitor nitrate concentration in downstream of combined GAC to determine if water is sent to sewer or the North Hollywood Forebay.
UV Building Analyzer Wall	Hydrogen Peroxide Analyzer No. 1	Hydrogen Peroxide	Measure the concentration of hydrogen peroxide prior to UV.
UV Building Analyzer Wall	Hydrogen Peroxide Analyzer No. 2	Hydrogen Peroxide	Measure the concentration of hydrogen peroxide downstream of combined GAC to confirm adequate quenching of hydrogen peroxide in GAC vessels.

The UVT analyzer is required to be calibrated every week. However, the system will alarm should the UVT be lower than 97% and in the case of analyzer failure. In both cases, the treatment will continue using the last stable UVT without treatment interruption.

In the instance that the nitrate analyzer fails, the treatment is not affected. The alarm will require the operator to troubleshoot the analyzer and check the GAC treated water for nitrate concentration.

If the hydrogen peroxide analyzer upstream of UV (No. 1) fails during operation, the system will continue treatment without interruption since the analyzer is only used for monitoring. The fail alarm requires the operator to troubleshoot the monitoring instrument and verify its calibration with the actual peroxide concentration. The same logic is applied to the hydrogen peroxide analyzer No. 2. This analyzer is

expected to drift due to the constant reading of zero hydrogen peroxide and will require regular maintenance.

2.2 Operational Experience at Tucson Water TARP

Operational experience is based on Tucson Water TARP, which has been in operation for more than five years with a similar treatment train. Note that the only difference between TARP and NHWWT is the additional pre-treatment at the NHWWT that is upstream of the UV AOP and GAC. Operational history of the Tucson Water TARP facility is summarized below.

The TARP cartridge filters experienced no failures while in operation. However, the cartridge filters were taken out of service due to high solids loading from wells and piping debris, resulting in high replacement frequency (2-3 weeks). The upstream basket strainers would also become loaded with gravel pack from the aging wells. UV AOP and GAC treatment performance has not been affected by the removal of the cartridge filters. Removal of the cartridge filters resulted in more frequent GAC backwashing and damage to the UV reactors as described below. Tucson Water added sand separators to manage sand and gravel and allow re-installation of the cartridge filters.

The peroxide feed pump system comprises diaphragm metering pumps, which require an automatic purge cycle to prevent air binding due to hydrogen peroxide off-gassing. During the purging, the system pressure drops, resulting in a loss of peroxide dosing until pressure is re-established, averaging 4-5 minutes. To mediate the loss of peroxide, the pumps are run at a higher speed during the purging process. No failures have been recorded at the pumps. The NHWWT will not require purging due to the selection of peristaltic pumps over diaphragm metering pumps.

The peroxide residual analyzers at TARP requires monthly calibration. Issues were reported with the post-GAC peroxide analyzer drifting due to the low peroxide levels post-GAC. The utility is evaluating alternative methods for monitoring peroxide breakthrough. Analyzer alarms were reduced to notification level alarms to prevent plant shutdown for false positive events. Periodic probe maintenance is also necessary. Calibration issues have not impacted the treatment performance of the facility.

UV AOP reactors at TARP have experienced wiper malfunction due to gravel and sediment build-up caused by the cartridge filters being removed from service. The wipers push gravel within the chamber and have resulted in two to three sleeve and lamp breaks at the bottom of the reactor. Fouling was observed when the wiper system failed. The fouling was removed when the wipers came back online or through manual cleaning of the sleeves. Approximately 5% of installed lamps failed prior to guaranteed life. Despite lamp failure and fouling, the operational activities have only resulted in less than a day of downtime without affecting the treatment performance.

GAC vessels have not experienced peroxide breakthrough since the TARP facility became operational. Reduced concentrations of peroxide have been detected at 25% and 50% of the GAC bed depth but not in the treated water. Some GAC fines have been noted in low flow areas downstream of GAC.

Table 2-2 summarizes the operational experience at TARP and the solutions at NHWWT to prevent these issues.

Table 2-2 Tucson Water TARP Operational Experience Summary

TARP Operational Experience	NHWWT Solution
• Periodic short-term loss of peroxide residual due to pump purging.	• Hose metering pumps will be utilized and do not require purging.
• UV equipment has experienced failures due to pre-filtration taken out of service.	• Pre-filtration will be comprised of two technologies: sand separators and cartridge filters.
• Peroxide analyzers have been challenging.	• Scheduled peroxide analyzer calibration.

3 ASSESSMENT OF POTENTIAL HUMAN HEALTH RISKS

In accordance with Section 5 of the DDW Draft Process Memo 97-005, the evaluation of human health risks associated with failure of the treatment system include the following information:

- The duration of exposure to contaminated water that would result from such a failure;
- The potential human health risks associated with such exposure to insufficiently treated or untreated water over the course of that failure, considering the risks of disease from microbiological organisms, and the risks of acute, chronic, non-cancer effects and cancer risks from chemical contaminants; and
- Potential cumulative risks, due to multiple failures over the course of operation.

In this chapter, the assessment of human health risks associated with complete failure of the proposed NHWWT is documented. The assessment adopted the methodologies developed by DDW as described in the Draft Process Memo 97-005 and satisfies the evaluation requirements listed above.

3.1 Duration of Exposure and Frequency

A conservative four (4) hour exposure duration estimate was determined based on plant operator response time to system alarms and monitoring data. Since the plant will be a monitored remotely, the response time considered operator travel time with contingency for natural disaster implications, and time to assess the troubleshooting necessary to respond to the alarm(s). The NHWWT design includes two types of alarms; i.e.: major and minor. The major alarms are deemed as high-level alarms that require response time of four hours or less because these are treatment based. If the major alarm is not troubleshot within the allowable four hours, it transitions into a facility interlock. An interlock is a condition that causes the equipment to stop. A second alarm reminder will be set for the operator to troubleshoot before the major alarm transitions into an interlock. A minor alarm is a less critical alarm that will not interrupt treatment but necessary for the facility to operate all equipment within design range. Table 3-1 provides information pertaining to the major and minor NHWWT alarms.

For the assessment of human health risks associated with the potential failure of the proposed NHWWT, an exposure duration of 24 hours was adopted to evaluate potential carcinogenic and non-carcinogenic effects resulting from a single failure. The adopted 24-hour (hr) exposure duration is considered to represent a very conservative exposure duration, as failure to troubleshoot a major alarm within four hours will result in a facility interlock (described in previous paragraph). Therefore, the maximum exposure duration would be 4 hours.

PHGs developed for cancer risks are protective (i.e., will not cause significant adverse health effects) of persons consuming two liters of water every day (i.e., over a **24-hr** period) for 70 years. As a first (conservative) step, the human health risk calculations upheld the 24-hr exposure duration incorporated in the development of PHGs protective of cancer risks instead of adjusting risk calculations to assume the more realistic 4-hr exposure duration. As presented in the following sections, even when adopting a 24-hr exposure duration, human health risks are small and within accepted risk limits. Additional analysis using a shorter duration was not necessary.

To evaluate potential cumulative carcinogenic effects from multiple failures, an exposure duration of 24 hours every year for 10 years, i.e., 10 days total exposure duration, was used in this analysis.

Table 3-1 Facility Alarm Levels

Condition	Controls Response	Level of Alarm[1]	Operator Response
AOP cannot maintain target log reduction	Alarm	Major	Troubleshoot and turn off well(s) as needed
Low hydrogen peroxide residual upstream of UV	Alarm	Minor	Verify peroxide residual via grab sample
Low UVT (<97%)	Alarm	Minor	Verify calibration
Peroxide measured in GAC treated water	Alarm	Minor	Verify peroxide residual via grab sample
High pressure within the treatment plant	Automatic Facility shutdown & Shutdown Alarm	Major/Interlock	Inspect and troubleshoot
High flow GAC	Alarm	Major	Inspect and troubleshoot
High pressure at individual wells	Automatic shutdown of wells & Shutdown Alarm	Minor	Inspect and troubleshoot
Low hydrogen peroxide feed rate	Start standby pump	Major	Inspect pumps
UVT Analyzer Failure	Alarm	Major	Troubleshoot
Loss of UV treatment (power quality event)	Restart UV system & Alarm (Ballast failure)	Major	Check power
Loss of communications with reactor LCP or UV SCC	Alarm	Major	Troubleshoot communications

3.2 Constituents of Potential Concern

The assessment of human health risks adopted the constituents of potential concern (COPCs) identified in the NHW Well Field Treated Water Goals Evaluation report (Step 4 of 97-005 Evaluation), with the exception of hexavalent chromium (CrVI)[1]. The list of COPCs include:

- All COPCs identified in the Step 2 report for the NHW Well Field 97-005 Evaluation for both production and monitoring wells;
- Constituents which exceeded 10% of their Maximum Contaminant Level (MCL) or Notification Level (NL) in production wells and fall into one or more of the following categories:
    - Semi-Volatile Organic Compounds (SVOCs);
    - Volatile Organic Compounds (VOCs);
    - Inorganic constituents which:
        - Are known contaminants in the San Fernando Basin (SFB); and
        - Were identified as COPCs with anthropogenic source(s) within the NHW Well Field Study Area in the Step 1 report for the NHW Well Field 97-005 Evaluation. For example, HPL, which is located within the NHW Study Area, is a known contamination source.

The list of constituents adopted for this assessment of human health risks posed by the failure of proposed treatment is provided in Table 3-2 below.

Table 3-2 Adopted NHW Well Field Constituents of Potential Concern (COPCs)

COPC
1,1-DICHLOROETHANE (1,1-DCA)
1,1-DICHLOROETHENE (1,1-DCE)
1,2,3-TRICHLOROPROPANE (1,2,3-TCP)
1,2-DICHLOROETHANE (1,2-DCA)
1,4-DIOXANE
BENZENE
CIS-1,2-DICHLOROETHENE (CIS-1,2-DCE)
DI(2-ETHYLHEXYL)PHTHALATE (DEHP)
NITRATE (AS NITROGEN [N])
TETRACHLOROETHENE (PCE)
TRICHLOROETHENE (TCE)

[1] DDW confirmed via email communication (sender: Jeff O'Keefe) on June 6, 2020, that Cr(VI) can be excluded from the NHW Well Field Step 5 assessment, as it was confirmed in Step 4 (adopted in the MCL-equivalent approach) that Cr(VI) is present at background concentrations and will not be treated by NHWWT to meet an MCL.

3.3 Constituents of Potential Concern Exposure Concentrations

For the purposes of this assessment of human health risks, the estimated concentrations of COPCs in the combined flow for two scenarios (or options) were considered. The concentrations were taken from water quality data analysis and treatment plant influent estimates provided in the NHW Well Field Raw Water Quality Characterization (RWQC) report (Step 2 of 97-005 Evaluation); values are summarized in Table 3-3.

As noted in Section 1, the NHWWT will treat impacted groundwater from up to five wells; i.e., three Remediation Wells with the option of treatment of five Remediation Wells. It is for this reason that two scenarios are considered herein, i.e., Three Remediation Well Treatment, and Five Remediation Well Treatment. As the NHWWT effluent (assumed to be untreated in a failure scenario) will be combined with the collective flow from other NHW production wells which are not being treated as part of the NHWWT (NH-04, NH-07, NH-22, NH-25, NH-26, NH-32, NH 33 and NH-36), it is considered appropriate to conduct the assessment of human health risks using the maximum concentrations calculated for the following Combined Flow scenarios:

- **Three Remediation Well Treatment Scenario** - *Combined Flow* comprising:
    - NHWWT effluent (untreated due to failure of proposed treatment) generated from three Remediation Wells (NH-34, NH-37 and NH-45); plus
    - Untreated Water (NH-04, NH-07, NH-22, NH-25, NH-26, NH-32, NH-33 and NH-36).
- **Five Remediation Well Treatment Scenario** (if system is expanded to include two additional wells**)** - *Combined Flow* comprising:
    - NHWWT effluent (untreated due to failure of proposed treatment) generated from five Remediation Wells (NH-34, NH-37, NH-43A, NH-44 and NH-45); plus
    - Untreated Water (NH-04, NH-07, NH-22, NH-25, NH-26, NH-32, NH-33 and NH-36).

A diagram showing the flows described above is provided in Figure 3-1. The locations of the Remediation Wells and other production wells are shown in Figure 1-1.

Table 3-3 Estimated Maximum Concentrations for the COPCs in the Combined Flow(s) For Failure Scenarios

COPC	MCL or NL (µg/L)	Max. Concentration for Three Well Scenario (µg/L)	Max. Concentration for Five Well Scenario (µg/L)
1,1-DICHLOROETHANE (1,1-DCA)	5	Non-Detect (<DLR)	Non-Detect (<DLR)
1,1-DICHLOROETHENE (1,1-DCE)	6	1.3	1.3
1,2,3-TRICHLOROPROPANE (1,2,3-TCP)	0.005	Non-Detect (<DLR)	Non-Detect (<DLR)
1,2-DICHLOROETHANE (1,2-DCA)	0.5	Non-Detect (<DLR)	Non-Detect (<DLR)
1,4-DIOXANE*	1	4.0	3.4
BENZENE	1	Non-Detect (<DLR)	Non-Detect (<DLR)

COPC	MCL or NL (µg/L)	Max. Concentration for Three Well Scenario (µg/L)	Max. Concentration for Five Well Scenario (µg/L)
CIS-1,2-DICHLOROETHENE (CIS-1,2-DCE)	6	Non-Detect (<DLR)	Non-Detect (<DLR)
DI(2-ETHYLHEXYL)PHTHALATE (DEHP)	4	Non-Detect (<DLR)	Non-Detect (<DLR)
NITRATE (AS N)	10,000	3,806	4,103
TETRACHLOROETHENE (PCE)	5	1.9	3.2
TRICHLOROETHENE (TCE)	5	4.9	7.0

Notes:

µg/L = micrograms per liter; MCL = Maximum Contaminant Level; NL = Notification Level

*As outlined in the Step 2 of the NHW Well Field 97-005 Evaluation, groundwater flow simulations and fate and transport modeling for 1,4-dioxane have been carried out for the NHW Well Field (Hazen, 2016a); projected concentrations for 1,4-dioxane in NHW production wells are incorporated in the failure scenario analysis presented herein.

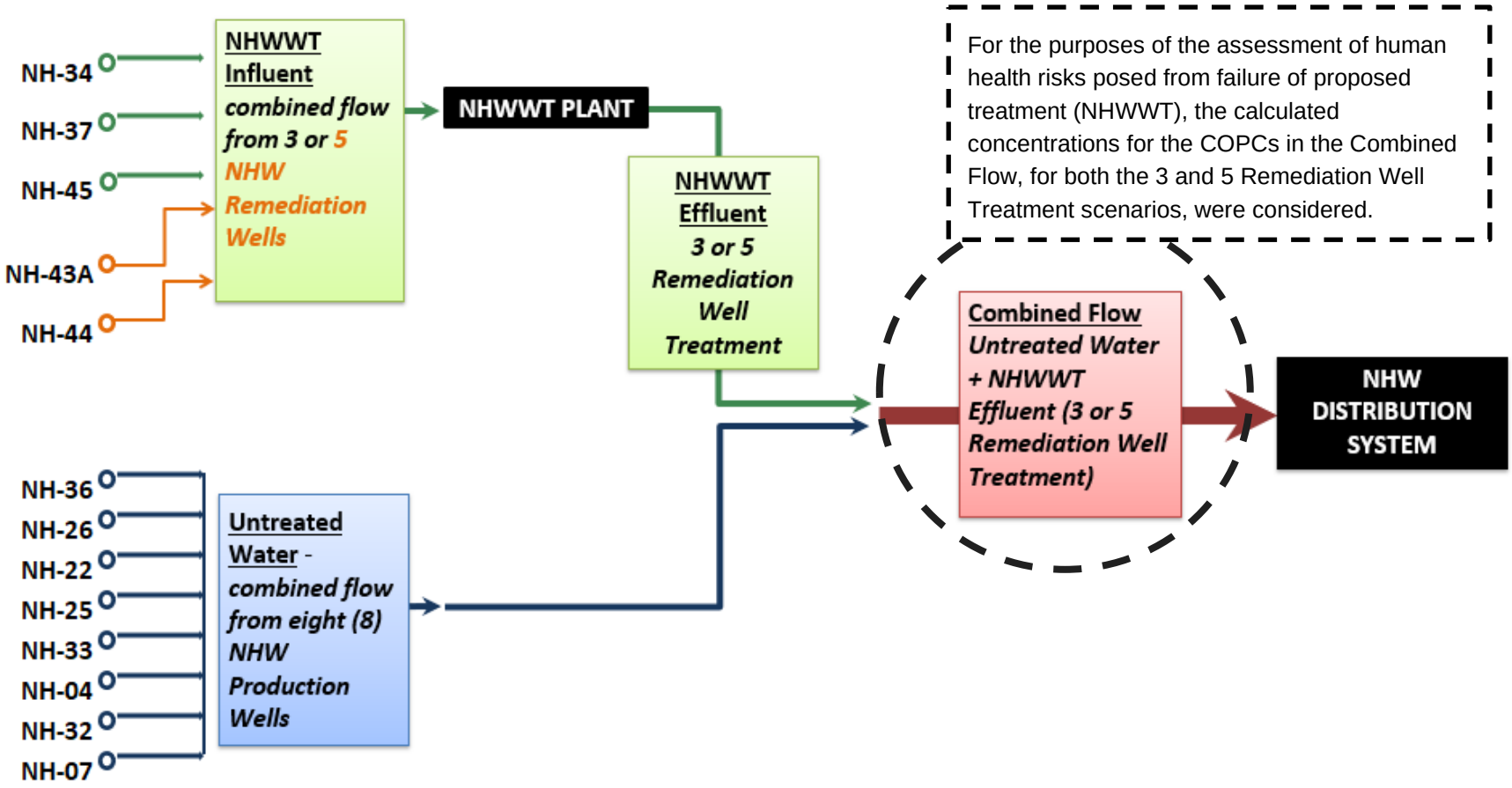

Figure 3-1 NHW Well Field Flows Diagram

3.4 Approach

The approach described herein aligns with the methodology described in the Draft Process Memo 97-005 and incorporates the outcome of discussions with DDW from July 2018 through January 2020.

3.4.1 Failure Scenario

The NHWWT includes multiple treatment technologies, i.e., UV AOP and GAC (Section 2), and therefore, multiple failure evaluations were considered. For example, each technology may be assumed to fail individually; various combinations of technologies may be assumed to fail together; and all may be assumed to fail at the same time.

For the purposes of this assessment, the simultaneous failure of all technologies was assumed (i.e., complete NHWWT failure). It should be noted that this assumption is considered highly conservative and presents the worst-case scenario whereby untreated water (i.e., influent = effluent) enters the distribution system. As described in Section 2, the likelihood of complete failure occurring is minimal due to online monitoring of key operational parameters and multiple barriers for many of the COPCs. Short term undertreated water due to the failure of one UV train is the most likely scenario. The undertreated water would be limited through automatic isolation of the failed UV train.

As described in subsequent sections, even when adopting the very conservative assumption of complete treatment failure, the risks to human health from exposure to untreated water are small and within accepted risk limits. However, if the analysis showed higher potential risks under this assumption, it may have been more appropriate to evaluate human health risks by assessing various failure modes instead of complete treatment failure.

In accordance with the 97-005 Process Memo, the assessment specifies the following guideline for each COPC:

- The MCL or NL; and
- The appropriate value for cancer- or non-cancer endpoints, based on the California Public Health Goals (PHGs) or PHG-like values.

The COPCs and relevant guidelines are presented in Table 3-4 below.

Table 3-4 NHWWT COPCs and Relevant Guidelines

COPC	MCL (µg/L)	PHG (µg/L)		NL (µg/L)
		Cancer	Non-Cancer	
1,1-DICHLOROETHANE (1,1-DCA)	5	3	140	--
1,1-DICHLOROETHENE (1,1-DCE)	6	--	10	--
1,2,3-TRICHLOROPROPANE (1,2,3-TCP)	0.005	0.0007	80	--
1,2-DICHLOROETHANE (1,2-DCA)	0.5	0.40	480	--
1,4-DIOXANE	1	0.35*	210**	1
BENZENE	1	0.15	26	--
CIS-1,2-DICHLOROETHENE (CIS-1,2-DCE)	6	--	13	--
DI(2-ETHYLHEXYL)PHTHALATE (DEHP)	4	12	100	--
NITRATE as NITROGEN (N)	10,000	--	10,000	--
TETRACHLOROETHENE (PCE)	5	0.06	11	--
TRICHLOROETHENE (TCE)	5	1.7	1,000	--

Notes:

MCL = Maximum Contaminant Level; PHG = Public Health Goal; NL = Notification Level; µg/L = micrograms per liter; "--" indicates not applicable; *the PHG-like value for 1,4-dioxane is the 10-6 risk level, based on USEPA's risk assessment (see discussion below) and DDW's NL documentation; **210 ug/L, calculated from the reference dose (RfD) of 3 $x10^{-2}$ mg/kg-day x 70 kg x 0.2 relative source contribution [RSC])/2 L/day from US EPA IRIS

In accordance with the DDW Process Memo 97-005, the assessment used PHGs whenever they were available for a given COPC. Where PHGs were not available, PHG-like values were adopted, as follows:

- For 1,4-dioxane, the Office of Environmental Health Hazard Assessment (OEHHA) is currently developing a PHG for 1,4-dioxane. EPA's tap water Regional Screening Level (RSL) Total Hazard Quotient of 0.1 (THQ = 0.1, to account for exposure to multiple constituents) of 60 micrograms per liter (µg/L) was used as a surrogate for the non-cancer PHG; EPA provides hazard quotient (HQ) values for non-carcinogens in the form of a number such as 0.1 or 1.0. Hazard quotient is the ratio of a predicted exposure concentration to the reference concentration (RfC) for a pollutant. For example, a hazard quotient of 1.0 means that the predicted exposure concentration equals the reference concentration, and a hazard quotient of 0.1 means the predicted exposure concentration is one-tenth the reference concentration. Reference concentration is an estimate of the continuous lifetime inhalation exposure that the EPA believes is likely to have no appreciable risk of deleterious non-cancer effects. Although exposures below the RfC are believed to be safe, exposures above the RfC are not necessarily associated with adverse effects. Nevertheless, as exposure increases above the RfC, the risk for adverse effects also increases; and

- For 1,4-dioxane, the 1E-06 lifetime cancer risk-related concentration of 0.35 ug/L was used as the PHG-like value. In 1998, the Drinking Water Program, now DDW, established its initial NL at 3.0 µg/L, based on an EPA (1990) drinking water concentration that corresponded to a 1E-06 theoretical lifetime cancer risk. Later, in 2010, EPA revised its 1,4-dioxane risk evaluation, such that a 1E-06 risk level corresponds to 0.35 µg/L (EPA 2010a, 2010b, 2013). DDW revised its NL to the 1.0 µg/L level in November 2010 (which corresponds to 3E-06) to reflect the detection limit for reporting (DLR) (cited from California State Water Resources Control Board [California Water Boards], online, 2018).

The risk from the exposure attributable to each COPC was assessed as follows:

- For a carcinogen, the lifetime cancer risk from the exposure attributable to each contaminant, in units of cancer case x 1E-06 was determined, whereby:
    - The cancer risk attributable to the contaminant in cancer case x 1E-06 = concentration during failure/*de minimis* risk concentration (e.g., PHG) x (period of exposure in days)/365 x 70 years).
- For non-cancer hazard attributable to each contaminant, expressed as a ratio (the hazard quotient, HQ), whereby:
    - HQ = the exposure in µg/L divided by (/) the PHG or PHG-like value in µg/L.

To determine the overall cancer risk for each Combined Flow (Section 3.3; Figure 2-1), the cancer risks calculated for each COPC were summed. A risk range of 1E-06 to 1E-04 is considered to fall within the EPA risk management range and was therefore adopted as the acceptable cancer risk range for this assessment.

Similarly, for non-cancer risk, the overall risk for each Combined Flow (Section 3.3; Figure 2-1) was calculated by summing the non-cancer risk (expressed as ratio = Hazard Quotient [HQ]) calculated for each COPC. The sum of the HQs is referred to as the Hazard Index (HI). An HI less than unity (one [1.0]) is considered acceptable. Because the HI is a ratio of the exposure level vs. a threshold (i.e., the PHG or its surrogate, in this case), an HI above or below unity suggests the potential magnitude of the occurrence of adverse effects (EPA 1989): if the HI is greater than 1.0, a potential may exist for adverse non-carcinogenic health effects; conversely, if the HI is equal to or less than 1.0, exposures to the COPCs are not expected to result in a systemic toxic response.

3.4.2 Exposure Equations

The following equations were used to calculate risks/hazards from exposure to untreated NHWWT effluent (Section 3.3; Figure 2-1).

Equation 1 - Carcinogenic risk (based on a 1E-06 target risk level) and averaged over a lifetime (equation adapted from EPA 1989)

Carcinogenic Risk = $\left(\frac{Maximum\ Estimated\ COPC\ Concentration\ (\mu g/L)}{PHG\ (\mu g/L)}\ x\ ED\right) \div AT \div 10^{-6}$

where:

PHG = California Environmental Protection Agency (CalEPA) Public Health Goal (µg/L)

ED = Exposure Duration, 1 day or 10 days

µg/L = micrograms per liter

AT = averaging time; 365 days/year x 70 years = 25,550 days

10^{-6} (also 1E-06) = acceptable incremental lifetime cancer risk.

Equation 2 - Non-carcinogenic hazard (equation adapted from DDW 2015)

Non-carcinogenic Risk = $\frac{Maximum\ Estimated\ COPC\ Concentration\ (\mu g/L)}{PHG\ (\mu g/L)}$

where:

PHG = California Environmental Protection Agency (CalEPA) Public Health Goal (µg/L)

µg/L = micrograms per liter.

3.5 Toxicity Assessment

For the toxicity assessment, the estimated maximum concentrations for the COPCs were compared to PHGs or equivalent for both carcinogenic and non-carcinogenic exposure.

3.5.1 Public Health Goals

The PHGs are levels of contaminants in drinking water based on human health risk assessments that are protective of public health and pose no significant health risk if consumed for a lifetime. The PHGs, which are not enforceable, are developed by the CalEPA's OEHHA. PHGs are used by the DDW to determine whether contaminant MCLs should be considered for possible revision. The California Safe Drinking Water Act of 1996 ("the Act", amended to be called Health and Safety Code, Section 116365 (h)) requires DDW to make public the list of chemicals for which a review of the existing MCL is to be completed. Additionally, Section 116365 specifies that the PHG is to be based exclusively on public health considerations without regard to cost impacts. A toxicity profile for each COPCs considered herein are provided in Appendix B and includes:

- Tabulated acute and chronic cancer and non-cancer PHGs (OEHHA) or surrogates used in this assessment, the basis for each PHG or surrogate with respect to the organs or system(s) affected and any relevant notes specific to this assessment;
- Industrial usage of COPCs;
- EPA carcinogenicity classification and Proposition 65 status in California; and
- A brief discussion of the study/studies and any uncertainty factors relevant to the development of the non-carcinogenic, acute and the carcinogenic and/or non-carcinogenic PHG or surrogate, whichever are applicable, used in this assessment.

3.6 Risk Characterization

The equations presented in Section 3.4.2 were used to calculate the potential risks/hazards from exposure to individual COPCs by comparing the maximum estimated concentration to a health-protective reference value and amortizing the ratio across an averaging time (lifetime for carcinogens). Potential risks from individual constituents may be added together when the same individuals or group of individuals are exposed to multiple constituents, with the expectation of similar endpoints (e.g.

carcinogenic vs. non-carcinogenic effects, etc.). The cancer risk equation below estimates the incremental individual lifetime cancer risk for simultaneous exposure to several carcinogens and is based on EPA's risk assessment guidelines (EPA 1989).

Equation 3 - Total excess lifetime cancer risk (equation adapted from EPA 1989)

$ELCR_T = \sum ELCR_i$

where:

$ELCR_T$ = total excess lifetime cancer risk, expressed as a unitless probability; and

$ELCR_i$ = excess lifetime cancer risk estimate for the i^{th} constituent.

This equation accounts for the joint probabilities of the same individual developing cancer as a consequence of exposure to two or more carcinogens. Additionally, it assumes that intakes of individual substances are small, the action by the compounds involved is additive, that there are no synergistic or antagonistic chemical interactions, and all carcinogenic chemicals produce the same effect (i.e. cancer).

For non-carcinogenic substances, the HI is equal to the sum of the HQ, as described by this equation:

Equation 4 - Non-carcinogenic hazard (equations adapted from EPA 1989)

$HI = \sum HQ_i$

where:

HI = hazard index

HQ_i = hazard quotient for the i^{th} constituent

This equation accounts for the joint probabilities of the same individual developing adverse effects to two or more COPCs.

3.7 Human Health Risk Assessment (HHRA) Results

Results of the human health risk calculations are provided in Appendix C for the single treatment failure event scenario, and Appendix D for the multiple treatment failure events scenario. The calculations use the approach detailed above. The risk calculations were based on the potential exposure from the estimated maximum concentrations of COPCs in the NHW Well Field Combined Flows (Section 3.3; Figure 2-1) under total treatment plant failure conditions. Exposure concentrations were compared directly to carcinogenic and non-carcinogenic PHGs. A summary of the results are presented in Table 3-5 and Table 3-6 below. These tables show the calculated cancer risk and non-carcinogenic hazard assuming: (1) a single treatment failure event (Table 3-5, Section 3.7.1), and the calculated cancer risk assuming: (2) multiple treatment failure events (Table 3-6, Section 3.7.2), for each scenario, i.e., Three Remediation Well Treatment and Five Remediation Well Treatment.

3.7.1 Single Treatment Failure

As presented in Table 3-5, the assessment results indicate that the risk of cancer from exposure during a single treatment failure is *1.8.E-9* for Three Remediation Well Treatment, and *2.6E-9* for Five Remediation Well Treatment. These calculated risk values are below the DDW (and EPA and CalEPA) *de minimis* cancer risk of 1E-06.

Also presented in Table 3-5, the calculated non-cancer hazard (i.e., the ratio of the maximum estimated arrival concentrations of COPCs to non-cancer PHGs) from a single treatment failure event is *0.70* assuming Three Remediation Well Treatment, and *0.85* when assuming Five Remediation Well Treatment. The calculated non-carcinogenic hazards for both remediation well options are below the DDW threshold value of 1.0. Results of the human health risk calculations for the single treatment failure scenario are tabulated and provided in Appendix C.

Table 3-5 Results Based on 1-day Exposure Duration

Scenario	DDW's *de minimis* Cancer Risk	Cancer Risk	DDW Threshold	Non-Cancer Hazard
Three Remediation Well Treatment	1E-06	1.8E-09	1.0	0.70
Five Remediation Well Treatment		2.6E-09		0.85

3.7.2 Multiple Treatment Failures

As presented in Table 3-6, multiple treatment failures (totaling 10 days over a 70-year lifetime) results in a calculated cancer risk of *6.4E-09* when adopting Three Remediation Well Treatment, and *6.1E-09* when assuming Five Remediation Well Treatment. The calculated cancer risk for both options are below DDW's *minimis* cancer risk of 1E-06. Results of the human health risk calculations for the multiple treatment failures scenario are tabulated and provided in Appendix D.

Table 3-6 Results Based on 10-day Exposure Duration (1-day x 10 years)

Scenario	DDW's *de minimis* Cancer Risk	Cancer Risk
Three Remediation Well Treatment	1E-06	6.4E-09
Five Remediation Well Treatment		6.1E-09

3.8 Microbiological Contaminants

The 97-005 Process Memo states that:

"*For microbiological contaminants, the risk assessment needs to consider the impact of single and multiple failures of the proposed multi-barrier treatment system, and the likelihood of exposure to virus, bacteria, or parasitic organisms, as well as the risk of infection.*"

The presence of microbial organisms in drinking water is regulated under the California MCL for the distribution system, which is based on the number of samples collected per month, and states:

- For public water systems collecting more than 40 samples per month, the MCL is exceeded when:
  - More than 5% of samples in a month are total coliform-positive.
- For public water systems collecting less than 40 samples per month, the MCL is exceeded when:
  - More than 1 sample per month is total coliform-positive.
- For all systems, regardless of sample size, the MCL is violated when:
  - Any repeat sample is fecal coliform-positive or E.coli positive; and
  - Any repeat sample following a fecal coliform-positive or E.coli positive routine sample is total coliform-positive.

NHW microbial data collected between 2012 and 2018 were evaluated for detections; out of 1,759 records, there were 0 positive detections of either E.coli or fecal coliforms. Thus, there is no measurable risk from exposure to microbial contaminants originating from the groundwater.

4 CONCLUSIONS

This report documents Step 5 of the 97-005 evaluation process, i.e., “Human Health Risks Associated with Failure of Proposed Treatment”, and satisfies the applicable requirement outlined in the DDW Process Memo 97-005. A summary of the evaluation outcome is provided below.

The assessment of mode of failure for each component of the NHWWT concluded the sand separators, cartridge filters, and GAC contactors do not affect the treatment performance and therefore do not pose a health risk to the public under a failure scenario. Failure of these components would result in increased maintenance activities. Peroxide feed and UV reactor failure would pose a limited and brief increase in risk to the public. However, online monitoring and a four-hour window of operator troubleshooting of the equipment would limit any potential of high exposure.

Human health risk calculations using the approach described in the DDW Process Memo 97-005 which includes the use of maximum calculated constituents of concern (COPCs) concentrations in untreated NHWWT effluent, indicate that, even in the event of total NHWWT failure, incremental cancer and non-cancer risks are small and within accepted risk limits. Multiple failures spanning several years, presented as a worst-case scenario and are not expected to reasonably occur, showed cancer risk below de minimis (1E-06), and the non-cancer hazard (i.e., the ratio of the maximum estimated arrival concentrations of COPCs to non-cancer PHGs) are below the DDW threshold value of 1.0. Additionally, exposure to microbial organisms is not considered to pose a risk of disease in the event of a treatment failure, based on comparison to the California MCL.

5 REFERENCES

California Water Boards, online. 2018. 1,4-Dioxane. California Water Resources Control Board. Accessed October 2018. https://www.waterboards.ca.gov/drinking_water/certlic/drinkingwater/14-Dioxane.html

DDW (Division of Drinking Water) (formerly California Department of Public Health). 2015. Addressing the Direct Domestic Use of Extremely Impaired Sources, Process Memo 97-005. Initially Established November 5, 1997, revised March 25, 2015 (Draft).

EPA (United States Environmental Protection Agency). 1989. Risk Assessment Guidance for Superfund (RAGS): Volume 1 - Human Health Evaluation Manual (Part A). EPA/540/1 89/002. December.

EPA (United States Environmental Protection Agency). 1990. 1,4-Dioxane. Integrated Risk Information System (IRIS), US Environmental Protection Agency, September 1 (cited by California Water Boards, online (2018).

EPA (United States Environmental Protection Agency). 2010a. 1,4-Dioxane, IRIS, US EPA, Accessed August 11, 2010 (cited by California Water Boards, online (2018).

EPA (United States Environmental Protection Agency). 2010b. Toxicological Review of 1,4-Dioxane, in support of summary information on IRIS. Accessed August 11, 2010 (cited by California Water Boards, online (2018).

EPA (United States Environmental Protection Agency). 2013. 1,4-Dioxane, IRIS, Accessed September 20, 2013 (cited by California Water Boards, online (2018).

Hazen (Hazen and Sawyer), 2016a. Interim Remedial Investigation / Feasibility Study Report, North Hollywood West Well Field. December 2016.

Hazen (Hazen and Sawyer), 2016b. Proposed Plan for Interim Remedial Action, North Hollywood West Well Field. December 2016.

Hazen (Hazen and Sawyer), 2017. Interim Remedial Action Decision, North Hollywood West Well Field. July 2017.

Office of Environmental Health Hazard Assessment (OEHHA). 2018. Cis- and Trans-1,2,-Dichloroethene in Drinking Water. July.

Appendices

Appendix A Bench-scale Ultraviolet Advanced Oxidation Process (UV AOP) Testing Report

TASK 301
BENCH-SCALE TESTING REPORT

North Hollywood West Treatability Testing Bench-Scale Report

Prepared for:

City of Los Angeles
Department of Water and Power
111 North Hope Street
Los Angeles, California 90012

Submitted by:

Hazen and Sawyer (Hazen) under Agreement No. 47329-6 (Owner's Agent for the SFB Remediation)

Prepared by:

Owner's Agent: Hazen, with primary input from Arcadis and University of Colorado at Boulder
800 West 6th Street, Suite 400
Los Angeles, California 90017

December 2020

CONTENTS

TABLES

FIGURES

1 Introduction

The City of Los Angeles Department of Water and Power (LADWP), in accordance with the Comprehensive Environmental Response, Compensation, and Liability Act of 1980 (CERCLA), the National Oil and Hazardous Substances Pollution Contingency Plan (NCP) and guidelines presented in the Guidance for Conducting Remedial Investigations and Feasibility Studies Under CERCLA (EPA 1988a), conducted an interim remedial investigation/feasibility study (RI/FS) to address the synthetic contaminant 1,4-dioxane dissolved in groundwater at the North Hollywood West (NHW) Well Field located within the San Fernando Groundwater Basin (San Fernando Basin [SFB]). An Interim Remedial Action including groundwater treatment was selected as the Preferred Alternative.

Treatment goals for NHW groundwater remediation wells are shown on Table 1-1. Influent design concentrations based on modelling results and use of a safety factor are also provided.

Table 1-1. Performance Treatment Goals

Contaminant	Design Influent	Design Effluent	Performance goal
Tetrachloroethylene (PCE)	25 μg/L	<0.5 μg/L	1.7-log reduction
Trichloroethylene (TCE)	50 μg/L	<0.5 μg/L	2.0-log reduction
1,4-Dioxane	20 μg/L	<0.25 μg/L	1.9-log reduction

1.1 Testing Objective

The purpose of this bench-scale testing is to support the technical evaluation of an Ultraviolet Advanced Oxidation Process (UV AOP) using UV light and hydrogen peroxide (UV/peroxide) for treating groundwater from the San Fernando Basin North Hollywood West Well Field.

The goals for bench-scale testing of UV/peroxide are listed below:

1. Generate site-specific data to evaluate the ability of UV/peroxide to treat 1,4-dioxane and volatile organic compounds (VOCs) present in the groundwater.
2. Evaluate regulated and unregulated byproduct formation of the UV/peroxide process.
3. Evaluate relative treatment efficiencies and byproduct formation with low pressure high output (LPHO) and medium pressure (MP) UV lamps.
4. Develop 1,4-dioxane UV dose response curves as a function of peroxide dose for comparison to full-scale design criteria.
5. Evaluate TTHM/HAA5 formation with blend of UV/peroxide treated groundwater with LADWP surface water through Simulated Distribution System (SDS) testing.

1.2 UV AOP Background

UV/peroxide uses UV light to photolyze hydrogen peroxide to form hydroxyl radicals. Hydroxyl radicals can oxidize 1,4-dioxane, PCE, TCE and 1,1-DCE, and UV/peroxide has been proven to be effective and

reliable potable water applications in Southern California and at other locations throughout the United States (EPA 2006). UV/peroxide uses hydroxyl radicals, which are powerful oxidizers, to break down contaminants. The reliability of this process has been proven at the regulatory level, and it is a preferred technology for 1,4-dioxane treatment. The EPA has found UV irradiation combined with hydrogen peroxide to be effective at removing 1,4-dioxane with up to greater than 99% effectiveness (EPA 2011).

Key design parameters for UV/peroxide systems included in this study are:

- Background water quality, specifically:
    - UV transmittance (UVT)
    - Hydroxyl radical scavenging demand
- Lamp technology selection
- Byproduct formation and change in toxicity

1.2.1 Background Water Quality

UVT and hydroxyl radical scavenging demand are the two most important water quality parameters for sizing UV/peroxide equipment. UVT is a measure of how much UV light is transmitted through the water and how much is absorbed by background constituents in the water (e.g., natural organic matter (NOM) or nitrate). Lower UVTs result in the UV/peroxide process being less efficient as more power is required to overcome the UV light that is absorbed by constituents other than peroxide.

Hydroxyl radicals are non-selective and will react with constituents in the water other than the target compounds. For most natural waters, the hydroxyl radical scavenging demand is driven by NOM and carbonates. However, the formation of nitrite with a MP UV reactor may increase the background hydroxyl radical scavenging demand. Increases in the hydroxyl radical scavenging demand decrease the efficiency of the AOP process, and, as such, more UV light and/or hydrogen peroxide is required to achieve the required level of reduction of the target contaminant.

1.2.2 Lamp Technology

Municipal scale UV/peroxide systems utilize two common types of UV lamps: low pressure, high output (LPHO) and medium pressure (MP) UV lamps. LPHO lamps emit UV light at a wavelength of 254 nm, while MP lamps emit a broader spectrum. LPHO UV lamps are more efficient at turning electrical energy into UV light, while MP UV lamps emit UV light at lower wavelengths where peroxide has a higher absorbance. The efficiency of the MP UV lamps can be negatively impacted by nitrate, which has a high UV absorbance in the same range that peroxide absorbs UV light. The broad spectrum of UV light emitted by MP UV lamps may also impact byproduct formation as discussed in the following section.

1.2.3 Byproduct Formation

For municipal scale applications, AOPs are typically not operated to achieve complete mineralization (i.e., oxidation to carbon dioxide, chloride, and water) of the target contaminants due to the power and peroxide doses that would be necessary. Since mineralization is not achieved, byproduct formation is a potential concern. The complete identity of byproducts from UV AOP oxidation of organic contaminants are not fully known (WRI, 2011), but several byproducts with regulatory limits have been identified. Potential byproducts for UV/peroxide include the following:

- Regulated disinfection byproducts [total trihalomethanes (TTHM) and five regulated haloacetic acids (HAA5)]
- Nitrite (MP UV only)
- Assimilable organic carbon (AOC), which includes biodegradable constituents such as aldehydes, carboxylic acids, and other small organic byproducts
- Unidentified chemicals contributing to toxicity
- Chloropicrin (MP UV only)

AOP technologies have been shown to transform organics in the water, which can result in higher formation of disinfection byproducts (DBPs), including TTHMs and HAA5, after free chlorine contact time (Dotson, et al. 2010, Andrews 2009). TTHMs and HAA5 are regulated under the Stage 1 and Stage 2 Disinfectants and Disinfection Byproduct Rule (DBPR). The increase in DBP formation is likely due to hydroxylation of aromatics or transformation of less reactive hydrophobic organic matter by hydroxyl radicals into more reactive hydrophilic organic matter (Dotson, et al. 2010).

Nitrite formation is specific to MP UV/peroxide systems. Nitrate has a high UV absorbance at the lower wavelengths emitted by MP UV lamps (i.e., <240 nm), and can be transformed (i.e., photolyzed) into nitrite and radical species when it absorbs UV light. The conversion of nitrate to nitrite must be considered with MP UV systems, as nitrite has a drinking water MCL of 1 mg/L as N and is a hydroxyl radical scavenger.

AOC is a measure of the potential bacterial regrowth or the ability of a water to support bacterial growth. Increases in AOC can be problematic because there is a potential to increase biological growth in the distribution systems. Ozone/peroxide (another AOP process) is known to increase AOC concentrations, but less data are available for AOC formation with UV/peroxide. Linden et al. (2015) found AOC formation with UV/peroxide was limited, but concluded that it may be site specific.

Toxicity testing can be a useful method to evaluate the aggregate health risk of water. Several studies have evaluated the effect of MP UV irradiation on nitrate-containing waters (Martjin and Kruithof 2012, Martijn, Boersma, et al. 2014, Martijn, Kruithof, et al. 2015). The studies evaluated the toxicity of waters prior to and after MP UV exposure. Nitrate-containing waters had increased toxicity after exposure to MP UV light at relevant doses for drinking water disinfection and advanced oxidation. However, the increase in toxicity was contingent on the presence of NOM in the water. It is hypothesized that nitrate photolysis leads to nitrogen-containing intermediate molecules that can react with NOM to increase toxicity by forming nitrated aromatic compounds (Martijn et al. 2014).

Oxidation byproducts have also been evaluated for their impact on toxicity. Linden et al. (2015) evaluated the byproducts of AOP treatment of the EPA Contaminant Candidate List 3 (CCL3) compounds, which includes 1,4-dioxane. It was found that the oxidation byproducts for the majority of the CCL3 compounds, including 1,4-dioxane, did not increase toxicity.

Chloropicrin (Cl_3CNO_2) is a known, unregulated byproduct associated with MP UV irradiation. Studies have shown increasing chloropicrin formation after MP UV exposure. The increase in chloropicrin concentrations is likely due to exposure of NOM or nitrate to UV, leading to more favorable conditions for chloropicrin formation (Reckhow et al. 2010).

1,1,2-TCA is another unregulated oxidation byproduct observed through Vacuum UV (VUV) irradiation. A study published by Baum et al. concluded that 1,1,2-TCA was formed through VUV in the presence of 1,2 DCE.

2 Methods

The following sections summarize the bench-testing methods used in the UV AOP evaluation of NHW groundwater. Testing was provided by Dr. Karl Linden's laboratory at the University of Colorado at Boulder.

2.1 Source Water

Source water was collected from two sources: well water from LADWP's Well NH-37 and surface water from LADWP's North Hollywood Pump Station (NHPS). All UV AOP tests were completed on water from NH-37, which is a Remediation Well. Surface water was only used for blending in the SDS evaluations. Two samples were collected from Well NH-37 (2016 and 2017 sample). The second sample was collected to extend the log reduction of 1,4-dioxane using MP lamps.

2.2 Test Matrix

Table 2-1 presents the goal test matrix to evaluate LPHO and MP technologies under a range of hydrogen peroxide and UV doses, as well as the SDS testing using NHPS water. Tests 2 and 6 were conducted first. The range of UV doses was increased for the remaining tests based on the results of tests 2 and 6. The 2017 water had noticeable particles in the water for test conditions 9 and 10. For test condition 12, the water was filtered through a 0.45-micron filter to remove the particulates. The full-scale facility includes sand separators and cartridge filters to minimize particulates from the wells.

Table 2-1. UV/Peroxide Test Matrix

Test Number	Water	Sample Collection Date	Nitrate/Alkalinity Spiking	Lamp Technology	H_2O_2 Dose (mg/L)	Target UV Dose (mJ/cm^2)[1]
Control 1	NH-37	2016	N/A	N/A	0	0
Control 2	NH-37	2016	N/A	N/A	15	0
Control 3	NH-37 + NHPS	2016	N/A	N/A	0	0
1	NH-37	2016	N/A	LPHO	5	0, 1000, 1700, 2400, 3200
2	NH-37	2016	N/A	LPHO	8	0, 300, 600, 1000, 1500
3	NH-37	2016	N/A	LPHO	12	0, 1000, 1700, 2400, 3200
4	NH-37	2016	N/A	LPHO	15	0, 1000, 1700, 2400, 3200
5	NH-37	2016	N/A	MP	5	0, 700, 1200, 1700, 2300
6	NH-37	2016	N/A	MP	8	0, 200, 400, 700, 1100
7	NH-37	2016	N/A	MP	12	0, 700, 1200, 1700, 2300
8	NH-37	2016	N/A	MP	15	0, 700, 1200, 1700, 2300
9	NH-37 (2017)	2017	Nitrate; Alkalinity	MP	8	0, 2000, 3000, 5000, 7000
10	NH-37 (2017)	2017	Nitrate; Alkalinity	MP	15	0, 2000, 3500, 4500, 6000
11	NH-37	2016	N/A	MP	10	0, 2000, 3000, 4000, 6000
12	NH-37(2017 Filtered)	2017	Nitrate	MP	15	0, 3000, 4500, 6000, 8000

[1]The actual UV dose achieved varied from the target dose. MP UV doses are presented as peroxide weighted doses.

2.3 Target Contaminant Spiking

The 1,4-dioxane concentration in the raw water from Well NH-37 was approximately 14 µg/L. To allow better detection of 1,4-dioxane in the treated water and to test higher log reductions given the uncertainties of the full-scale design criteria at the time of testing, 1,4-dioxane was spiked to approximately 60 µg/L for the bench-scale testing.

VOCs are also present in the North Hollywood West Well Field, including trichloroethylene (TCE), tetrachloroethylene (PCE), and 1,1-dichloroethylene (1,1-DCE). This study also includes testing of 1,2-3-trichloropropane (1,2,3-TCP). While 1,2,3-TCP has never been detected in any operating production wells in the North Hollywood West Well Field (it has only been detected above the newly adopted MCL in 6 out of 84 samples and those detections occurred many years ago when the wells were not pumping), the chemical has had sporadic detections in other San Fernando Basin wellfields. Thus, the chemical was included in the testing to provide information on removal for potential projects in other well fields. VOCs were spiked in the test water to the following concentrations for testing purposes: 30 to 40 µg/L TCE, 4 to 5 µg/L 1,1-DCE, and 0.050 µg/L 1,2,3-TCP. PCE was not spiked due to it having a similar hydroxyl radical rate constant as TCE. Subsequent testing at other wellfield with spiked PCE concentration showed no negative changes to toxicity. Background PCE concentrations were approximately 0.16 µg/L. 1,4-dioxane and VOCs were purchased as neat chemicals and diluted with deionized water. 1,4-dioxane and all VOCs except 1,1-DCA were purchased from Fluka. 1,1-DCA was purchased from Ultra Scientific.

For the 2017 water sample, nitrate was spiked to match the 2016 sample nitrate concentration of approximately 6 mg/L as N. To make the results comparable with similar hydroxyl radical scavenging demands, the alkalinity was also spiked to 290-295 mg/L as $CaCO_3$ to account for the lower modeled hydroxyl radical scavenging demand due to the lower TOC concentration of the 2017 sample.

2.4 Hydrogen Peroxide Dosing

Analytical grade hydrogen peroxide was used for UV AOP testing, with target concentrations of 5, 8, 10 (MP only), 12, and 15 mg/L. A hydrogen peroxide stock of 5,000 mg/L hydrogen peroxide was used, and diluted in ultra-pure deionized water to achieve the desired hydrogen peroxide dose for each sample. All peroxide doses were determined before and after exposure, using the triiodide method by Klassen et al. (1994). Hydrogen peroxide was purchased from BDH VWR Analytical.

2.5 Collimated Beam Testing

UV/peroxide experiments were performed using both LP UV and MP UV collimated beam systems (Figure 2-1). The LP UV system was equipped with four 15-watt bulbs. The MP UV system was equipped with a single ozone free, 1 kilowatt lamp. Incident UV irradiance was measured by a calibrated radiometer (International Light Inc., Model 1700/SED 240/W). UV dose was calculated by multiplying the average irradiance (incident irradiance corrected for sample depth, absorbance at 254 nm (LP) or across the 200-300 nm range (MP), sample reflectance, divergence factor, and petri factor) by the irradiation time in seconds, as per the published standard method (Bolton and Linden, 2003). The UV dose for the MP system was further calculated using a hydrogen peroxide weighting factor that was normalized to 254 nm. The LP UV doses were not weighted to hydrogen peroxide as the LP lamps are

monochromatic. Note that the use of the divergence factor, which corrects for the photons of light that exit the water column before reaching the full depth of water due to divergence, is relatively new and not included in all bench-scale studies. Its precise use for MP UV dosimetry is an area of research. The use of the DF here results in a decrease in the reported UV dose of approximately 13 percent. While the UV doses reported include the divergence factor, if it were not used the required UV doses reported would be higher. The divergence factor was also applied to the LP UV doses.

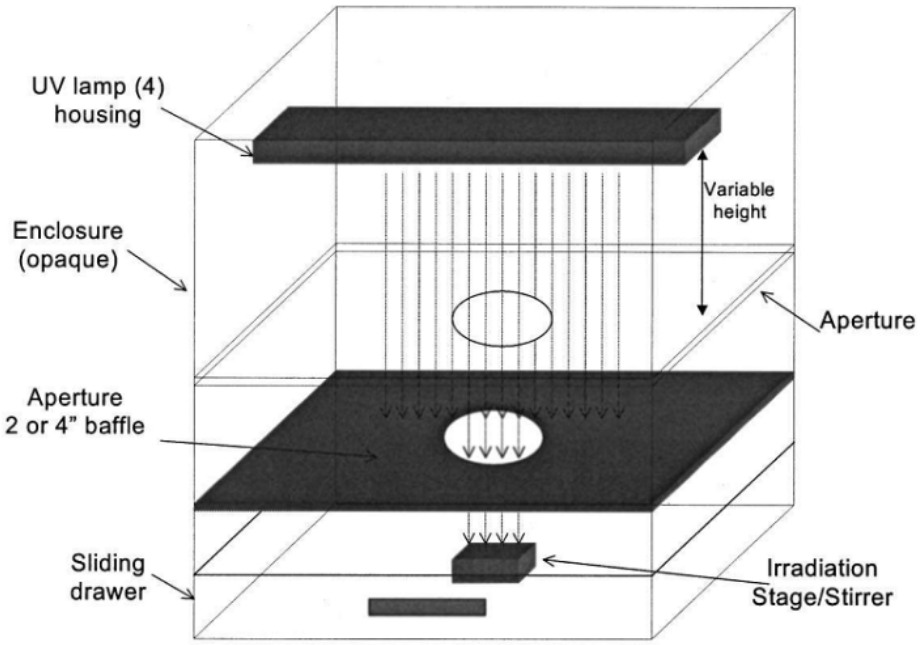

Figure 2-1. Bench-scale collimated LPHO and MP UV system (Bolton and Linden 2003).

UV exposures were performed in both open and closed vessels. The open vessels were used for DBP, nitrate/nitrite, and TOC determinations. The closed vessels were used for spiked VOC and 1,4-dioxane analysis to minimize volatilization losses. Open exposures were performed in a 600 mL glass petri dish, while the closed exposures were conducted in a custom quartz vessel with a volume of roughly 300 mL (Figure 2-2). Samples were completely stirred for the duration of the UV exposure. Due to the exposure times required for the target doses, ice packs were added to the chambers and airflow allowed to minimize temperature changes.

Figure 2-2. Quartz vessel used in the UV AOP analysis of VOCs and 1,4-Dioxane

2.6 Simulated Distribution System Testing

SDS testing was conducted to evaluate potential changes in DBP formation downstream of UV AOP treatment. SDS testing utilized chlorine quenching for removing the remaining peroxide residual prior to the SDS hold period. Full-scale DBP formation is expected to be less due to utilizing GAC for peroxide quenching, which reduces the potential for DBP formation by removing organics through adsorption and biological removal. SDS testing was conducted using the following method:

1. Filled two 250 mL amber glass bottles with target water (raw water, AOP treated water, or surface water blend). For SDS tests sampling nitrosamines, one 250 mL and one 1L amber glass bottles were filled. Filled bottles were headspace free.
2. Chlorine was added to achieve the target residual chlorine concentration (2.5 mg/L). Peroxide residual was quenched with chlorine prior to achieving a free chlorine residual.
3. Lids were closed and the bottles were shaken for 1 min.
4. The bottles were left for 20 mins to simulate free chlorine contact time.
5. The ammonia stock solution was used to dose at a target 5:1 ratio chlorine-to-ammonia mass ratio based on the measured residual chlorine concentration.
6. The bottles were shaken vigorously for 2 minutes.
7. Total chlorine residual was measured after 2 min of mixing time (time zero concentration).
8. The samples were stored in the dark at room temperature.
9. Total chlorine residual, TTHM, and HAA5 was measured after 3 days (72 hours) and 5 days (120 hours).
10. TTHM and HAA5 samples were taken in the appropriate vials containing quenching agents. TTHM bottles used sodium thiosulfate and HAA5 bottles used ammonium chloride as quenching agents. Nitrosamines were sampled after 5 days for the SDS tests.

2.7 Analytical Methods

Water quality before and after UV exposure was analyzed for numerous constituents by different laboratories. These details and the methods are presented in Table 2-2.

Table 2-2. Constituent Analysis Information

Analysis	Analysis Location	Method
AOC	Eurofins	Weinrich et al. - Assimilable Organic Carbon
THMs	Colorado University	EPA Method 552.2 (Agilent 6890 GC-µECD)
HAAs	Colorado University	EPA Method 552.2 (Agilent 6890 GC-µECD)
1,4-Dioxane	North Carolina State University	Modified EPA 522 (Sun, Lopez-Velandia and Knappe 2016)
VOCs	North Carolina State University	EPA Method 524.3
H_2O_2	Colorado University	Triiodide colorimetric method (Klassen, Marchington and McGowan 1994)
TOC	Colorado University	UV persulfate oxidation/conductivity method - Standard Methods 5310C and EPA 415.3 compliant.
Alkalinity	Colorado University	Hach digital titrator method, in compliance with EPA method 310.2
UV254	Colorado University	Cary Bio 100 spectrophotometer (Varian Inc., Palo Alto, TX)
Nitrate	Colorado University	Hach TNT 835 kit. Approved by the EPA. Reference Method: 40 CFR 141
Nitrite	Colorado University	Hach TNT 839 kit. Equivalent to EPA method. Reference Method EPA 353.2

2.8 Background Scavenging

Background radical scavenging experiments were carried out using 500 µg/L of para-Chlorobenzoic Acid (pCBA) as a probe compound to measure hydroxyl radical scavenging. pCBA reacts with hydroxyl radicals at a rate that far exceeds its reaction rate with UV light, making it an ideal probe to measure the formation and scavenging of hydroxyl radicals (HO·).

Samples were analyzed for the concentration of pCBA using an Agilent 1100 series high performance liquid chromatograph (HPLC) and UV detector (at 235 nm) equipped with a reverse phase C-18 column. The mobile phase flowrate was 1 mL/min. Eluents gradient began at 30% HPLC grade methanol and 70% formic acid solution (1% formic acid in lab grade water) increasing to 100% methanol by 6 minutes, followed by a 1 mL/min flow rate of 100% HPLC grade methanol for 2 minutes.

The concentration of HO· was then calculated using the following relationship:

$$\ln\frac{[\mathrm{pCBA}]}{[\mathrm{pCBA}]_0} = \frac{-k_{\mathrm{HO,pCBA}}[\mathrm{HO}\bullet]}{E_0} \times F$$

Equation 2-1

In Equation 2-1, E_0 is the average fluence rate (mW/cm²), F is the fluence (mJ/cm²) and $k_{HO,pCBA}$ is a time-based reaction rate constant between pCBA and hydroxyl radicals ($M^{-1}s^{-1}$). In this equation, the quantity $\frac{-k_{HO,pCBA}[HO\bullet]}{E_0}$ represents the slope of the plot of $\ln\frac{[pCBA]}{[pCBA]_0}$ vs F, and HO· can be calculated as in Equation 2-2:

$$[\mathrm{HO}\bullet] = \frac{-\mathrm{slope}\cdot E_0}{k_{\mathrm{HO,pCBA}}}$$

Equation 2-2

The value for $k_{HO,pCBA}$ has been reported as 5×10^9 $M^{-1}s^{-1}$ (Buxton, et al. 1998). A UV/peroxide model (Glaze, Lay and Kang 1995) can then be rearranged to calculate the total HO· scavenging coming from the sample background, as shown in Equation 2-3.

$$\sum k_s\,[S] = \frac{E_0\varepsilon_{254}\Phi[H_2O_2]}{U_{254}}\cdot\frac{1}{[\mathrm{HO}\bullet]}$$

Equation 2-3

In this equation, k_s is the HO· reaction rate constant for a given scavenging compound ($M^{-1}s^{-1}$), [S] is the concentration of the corresponding scavenging compound (M), ε_{254} is the molar absorption of H_2O_2 at 254 nm ($M^{-1}cm^{-1}$), Φ is the quantum yield of hydroxyl radical formation by photolysis of hydrogen peroxide at 254 nm, $[H_2O_2]$ is the concentration of hydrogen peroxide (M), and U_{254} is the wavelength energy (J/mol). Substituting Equation 2-2 into Equation 2-3 yields Equation 2-4:

$$\sum k_s\,[S] = \frac{E_0\varepsilon_{254}\Phi[H_2O_2]}{U_{254}}\cdot\frac{k_{\mathrm{HO,pCBA}}}{-\mathrm{slope}\cdot E_0} = \frac{\varepsilon_{254}\Phi[H_2O_2]}{U_{254}}\cdot\frac{k_{\mathrm{HO,pCBA}}}{-\mathrm{slope}}$$

Equation 2-4

2.9 Toxicity Testing

As a way of testing the combined impact of potential byproducts in an AOP treated water, toxicity testing was applied. Well NH-37 groundwater was spiked with VOCs and 1,4-dioxane and treated by LPHO- or MP- UV/peroxide advanced oxidation in a batch treatment system (collimated beam). Various UV doses and hydrogen peroxide concentrations were tested. The toxicity of raw, spiked, and treated waters was assessed by a battery of *in vitro* toxicity assays. These tests measured the acute cellular toxicity, estrogenic activity, and mutagenic activity of samples via the bioluminescence inhibition assay (BLIA), yeast estrogen screen (YES), and Ames II mutagenicity assay (AMES), respectively. For AMES testing, samples were assayed after concentration by solid phase extraction (SPE; 50x).

2.9.1 Bioluminescence Inhibition Assay (BLIA)

Acute cytotoxicity is measured by the BLIA over a short incubation of samples by measuring the kinetic change in cellular respiration, indicated by luminescence of a naturally bioluminescent marine bacterium, *Vibrio fischeri* (Shemer and Linden 2007). Toxic samples inhibit cellular respiration and luminescence in comparison to a non-toxic control. Data are represented as percent cell inhibition of samples relative to the non-toxic control, where the maximum toxicity is 100% as verified by assaying cytotoxic copper sulfate. Error bars represent standard deviation of three technical replicates.

2.9.2 Yeast Estrogen Screen (YES)

Estrogenic activity of samples is measured by YES using recombinant *Saccharomyces cerevisiae* yeast containing the human estrogen receptor (Routledge and Sumpter 1996, Routledge and Sumpter 1997). When an estrogen molecule in the sample binds to the receptor, a reporter gene induces synthesis of an enzyme that changes the color of a chromophore in the media. After correcting for differences in turbidity, estrogen induction is expressed as the induction of response relative to the maximum response (=100%) of the positive control estrogen compound, 17β-estradiol. The estrogenic activity for each sample is reported as equivalent of 17β-estradiol (EEQ) (Linden, et al. 2015). Error bars represent standard deviation of three technical replicates. Increases in estrogenic activity would indicate the formation of potentially toxic compounds.

2.9.3 Ames II Mutagenicity Assay (AMES)

The Ames II assay is a reverse mutation fluctuation assay that utilizes *Salmonella typhimurium* to detect genomic point mutations frame shift (by TA98 strain) or base pair substitution (by TAMIX mixture of six strains) (Kamber, et al. 2009, Mortelmans and Zeiger 2000). Mutagenic samples cause these point mutations to reverse, enabling revertant cells to survive and be enumerated. Samples are assayed alone, or with S9 enzyme to determine mutagenicity of abiotic degradation products. Samples were 0.45 µm filtered and concentrated 50X by SPE using HLB columns prior to analysis. Mutagenicity is expressed as the percent reversions compared to the maximum response of mutagenic positive controls (PC) 2-aminoanthracene, 4-nitroquinoline, and 2-nitrofluorene. If the number of revertant wells counted is at least twice the number of revertant well in the blank (control), then that concentration of chemical is said to be genotoxic. If the number or revertant wells decreases after reaching a maximum, the cells are said to be cytotoxic (Linden, et al. 2015).

3 Results

The following sections summarize the bench-testing results for the AOP evaluation.

3.1 Source Water Quality

The following sections summarize the background source water quality for samples used in the bench-scale testing.

3.1.1 Well Water – NH-37

The source water for the bench-scale testing was raw water collected from Well NH-37. Water was collected and sent by 2-day air to the University of Colorado for testing. While the AOP treatment facility will treat a blend of wells within the North Hollywood West Wellfield, water was only collected from well NH-37, because modeling predicts this well will have the highest 1,4-dioxane concentration of the remediation wells. Historical concentrations for the wellfield are shown in Table 3-1. Water quality analyzed before (by LADWP) and after (by University of Colorado) shipment are shown in Table 3-2. Two water samples were collected (2016 and 2017). The second water sample was collected to expand the MP testing to achieve higher log reductions. Figure 3-1 presents the UV absorbance scans for both samples.

Table 3-1. Historical Operating Well Water Quality

Well	1,4-Dioxane (µg/L)[1]	Alkalinity (mg/L as $CaCO_3$)	Nitrate (mg/L as N)	TOC (mg/L)	pH (S.U.)
		Avg (Max) [2000 – 2016]			
NH-34	1.62	209 (214)	3.5 (7.3)	0.46 (0.63)	7.6 (7.7)
NH-37	11.8	209 (234)	3.1 (7.7)	0.41 (0.76)	7.7 (7.8)
NH-45	1.85	210 (218)	2.4 (4.2)	0.45 (0.68)	7.8 (8.3)

[1] 1,4-dioxane data from March 2016

Table 3-2. 2016 NH-37 Raw Water Quality

Constituent	Unit	LADWP Laboratory	University of Colorado Laboratory	
			2016	2017
1,4-Dioxane	µg/L	15.9	14.2	<15
TCE	µg/L	13.6	10.7	<0.03
1,1-DCA	µg/L	0.662	N/A	N/A
1,1-DCE	µg/L	1.49	0.285	<0.08
1,2,3-TCP	µg/L	< 0.5	<0.03	1.8
Alkalinity	mg/L $CaCO_3$	253	209	170
Nitrite	mg/L as N	< 0.005	0.01	<0.003
Nitrate	mg/L as N	5.95	5.95	1.37
pH	S.U.	7.34	N/A	N/A
TOC	mg/L	N/A	0.64	0.47
TTHM	µg/L	0.572	N/A	N/A
Turbidity	NTU	0.10	N/A	N/A
UVT_{254}	%	N/A	97.5	97.3

*N/A means the constituent was not tested.

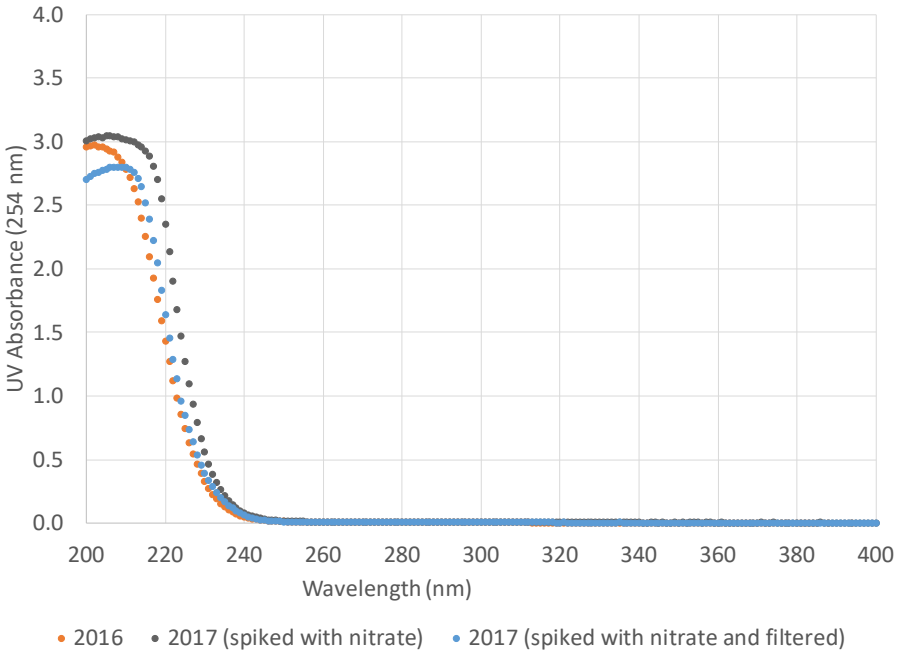

Figure 3-1. UV Absorbance Spectrum of Well NH-37

3.1.2 Surface Water – NHPS

Surface water taken from LADWP's NHPS (distribution system water) intended for SDS testing was analyzed by LADWP; relevant results are shown in Table 3-3.

Table 3-3. NHPS Water Quality

Constituent	Unit	LADWP Laboratory
TCE	µg/L	< 0.5
1,1-DCA	µg/L	< 0.5
1,1-DCE	µg/L	< 0.5
Ammonia (free)	mg/L as N	0.114
Ammonia (total)	mg/L as N	0.623
Chlorine (total)	mg/L	2.26
HAA (total)	µg/L	8.74
HAA5	µg/L	6.1
Turbidity	NTU	18.31

3.1.3 Hydroxyl Radical Scavenging Demand

The pH, absorbance (at 254 nm), alkalinity, and TOC of the 2016 water samples are shown in Table 3-4.

In most natural waters, hydroxyl radicals are scavenged mainly by two constituents: carbonates ($k_{HO,HCO3}$ = 8.5 x 10^6 M^{-1} s^{-1} and $k_{HO,CO3}$ = 3.9 x 10^8 M^{-1} s^{-1}) and TOC ($k_{HO,TOC}$ = 2.5 X 10^4 M^{-1} s^{-1}) (Buxton, et al. 1998). While hydrogen peroxide (~8 mg/L) was added to promote formation of hydroxyl radicals, it is also capable of scavenging radicals ($k_{HO,H2O2}$ = 2.7 x 10^7 M^{-1} s^{-1}). Given their established rate constants, the relative contribution of each water quality parameter to the overall scavenging demand can be calculated (Table 3-4).

Hydrogen peroxide (H_2O_2) concentration was determined prior to UV exposure ([H_2O_2] initial), shown in Table 3-4. Since H_2O_2 has a relatively low molar absorption coefficient at 254nm, only a small fraction is consumed during UV exposure. Hydrogen peroxide concentrations were measured using the molybdate-activated iodide method. This method utilizes a color change that occurs when H_2O_2 reacts with potassium iodide (KI) in a buffered solution containing ammonium molybdate, forming I_3^- which can be detected spectrophotometrically at 352 nm (Klassen, 1994).

Figure 3-2 presents the measured degradation of pCBA in the water from Well NH-37 by LPHO UV/peroxide with ~8 mg/L H_2O_2, and the theoretical decay of pCBA (term "model"). The modeled value was calculated using the measured water quality, associated scavenging rates from Table 3-4, and a steady-state hydroxyl radical model previously described by Rosenfeldt and Linden (2007). This model incorporates the water quality parameters and the spectral characteristics of the LPHO UV setup.

Table 3-4. Hydroxyl Radical Scavenging Demand Analysis (2016 Water Sample)

Constituent		Test 1	Test 2
pH		7.6	7.6
Alkalinity as $CaCO_3$		209	209
TOC (mg/L)		0.45	0.45
UV abs $_{254nm}$ (cm^{-1}) (Transmittance)		0.01874 (95.8%)	0.01874 (95.8%)
[H_2O_2] initial (mg/L)		8.10	7.58
Scavenger [S]	**$k_{OH/S}$ (M^{-1} s^{-1})**	**$k_{HO,S}$[S] (s^{-1})**	
TOC	2.50×10^4	1.13×10^4	1.13×10^4
HCO_3^-	8.50×10^6	1.77×10^4	1.77×10^4
CO_3^{2-}	3.90×10^8	1.62×10^3	1.62×10^3
H_2O_2	2.70×10^7	6.43×10^3	6.02×10^3
pCBA	5.00×10^9	1.65×10^4	1.67×10^4
	$\Sigma k_{OH,S}$[S] (s^{-1})	5.35×10^4	5.32×10^4
	$\Sigma k_{OH,S}$[S-pCBA] (s^{-1})	3.70×10^4	3.66×10^4

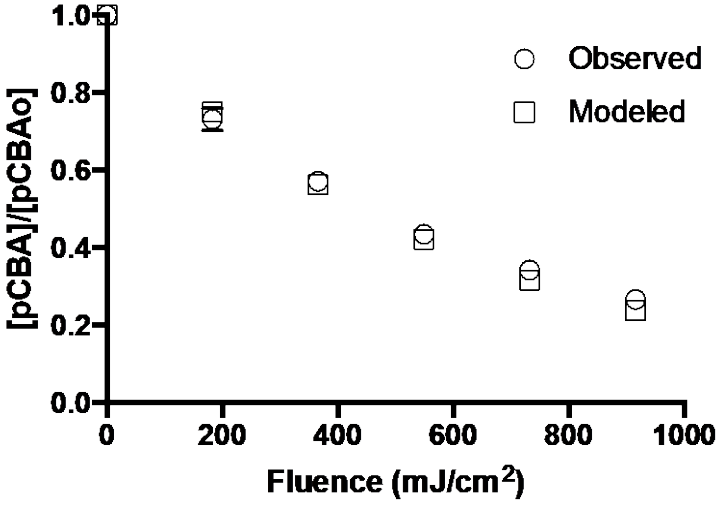

Figure 3-2. Modelled degradation of pCBA in Well NH-37 for Test 1 and 2, with 8 mg/L H2O2. Error bars represent one standard deviation.

Table 3-5 summarizes the experimental and theoretical HO• concentration and scavenging rates of the water samples. Refer to Appendix B of this document for more details on the scavenging methods and results.

Table 3-5. Comparison of Modelled and Experimentally Determined Hydroxyl Radical Concentrations and Scavenging Rates

Constituent	Test 1	Test 2
$[H_2O_2]$ mg/L	8.10	7.58
Scavenging Rate	**$k_{OH}[S]$ (s^{-1})**	
$k_{OH}[S]$, TOT-Model	3.70×10^{4}	3.66×10^{4}
$k_{OH}[S]$, TOT-Exp.	3.78×10^{4}	3.79×10^{4}
Steady State HO• Concentration	**$[OH]_{ss}$(M)**	
$[OH]_{ss}$ – Model	2.52×10^{-13}	2.38×10^{-13}
$[OH]_{ss}$ – Exp.	2.21×10^{-13}	2.18×10^{-13}

3.2 Treatment Performance

Figure 3-3 through Figure 3-15 show the results for 1,4-dioxane, TCE, and 1,1-DCE log reduction for LPHO and MP UV/peroxide treatment. LPHO was shown to be effective for 1,4-dioxane reduction and achieved the project goal of a 1.9-log reduction for 1,4-dioxane. TCE and 1,1-DCE concentrations were also simultaneously reduced at rates higher than 1,4-dioxane. 1,1-DCA was inadvertently spiked in place

of 1,1-DCE for the 8 mg/L hydrogen peroxide tests. 1,1-DCA showed minimal removal, as would be expected based on its lower hydroxyl radical rate constant (Figure 3-14 and Table 3-6). 1,2,3-TCP was also monitored but showed no reduction with either LPHO or MP UV/peroxide (Figure 3-14).

MP was less effective for 1,4-dioxane and VOC removal (Figure 3-6 and Figure 3-7). Once the MP UV doses are weighted to hydrogen peroxide, the required doses should be identical to the LPHO UV doses, if no other water quality changes occur. However, even after adjusting to a hydrogen peroxide weighted UV dose, the MP UV/peroxide results showed lower removals than the LPHO results. This indicates a change in hydroxyl radical scavenging demand with the MP UV/peroxide tests as the hydroxyl radical formation would be similar at a given LPHO or peroxide weighted MP UV dose. The MP UV lamps emit wavelengths below 240 nm, which is where hydrogen peroxide has a high absorbance. The peroxide absorbance and MP emission spectrum allows for the potential for more efficient hydroxyl radical formation. In water containing nitrate, the water can have a high UV absorbance below 240 nm, which reduces the overall efficiency. NH-37 has high UV absorbance in the wavelengths absorbed by hydrogen peroxide, due to background nitrate concentration (Figure 3-16). The absorbance difference is accounted for in the peroxide weighted dose calculation. The low wavelengths emitted by MP UV lamps will also photolyze nitrate into nitrite (Section 3.3.2) and potentially other nitrogen radicals. Nitrite is a strong hydroxyl radical scavenger (Table 3-6). The formation of additional nitrogen radicals may off-set the increased hydroxyl radical scavenging demand from nitrite. However, the MP UV/peroxide results indicate that additional hydroxyl radical scavenging was occurring in excess of any additional nitrogen radical formation and reaction, which decreased the overall efficiency of the process. Nitrate photolysis was negligible with LPHO UV lamps.

Additional testing and modeling were completed to evaluate the impact of nitrate on MP UV AOP (Appendix A). The testing examined the impact of hydroxyl radical production on the following parameters:

- nitrate concentration
- water depth
- hydrogen peroxide concentration
- background water matrix (lab water vs groundwater)

With no peroxide present, higher nitrate concentrations resulted in higher formation of radicals (hydroxyl or nitrogen radicals). In the present of hydrogen peroxide, the experimental and model results indicated that nitrite detrimentally affects MP UV AOP performance. This effect can be ascribed to the nitrite formed during nitrate photolysis. Elevated nitrate will likely be detrimental to MP UV AOP, despite the additional hydroxyl radicals that are produced. The data indicates that LPHO UV AOP should not suffer this effect nearly as much. The results showed a net neutral effect of nitrate addition with LPHO UV AOP.

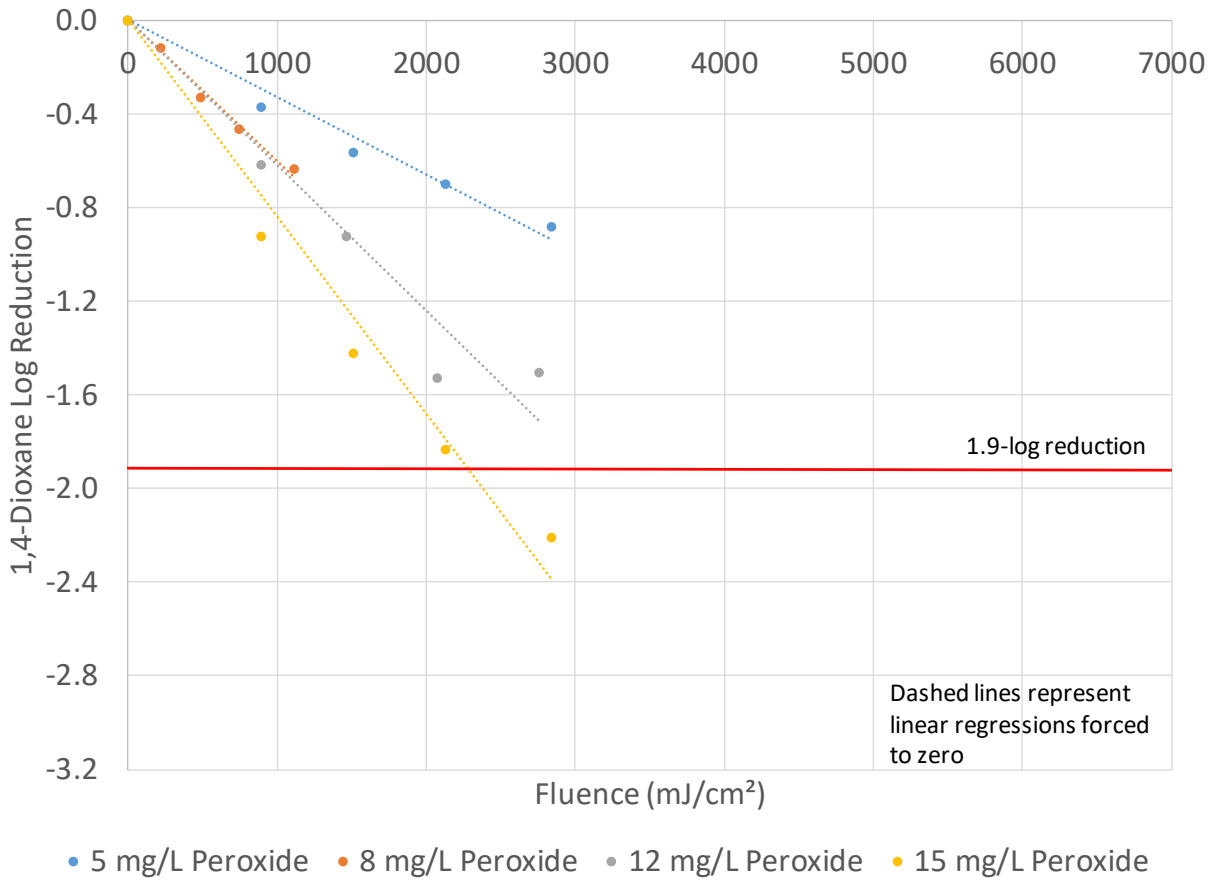

Figure 3-3. 1,4-Dioxane Log Reduction by LPHO UV/Peroxide Treatment

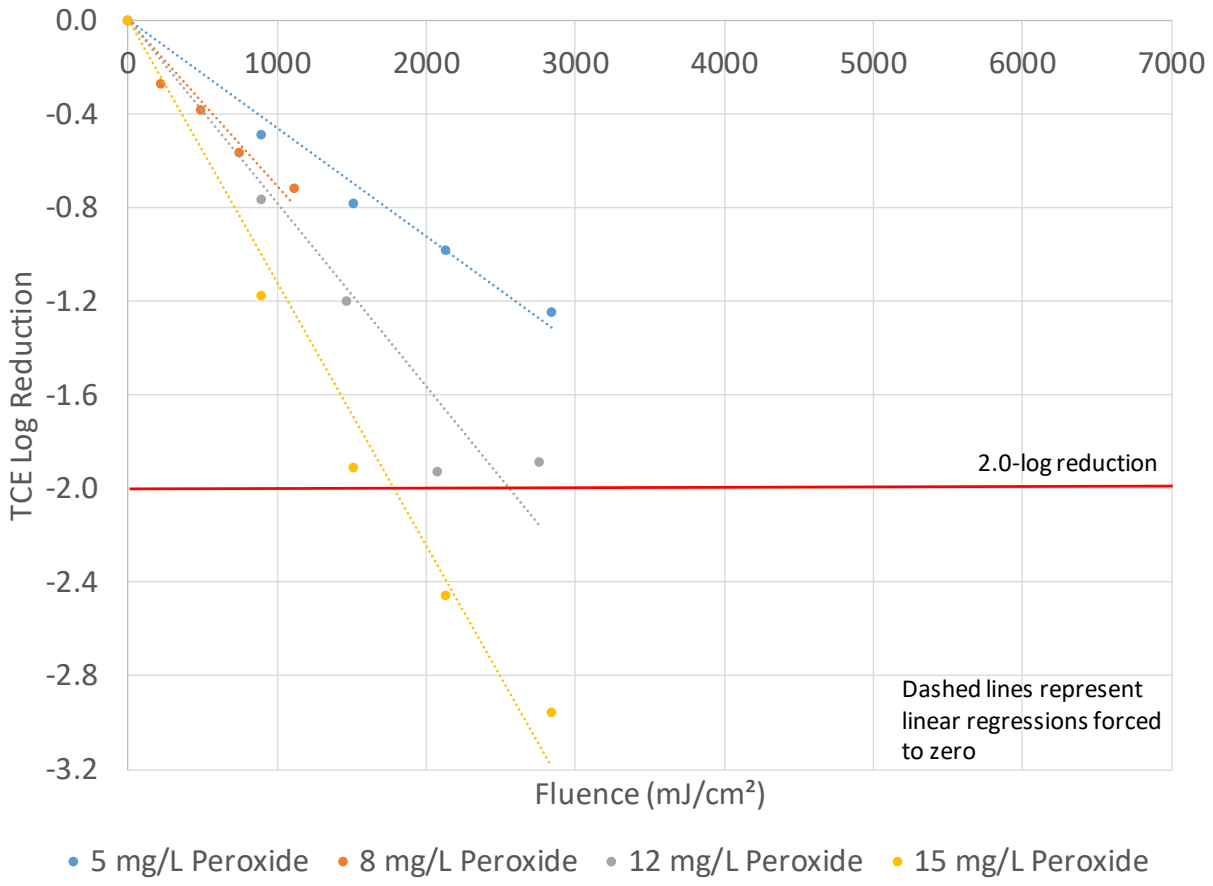

Figure 3-4. TCE Log Reduction by LPHO UV/Peroxide Treatment

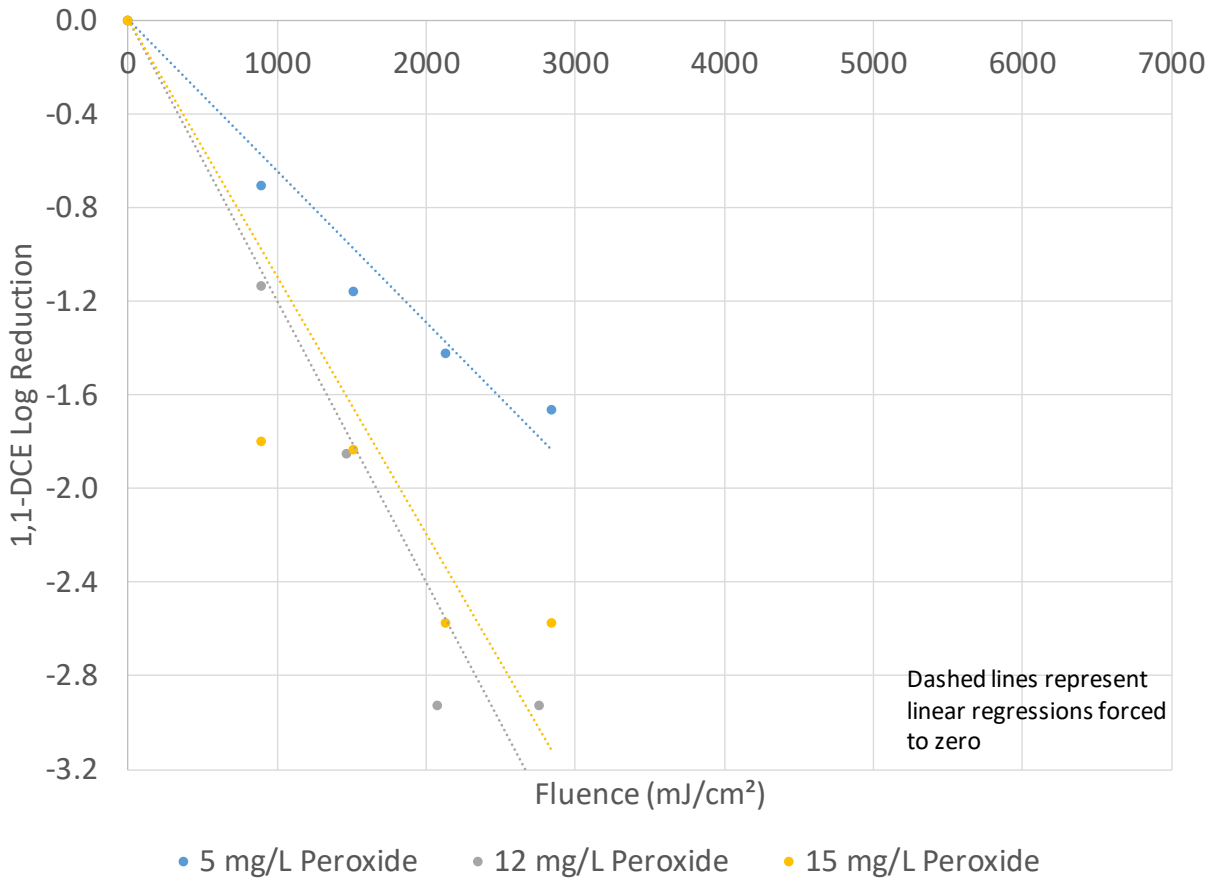

Figure 3-5. 1,1-DCE Log Reduction by LPHO UV/Peroxide Treatment

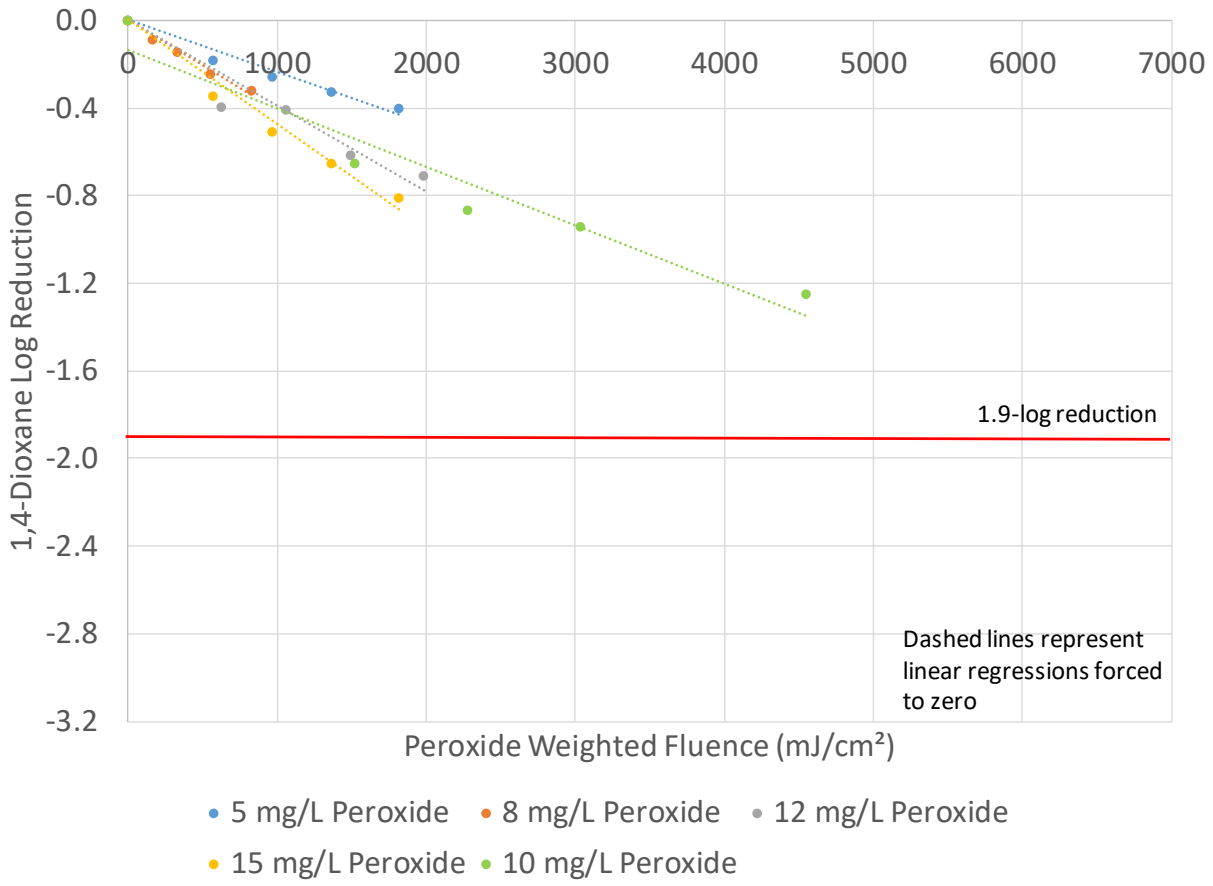

Figure 3-6. 2016 1,4-Dioxane Log Reduction by MP UV/Peroxide Treatment

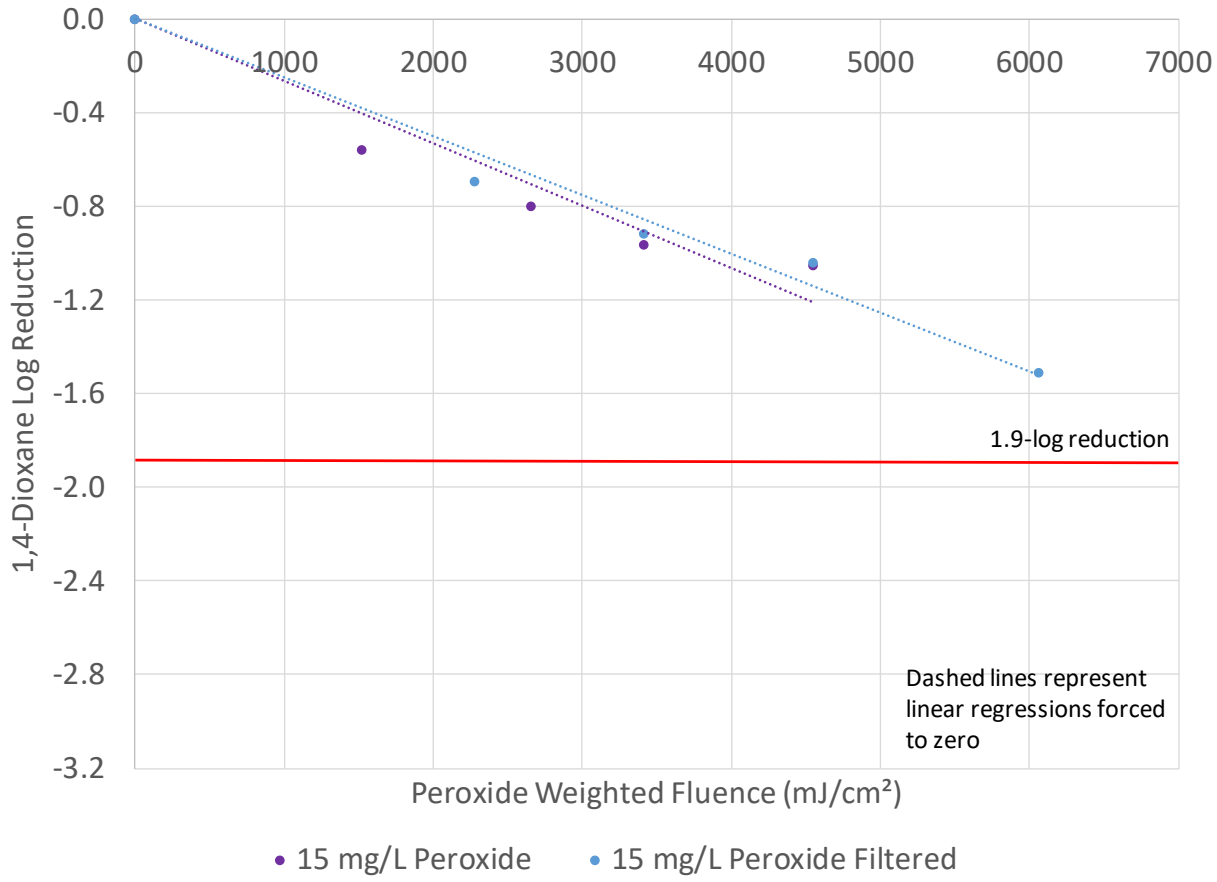

Figure 3-7. 2017 1,4-Dioxane Log Reduction by MP UV/Peroxide Treatment

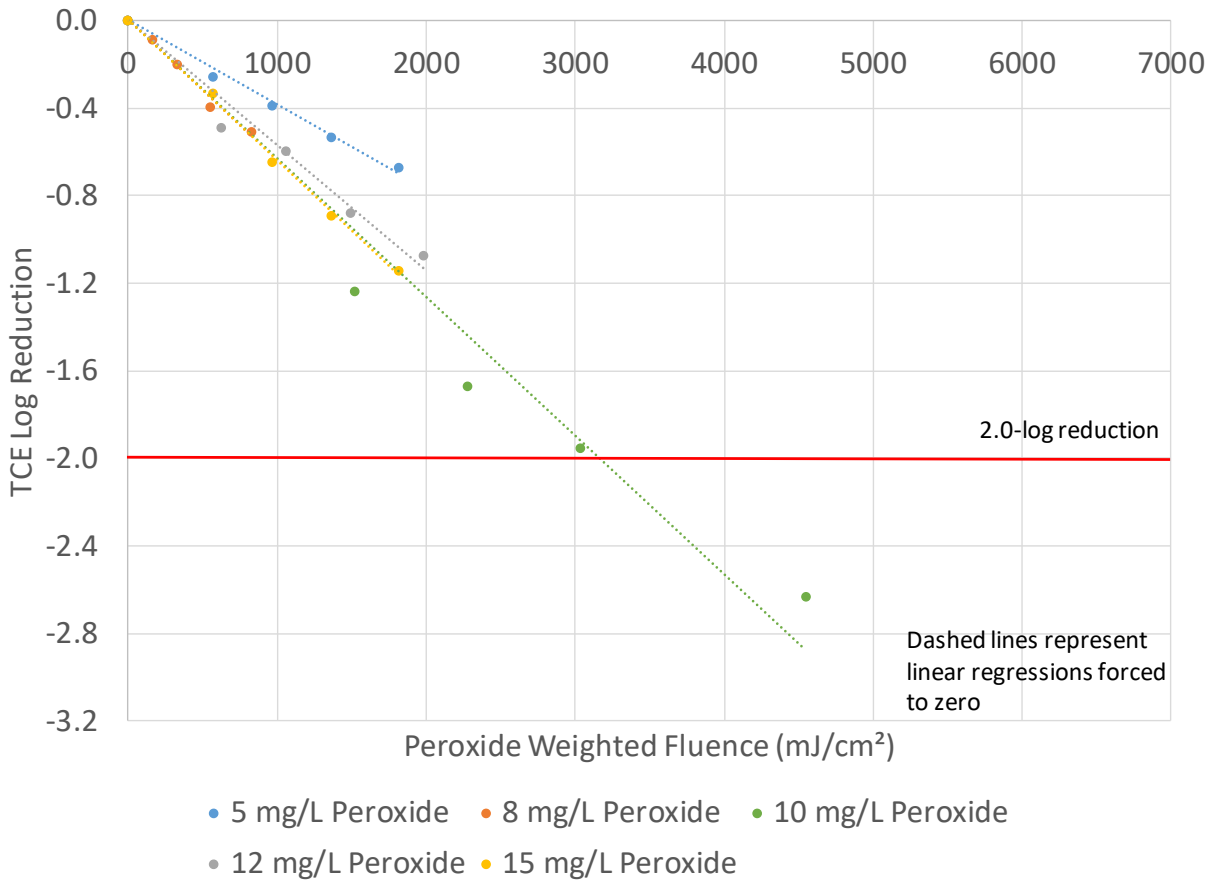

Figure 3-8. 2016 TCE Log Reduction by MP UV/Peroxide Treatment

In general, at a given UV dose, the target contaminant log reduction increases with increasing hydrogen peroxide doses. However, the increase is not linear due to the added hydroxyl radical scavenging demand of the hydrogen peroxide.

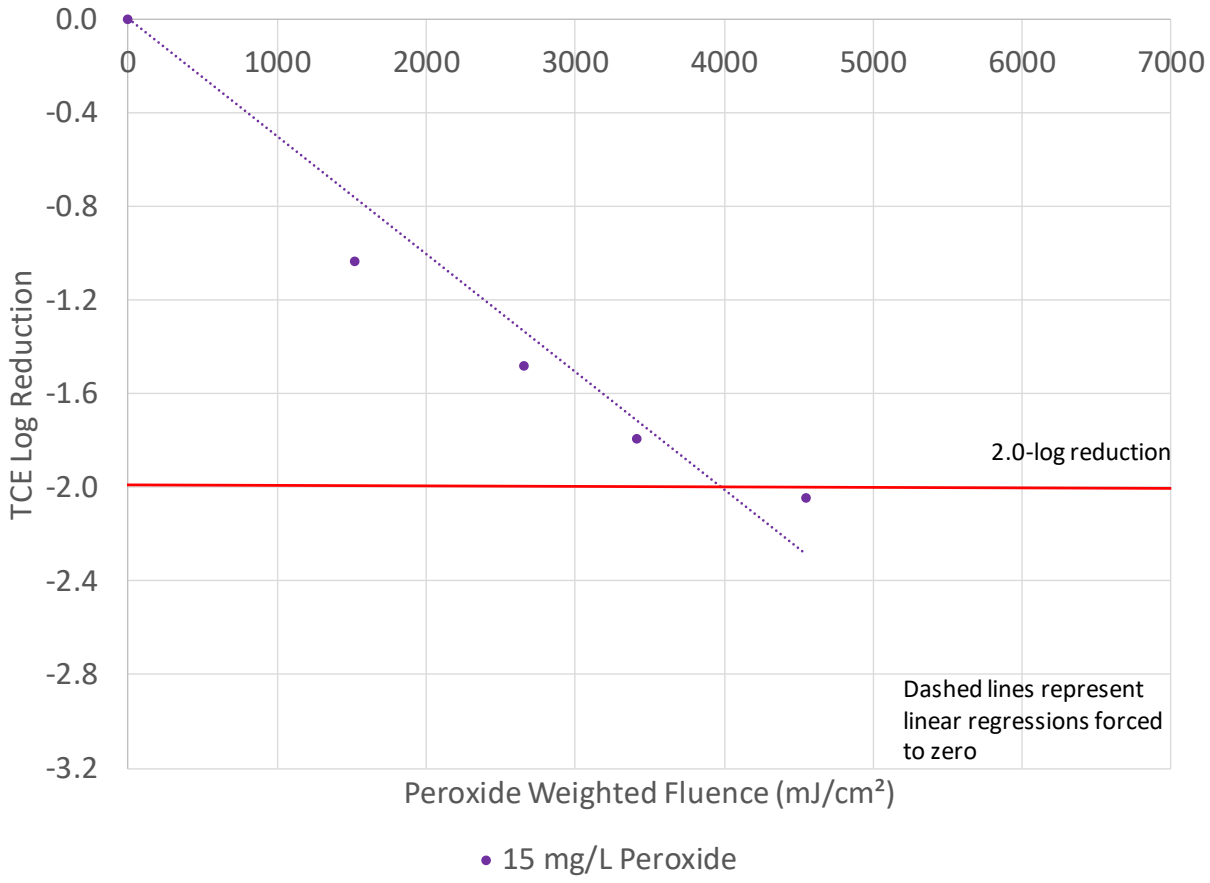

Figure 3-9. 2017 TCE Reduction by MP UV/Peroxide Treatment

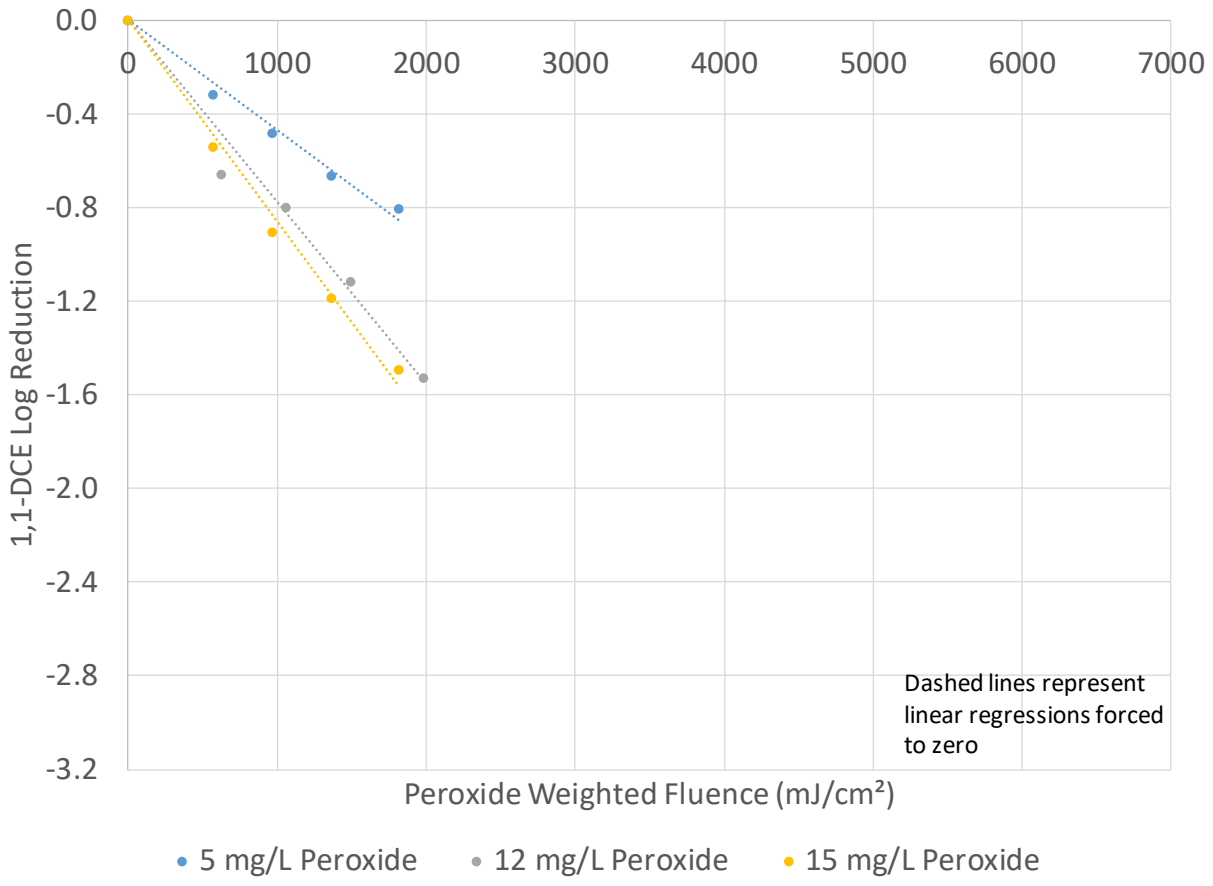

Figure 3-10. 2016 1,1-DCE Log Removals by MP UV/Peroxide Treatment

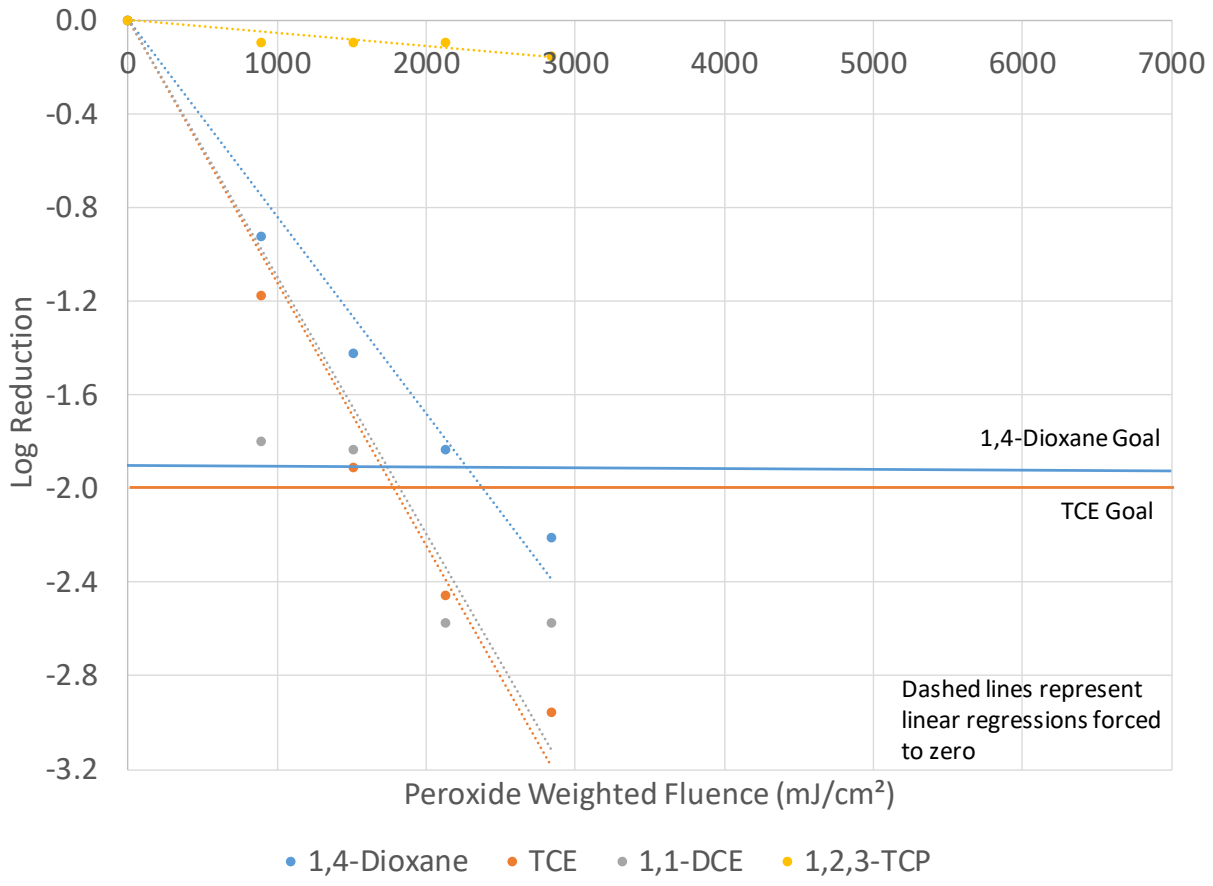

Figure 3-11. Comparison of Contaminant Removal by LPHO UV/Peroxide Treatment at 15 mg/L Hydrogen Peroxide (2016)

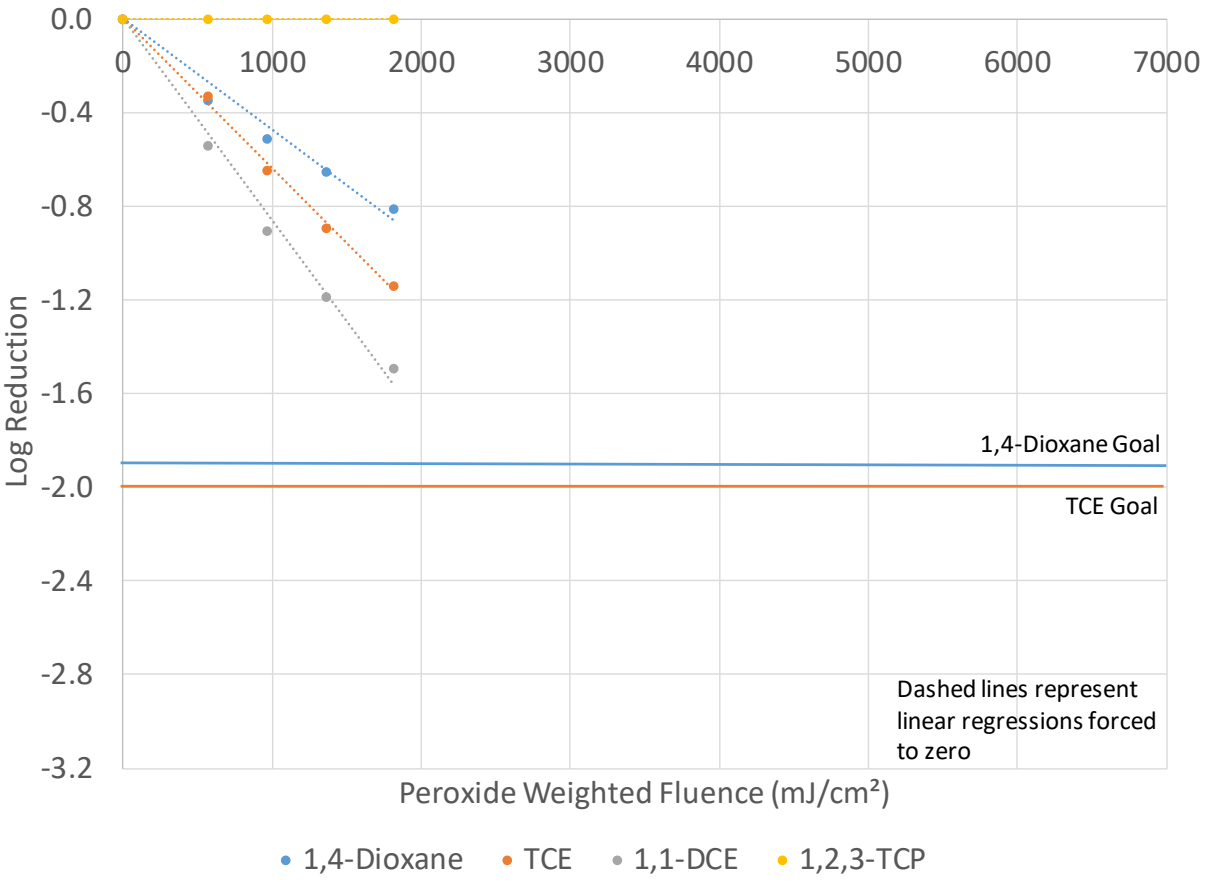

Figure 3-12. Comparison of Contaminant Removal by MP UV/Peroxide Treatment at 15 mg/L Hydrogen Peroxide (2016)

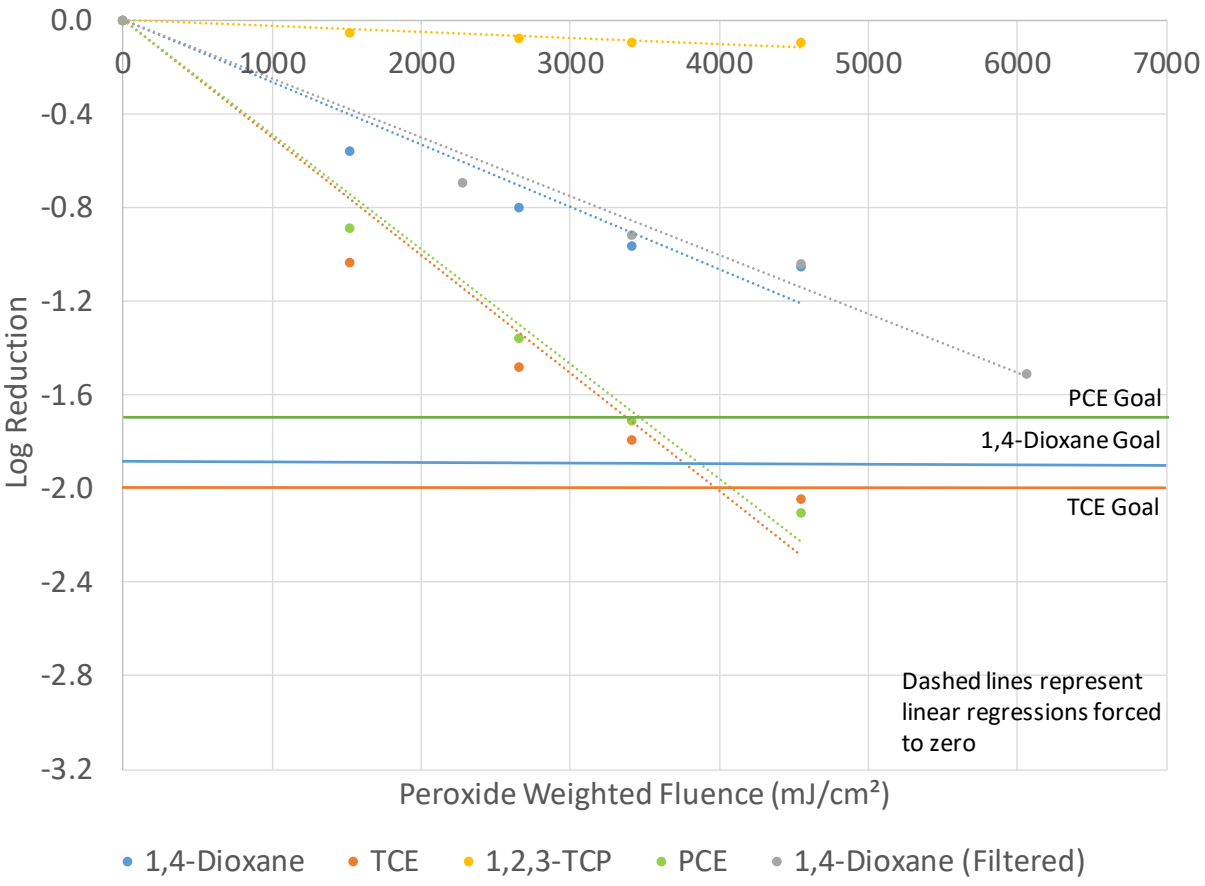

Figure 3-13. Comparison of Contaminant Removal by MP UV/Peroxide Treatment at 15 mg/L Hydrogen Peroxide (2017)

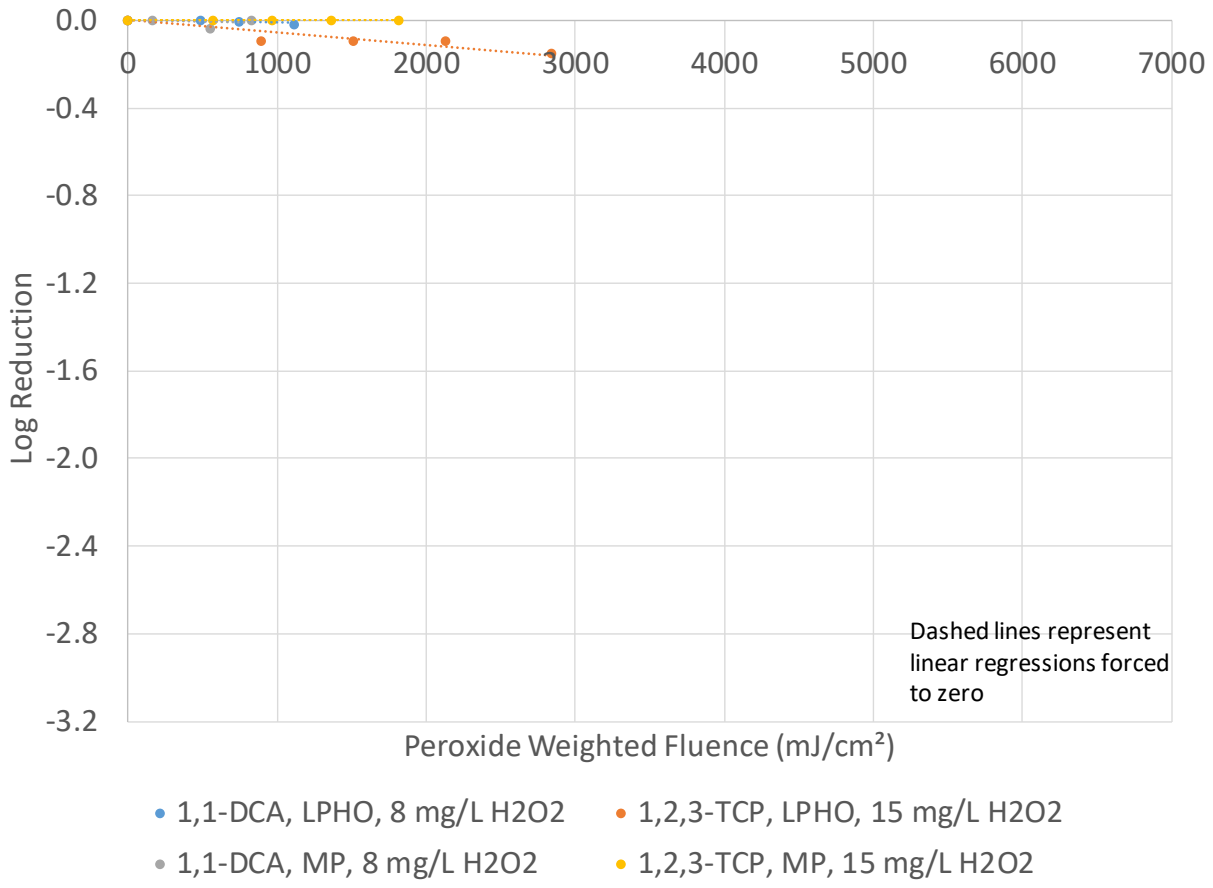

Figure 3-14. 1,1-DCA and 1,2,3-TCP Log Removals by LPHO and MP UV/Peroxide Treatment

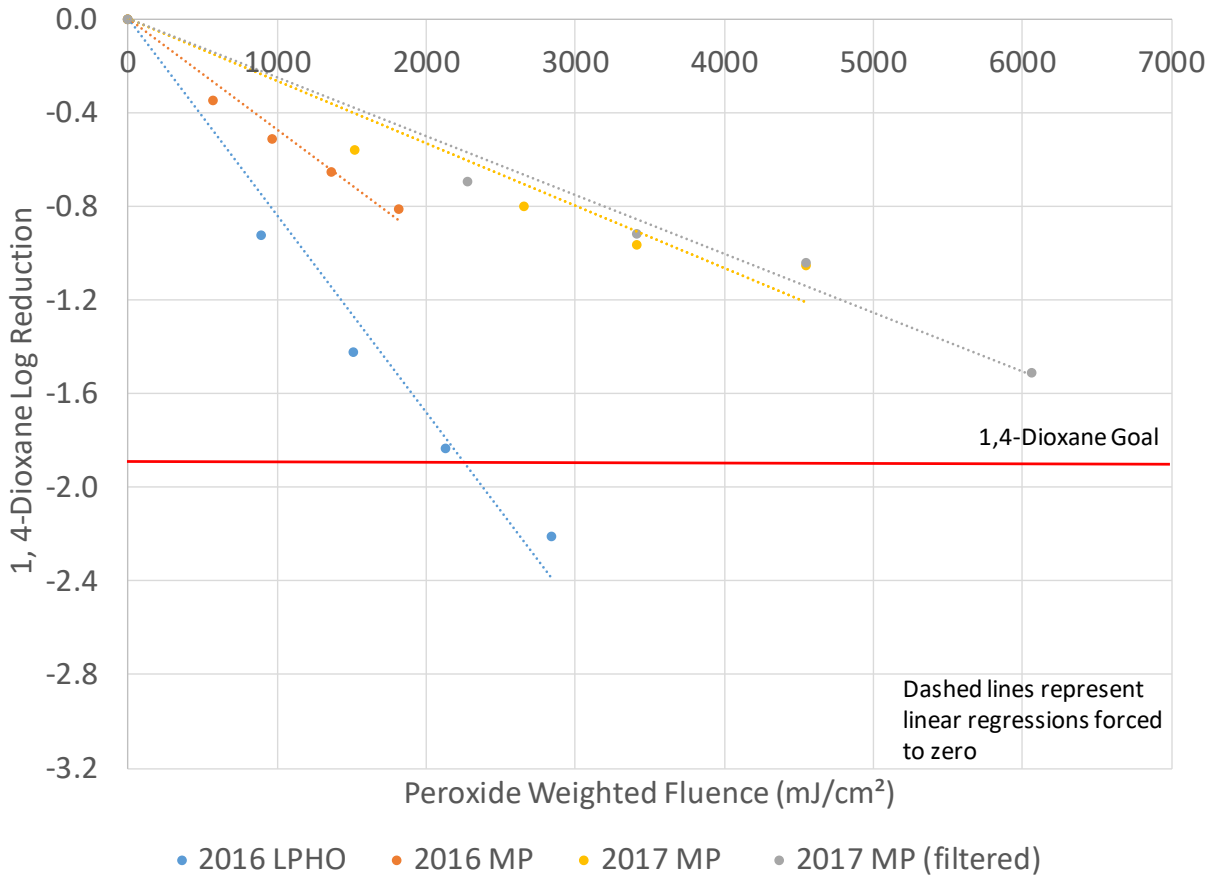

Figure 3-15. LPHO and MP UV/Peroxide 1,4-Dioxane Log Reduction at 15 mg/L Hydrogen Peroxide

Table 3-6. Hydroxyl Radical Rate Constants

Compound	Hydroxyl Radical Rate Constant ($L\ mol^{-1}\ s^{-1}$)
Hydrogen Peroxide	2.7×10^{7}
1,4-Dioxane	$2.3 - 3.1 \times 10^{9}$
TCE	$2.9 – 4.3 \times 10^{9}$
PCE	$2.0 – 2.8 \times 10^{9}$
1,1-DCE	6.8×10^{9}
Cis-1,2-DCE	3.8×10^{9}
1,1-DCA	1.3×10^{8}
Nitrite	1.1×10^{10}

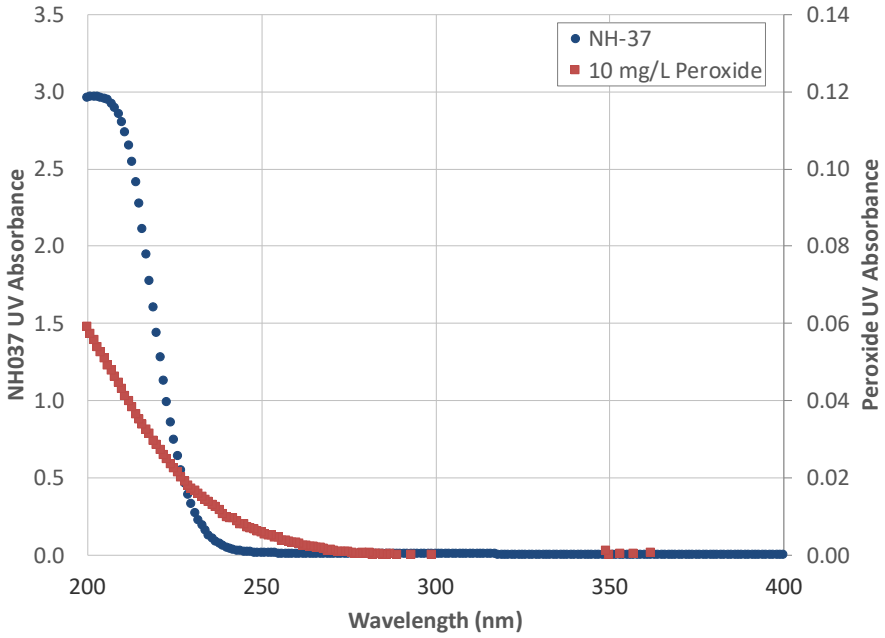

Figure 3-16. NH-37 and Hydrogen Peroxide UV Absorbance

3.3 Treatment Byproducts

The following sections summarize the AOP byproducts that were evaluated as part of the bench-scale testing.

3.3.1 Regulated DBPs

AOPs are known to increase the formation potential for regulated DBPs (i.e., TTHMs and HAA5) after the addition of chlorine. SDS testing was completed to evaluate changes in DBP formation potential after UV AOP treatment.

Figure 3-17 through Figure 3-22 show the results of the SDS testing for NH-37 1,4-dioxane and VOC spiked well water. The raw water was used as the control and the UV AOP treated water was tested with a variety of LPHO and MP dose and hydrogen peroxide doses. Figure 3-21 and Figure 3-22 show SDS results for NH-37 well water blended with NHPS surface water. The results show an increase in TTHM and HAA5 formation after UV AOP treatment for both the NH-37 well water and the blended water. However, TTHM and HAA5 formation was well below the regulatory limit for both waters. TTHM concentrations ranged from 17 to 26 μg/L for the AOP treated water compared to 6 to 8 μg/L for the raw water (Figure 3-17 and Figure 3-18). HAA5 increases were lower, with concentrations ranging from 4 to 19 μg/L for the AOP treated water compared to 3 to 4 μg/L for the raw water (Figure 3-19 and Figure 3-20). As expected, the blended raw water control had higher DBP concentrations than the raw well water. However, TTHMs were similar in the AOP treated well water and blended waters (Figure 3-21). HAA5 concentrations were slightly higher in the blended water but this is likely due to the DBP precursors in the raw water (Figure 3-22).

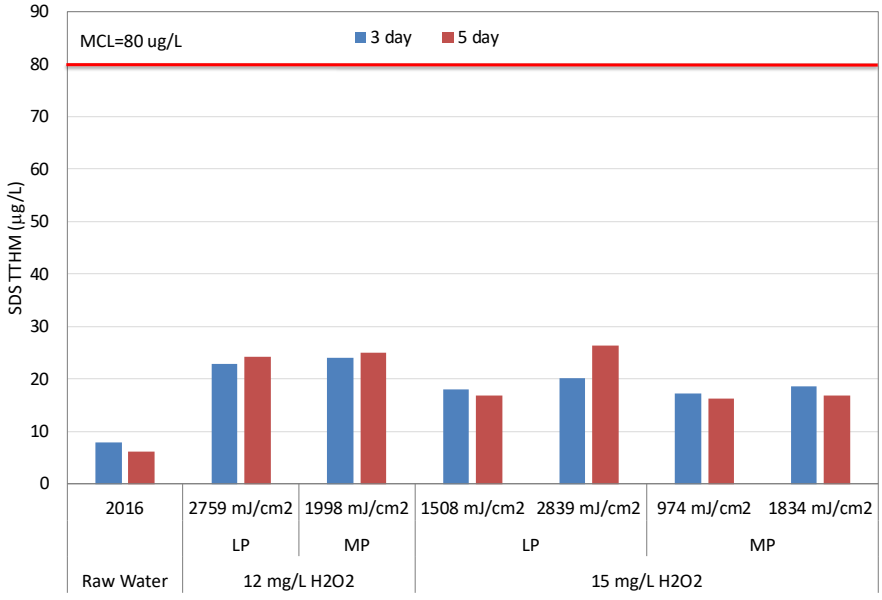

Figure 3-17. 2016 NH-37 TTHM SDS Results

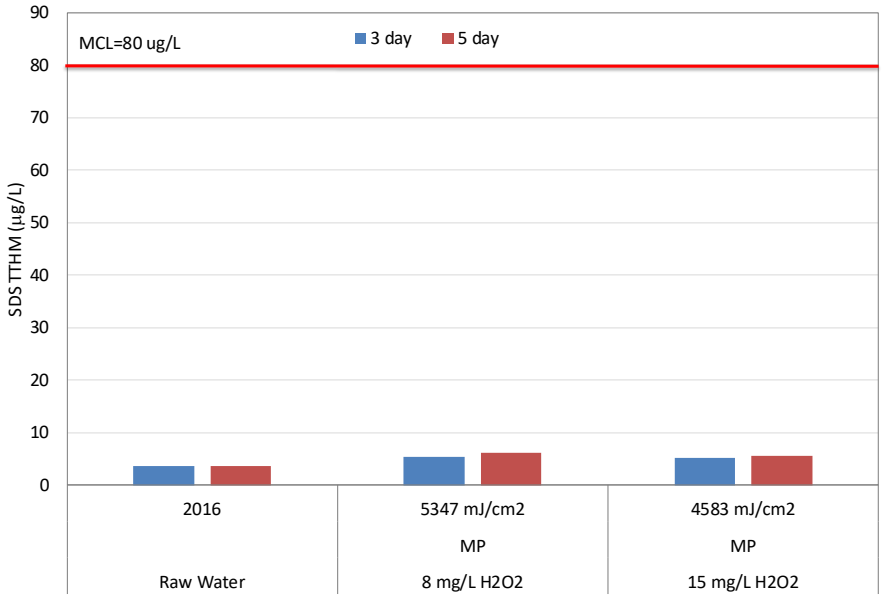

Figure 3-18. 2017 NH-37 TTHM SDS Results

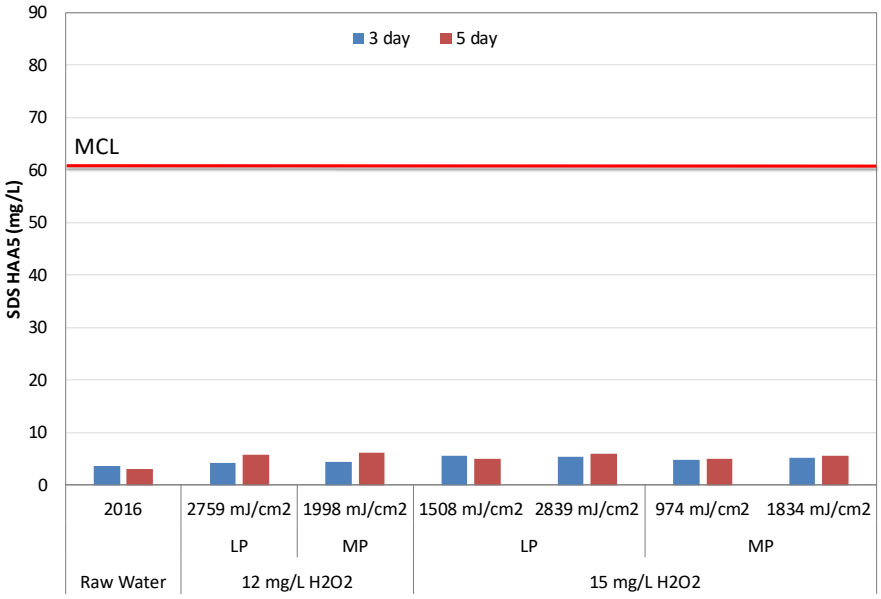

Figure 3-19. 2016 NH-37 HAA5 SDS Results

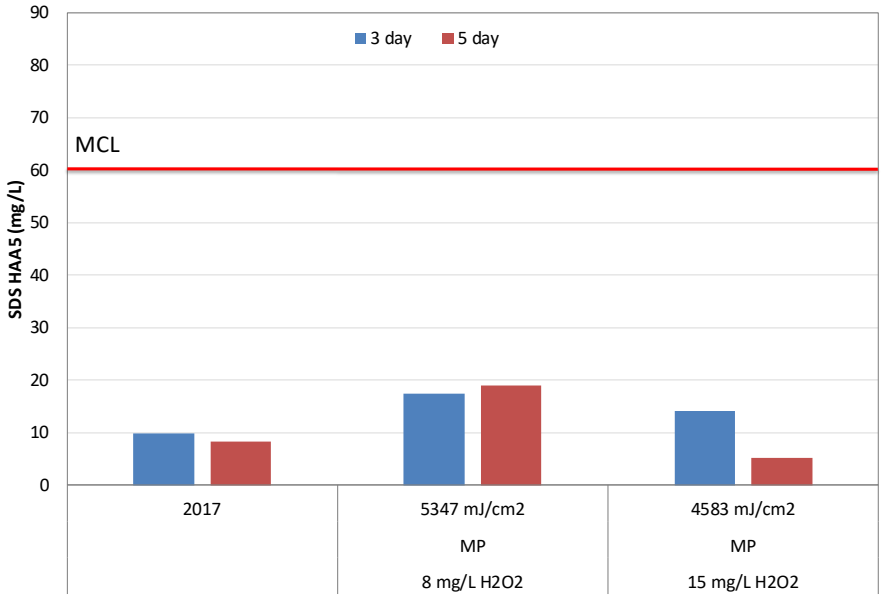

Figure 3-20. 2017 NH-37 HAA5 SDS Results

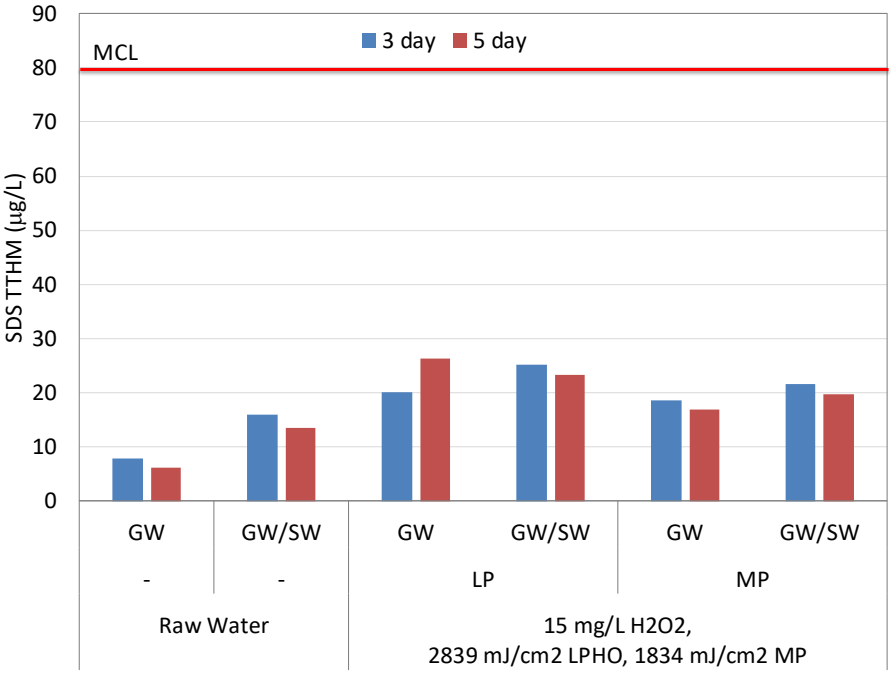

Figure 3-21. 2016 NH-37 (GW) and NHPS Surface Water (SW) Blended TTHM SDS Results

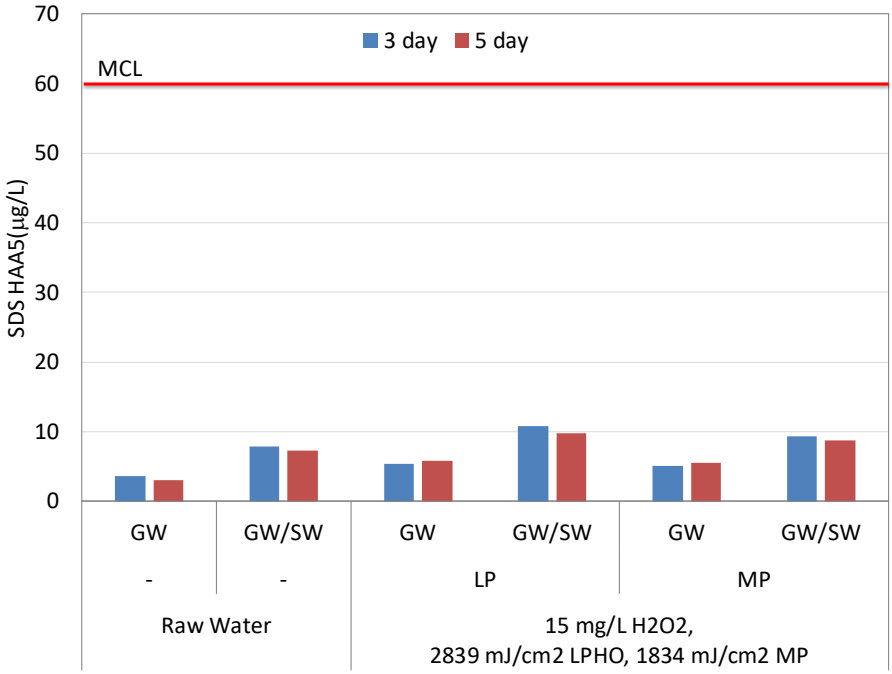

Figure 3-22. 2016 NH-37 (GW) and NHPS Surface Water (SW) Blended HAA5 SDS Results

The LPHO and MP samples were both exposed to the same unweighted UV dose (i.e., 1,700 or 3,200 mJ/cm^2). When the unweighted MP UV dose was converted to a peroxide weighted dose, the resulting MP peroxide weighted dose was lower than for the LPHO UV dose (e.g., 2839 vs 1834 mJ/cm^2). In addition, due to MP being less effective than LPHO (Figure 3-3 to Figure 3-10), the treatment level and corresponding potential for transformation of background organics would have been lower for the MP tests, which limits the ability to directly compare the LPHO and MP DBP results. However, despite the measured increases in DBP concentrations, TTHM and HAA5 concentrations were well below the regulatory limits for both lamp technologies.

3.3.2 Nitrite

Nitrite is a known by-product of the photolysis of nitrate with MP UV lamps. Nitrite formation is a function of UV dose and was measured up to 0.5 mg/L as N in NH-37 well water after MP UV AOP treatment (Figure 3-23). The actual nitrite formation during full-scale operation may vary compared to the bench-scale evaluations. Nitrate photolysis is a function of the presence of UV wavelengths below 240 nm, which is a function of the low wavelength output of the UV lamps, applied UV dose, UV absorbance of the lamp sleeve and water, nitrate concentration, and lamp spacing.

Nitrite formation was measured in all LPHO tests. The LPHO tests had negligible formation with concentrations less than 0.04 mg/L as N.

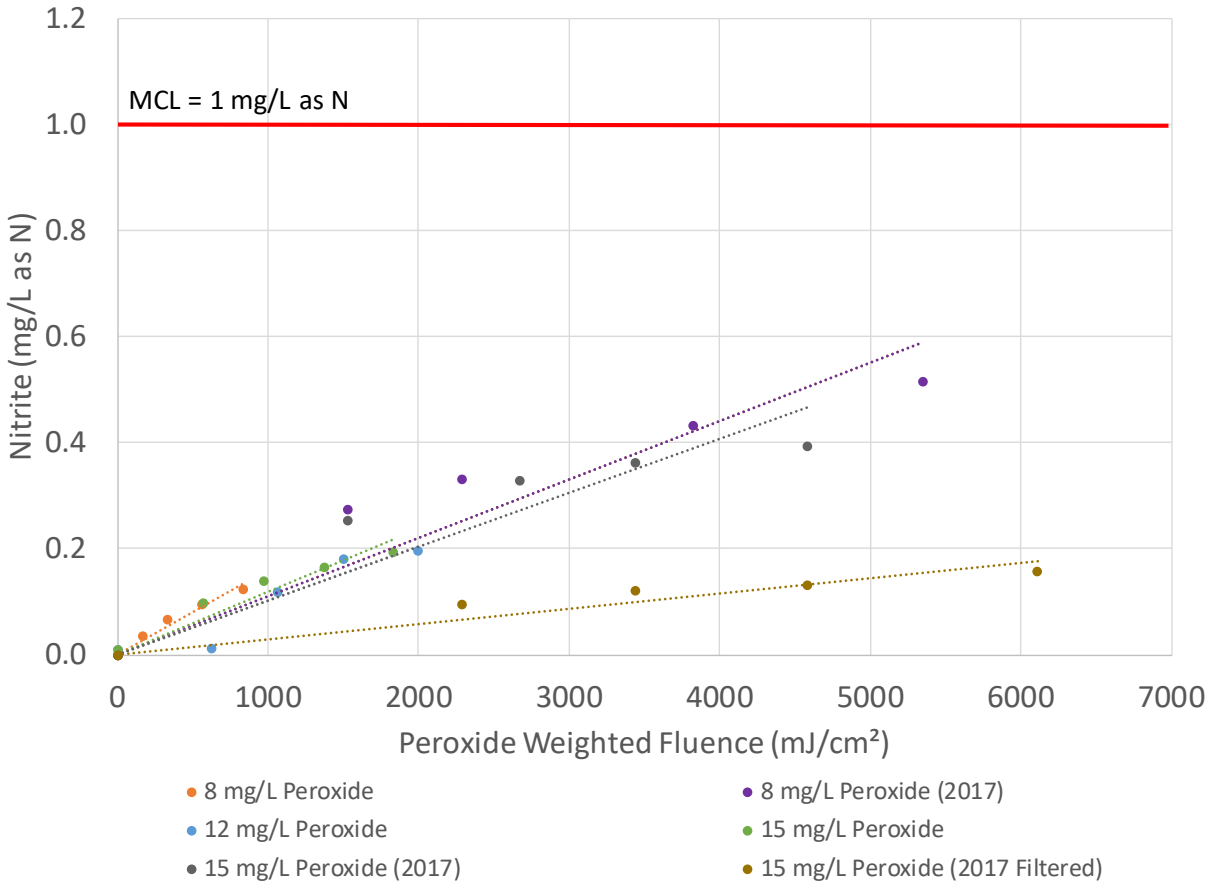

Figure 3-23. Nitrite Formation with MP UV/peroxide

3.3.3 AOC

No increases in AOC were measured after LPHO or MP UV AOP (Table 3-7). All AOC samples after treatment were below the method detection limit of 10 µg/L. UV AOP is not expected to reduce AOC. Linden et al (2015) showed no significant changes to AOC after LPHP UV AOP treatment and a slight increase with MP UV AOP. AOC formation is site-specific and depends on the organic material present. It is unknown why AOC was less than the detection limit after UV AOP treatment of the NH-037 water.

Table 3-7. AOC Formation

	Peroxide Dose	UV Dose[1]	AOC
Raw	0 mg/L	0 mJ/cm^2	73.5 µg/L
LPHO	12 mg/L	1700 mJ/cm^2	<10 µg/L
		3200 mJ/cm^2	<10 µg/L
	15 mg/L	1700 mJ/cm^2	<10 µg/L
		3200 mJ/cm^2	<10 µg/L
MP	12 mg/L	1200 mJ/cm^2	<10 µg/L
		2300 mJ/cm^2	<10 µg/L
	15 mg/L	1200 mJ/cm^2	<10 µg/L
		2300 mJ/cm^2	<10 µg/L

[1] MP UV doses are weighted to hydrogen peroxide

3.3.4 Toxicity

Three bioassays were utilized to evaluate any potential changes in toxicity after AOP treatment. Testing was completed on a range of UV doses and hydrogen peroxide concentrations for both LPHO and MP UV AOP (Table 3-8 and

Table 3-9). These tests measured acute cellular toxicity, estrogenic activity, and mutagenic activity of samples via the bioluminescence inhibition assay (BLIA), yeast estrogen screen (YES), and Ames II mutagenicity assay (AMES), respectively. For AMES testing, samples were assayed after concentration by solid phase extraction (SPE).

Table 3-8. 2016 NH37 Toxicity Sample Description

Test Number	Description/ UV Lamp	1,4-dioxane and VOCs[2]	Peroxide (mg/L)	UV Dose[1] (mJ/cm^2)
NC	Negative Control (DI water)	-	0	0
1	Raw NH-037 Groundwater	-	0	0
2	Spiked NH-037 Groundwater	+	0	0
3	Spiked NH-037 Groundwater	+	15	0
4	LPHO UV	+	5	2843
5	LPHO UV	+	8	486
6	LPHO UV	+	8	1111
7	LPHO UV	+	12	1468
8	LPHO UV	+	12	2759
9	LPHO UV	+	15	2839
10	MP UV	+	5	1833
11	MP UV	+	8	335
12	MP UV	+	8	838
13	MP UV	+	12	1063
14	MP UV	+	12	1998
15	MP UV	+	15	1834
B	SPE Blank (50X SPE of DI Water)	-	0	0
PC	Positive Control (toxic)	-	0	0

[1] MP UV doses are weighted to hydrogen peroxide

[2] + indicates 1,4-dioxane and VOCs added/ - indicates no 1,4-dioxane and VOCs spiked

Table 3-9. 2017 Toxicity Sample Descriptions

Test Number	Description/ UV Lamp	VOCs	H_2O_2 (mg/L)	UV (mJ/cm²)[1]
NC	Negative Control (DI water)	-	0	0
1	Raw Groundwater	-	0	0
2	Spiked Groundwater	+	15	0
3	MP UV	+	15	2673
4	MP UV	+	15	4583
5	MP UV	+	8	2292
6	MP UV	+	8	5347

[1] MP UV doses are weighted to hydrogen peroxide

[2] + indicates VOCs added/ - indicates no VOCs present

3.3.4.1 Bioluminescence Inhibition Assay (BLIA)

Figure -3-24Figure -3-24 represents the data from the BLIA. All samples induced acute cytotoxicity by about 20%, but UV AOP treatment of the samples did not significantly impact this response. As shown in Figure -3-24, consolidated data from all samples indicated an initial induced luminescence that was greater than the negative control (NC), but luminescence for samples decreased more rapidly than for the NC. This greater initial luminescence of samples indicates that sample constituents increased respiration and luminescence greater than the NC (Figure 3-25). The assay compares the initial luminescence to luminescence at 15 and 30 min, so this steep decrease in luminescence resulted in the ~20% cytotoxic response that is observed. The waters likely contained a constituent that caused the cells to initially produce more light, which would indicate a nutrient source in the native water. However, as this nutrient source was consumed, the kinetic response indicates the presence of something inhibitory of respiration (cytotoxic), which could be the result of the nutrient source being consumed rather than the presence of a toxic substance. Furthermore, none of the treatments induced or decreased the assays response, indicating that no new inhibitory compounds were formed by treatment.

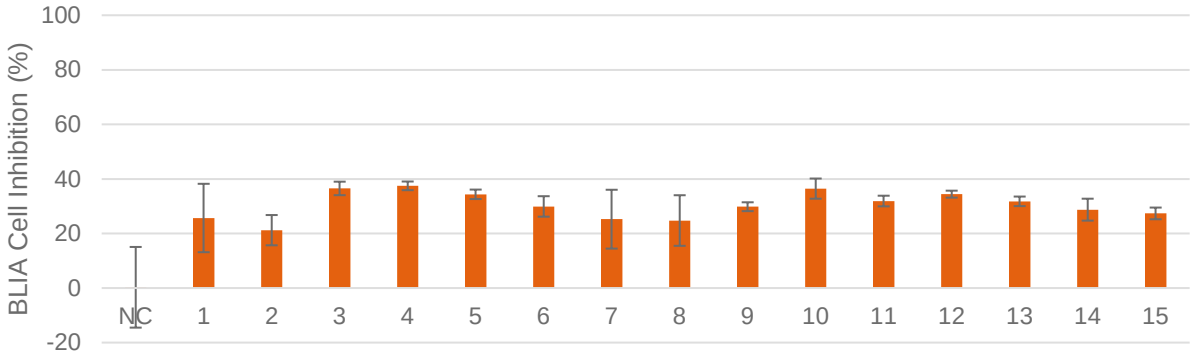

Figure -3-24. 2016 BLIA Percent Cell Inhibition

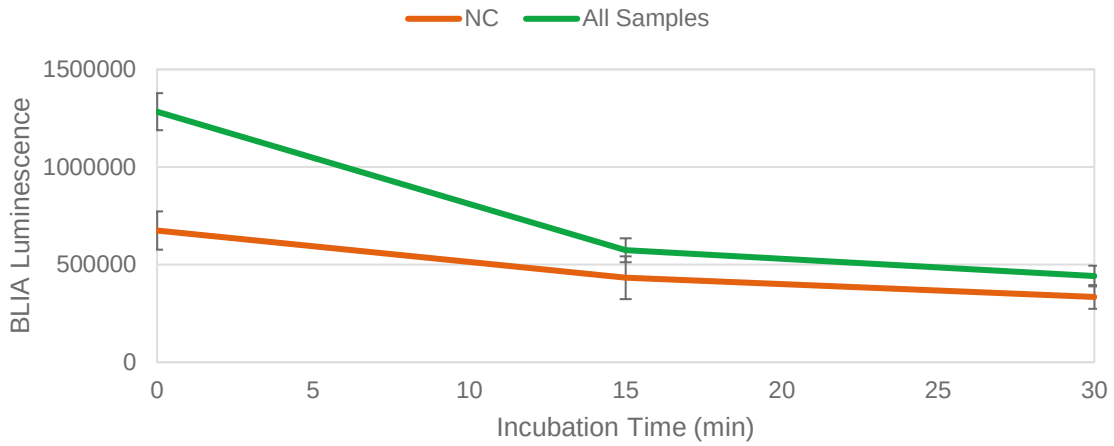

Figure 3-25. 2016 BLIA Raw Luminescence Measurement Averaged for all Negative Controls (NC) and Samples. Error Bars Represent Standard Deviation of 12 Replicates for NC and 3 Replicates of 15 Samples (45 Total) for All Samples

The results for the 2017 MP lamp data are shown on Figure 3-26. The control samples (raw water) induced a small acute cytotoxicity of around 10%, with the addition of H_2O_2 alone showing a slightly reduced level of about 5%. The samples treated with both peroxide and UV showed an insignificant assay response of less than 3%. For this assay, luminescence in sample wells was greater than that for NC, indicating presence of respiration-stimulating components in the sample. However, the luminescence in samples decreased more quickly for sample wells than for NC, indicating inhibitory components to have a greater effect than the stimulating components, resulting in consistent low-level inhibition. Overall, since treatment did not increase the inhibition, it appears that UV-AOP of these treated waters did not result in "new" inhibitory products for BLIA that formed during treatment.

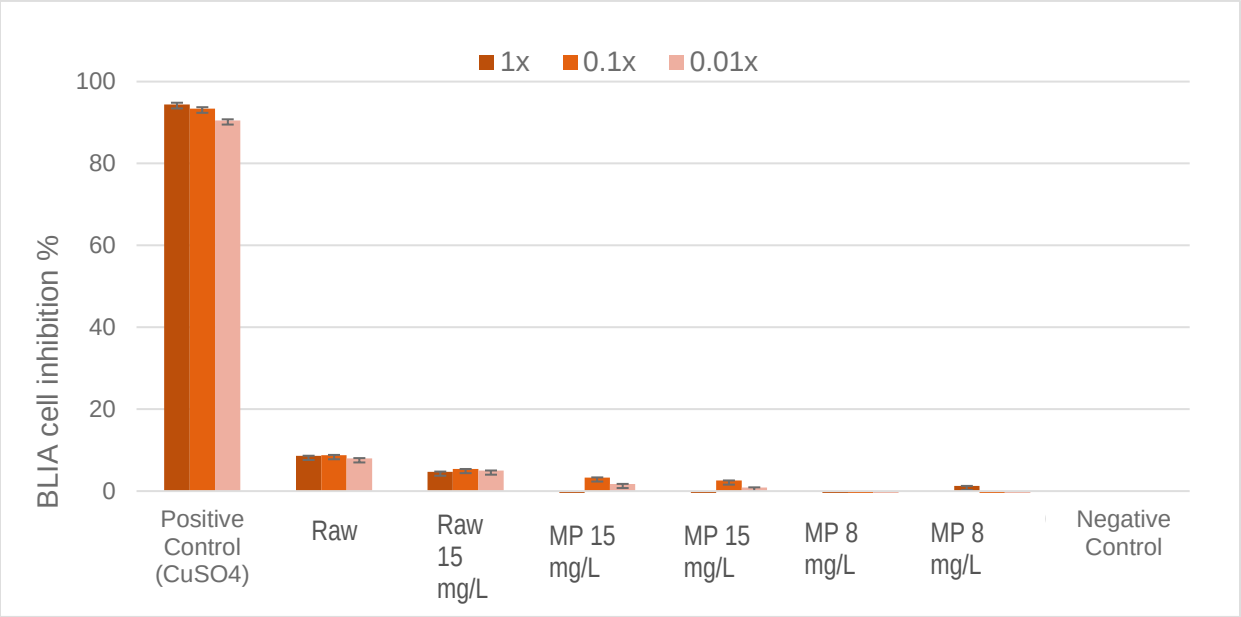

Figure 3-26. 2017 BLIA Percent Cell Inhibition

3.3.4.2 Yeast Estrogen Screen (YES)

Figure 3-27 shows the results of the YES. No samples induced significant estrogenicity. All samples induced similar cellular inhibition to that of BLIA, which resulted in low level cellular inhibition of about 20% ± 10%, but no treatment condition significantly impacted this response except for test 13, which lowered the cellular inhibition (lowest dose MP UV treatment with intermediate H_2O_2 concentration). Even though YES uses a eukaryotic microorganism and measures long term cell inhibition, and BLIA uses a bacterium to measure short term cell inhibition, the level of cell inhibition observed was similar for all samples in both YES and BLIA. Data for the 2017 tests performed on MP lamp are shown on Figure 3-28. The raw NH-37 water showed an estrogenicity of 15% while the treated samples showed an average estrogenicity of 20%, both of which do not fall into significant induction range. Most of the samples showed negative yeast inhibition (slight yeast growth) and no treatment condition significantly impacted this response.

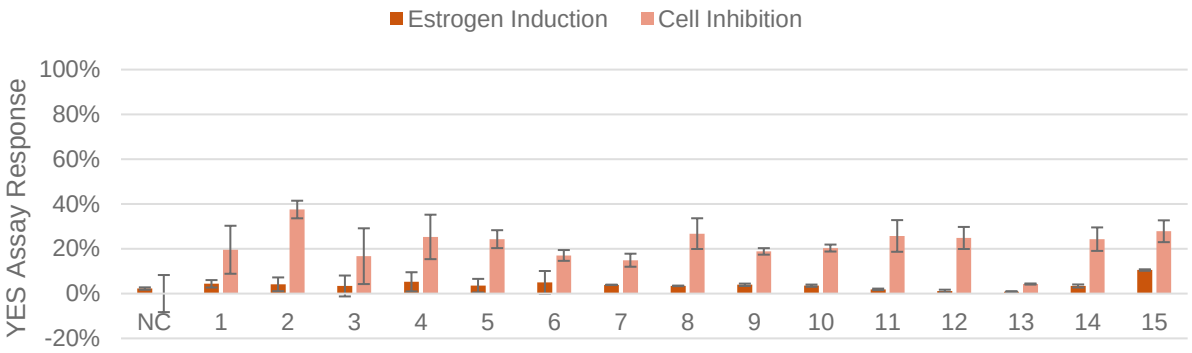

Figure 3-27. 2016 YES Percent Cell Inhibition and Percent Estrogen Induction

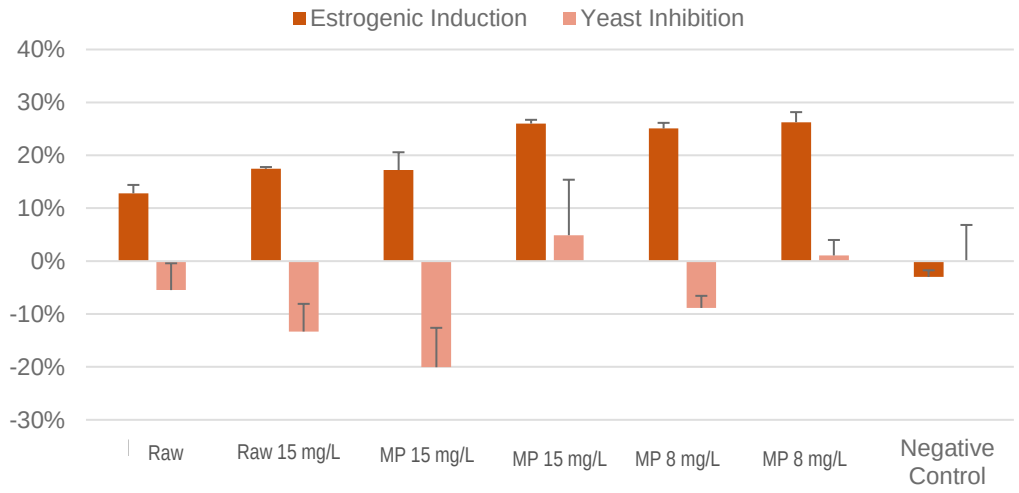

Figure 3-28. 2017 YES Percent Cell Inhibition and Percent Estrogen Induction

3.3.4.3 Ames II Mutagenicity Assay (AMES)

Figure 3-29 and Figure 3-30 presents the data from the AMES. Error bars for samples 14, 15, and B for the TA MIX-S9 are not included due to contamination of the replicate plate. No samples induced mutagenicity, even after the 25X or 50X concentration through SPE. AMES testing on select samples (not shown) indicated that non-SPE concentrated samples also did not induce mutagenicity.

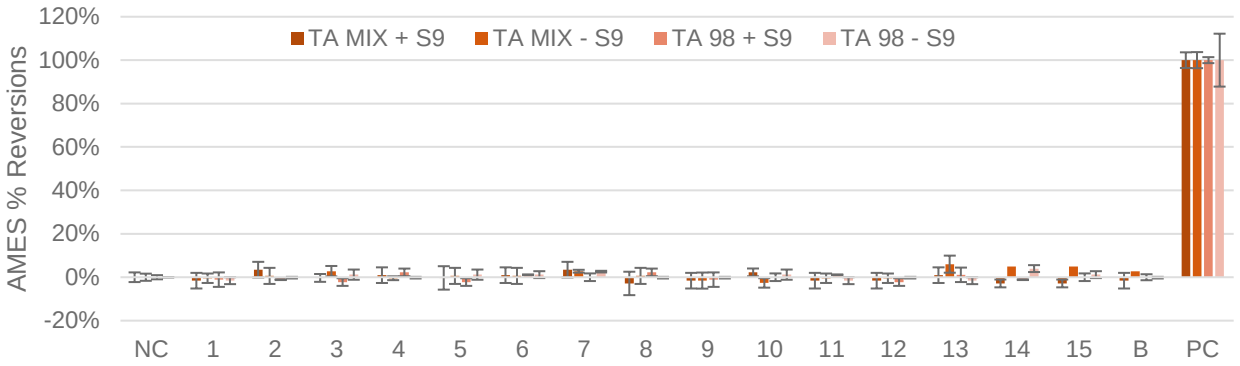

Figure 3-29. 2016 AMES Percent Reversions (50x Concentration)

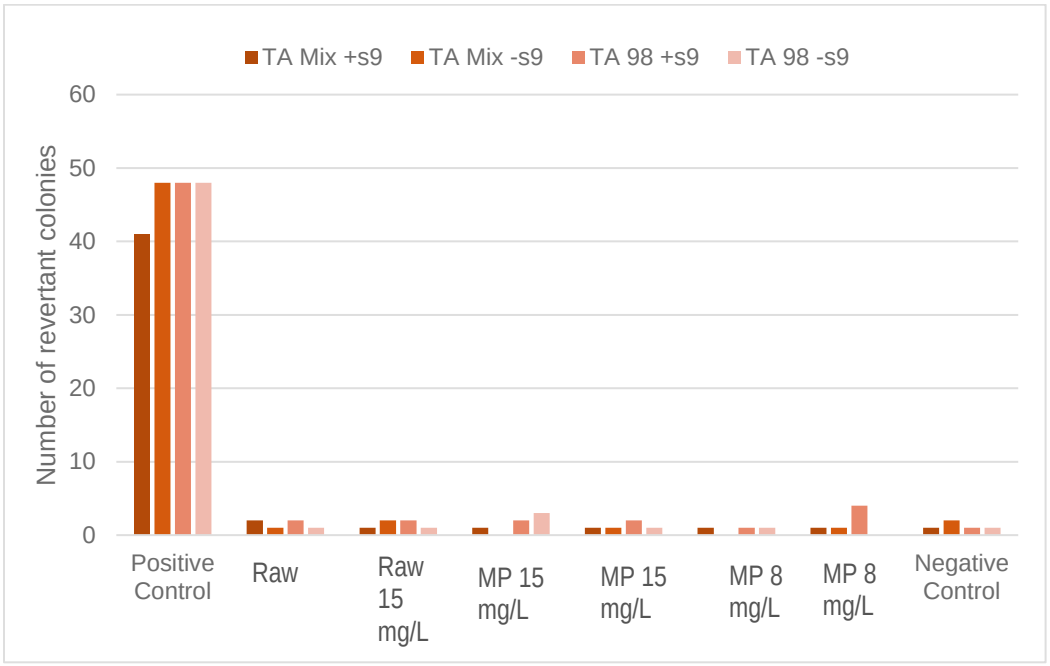

Figure 3-30. 2017 AMES Percent Reversions (25x Concentration)

3.3.5 Chloropicrin

Chloropicrin is a known byproduct with MP UV when nitrate is present, as is the case with NHW. Chloropicrin is not a regulated contaminant, but California has an archived advisory level of 50 µg/L for chloropicrin that was established in 1986. Due to a laboratory error, chloropicrin results were limited to the SDS results. In addition to UV light, chloropicrin can also be formed as a byproduct of chlorination (Merlet, Thibaud and Dore 1985), which may have impacted the results. Chloropicrin in the NH-37 raw water control was approximately 1 µg/L. After LPHO and MP UV/peroxide treatment, the chloropicrin concentrations ranged from 0.6 and 2.1 µg/L (Figure 3-31). The blend of surface water and groundwater showed higher chloropicrin results with concentrations ranging from 6 to 11 µg/L.

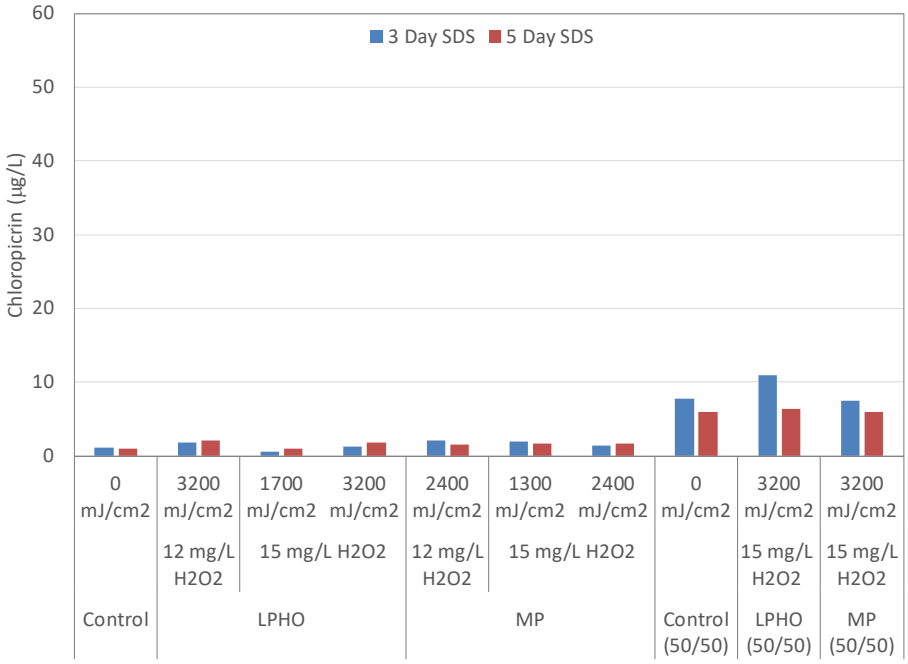

Figure 3-31. Chloropicrin Results from SDS Tests

4 CONCLUSIONS

Bench-scale testing was completed to assist with evaluating UV advanced oxidation for 1,4-dioxane treatment of North Hollywood West groundwater. The testing evaluated the relative efficiency of LPHO and MP UV/peroxide based on the site-specific water quality and the potential for oxidation byproducts.

LPHO UV/peroxide was able to achieve the target 1.9-log reduction of 1,4-dioxane while simultaneously reducing TCE and 1,1-DCE concentrations. As seen on Figure 3-15, MP UV/peroxide was not able to achieve the target log reduction at the evaluated UV doses compared to the LPHO lamps. Due to time limitations, higher doses were not able to be evaluated under the first phase of testing.

The MP UV/peroxide was shown to be less efficient than LPHO UV/peroxide after the MP UV doses were converted to peroxide weighted UV doses, which would account for the additional absorbance of hydrogen peroxide at the lower wavelengths and the site-specific water UV absorbance. The efficiency of the MP UV/peroxide appears to be limited due to the nitrate concentrations present in the NHW groundwater. Nitrate is photolyzed by MP UV to nitrite, which is a hydroxyl radical scavenger. Nitrate specific testing showed that the added hydroxyl radical scavenging demand from nitrate photolysis negatively impacts MP UV AOP efficiency. Table 4-1 presents the relative differences between the doses required for MP and LPHO UV/peroxide for 1,4-dioxane and VOC removal. UV doses were extrapolated when targets were not achieved.

Table 4-1. Comparison on LPHO and MP UV/Peroxide Efficiency for 1,4-Dioxane, TCE, and 1,1-DCE Reduction

Lamp Technology	Log Reduction	Required UV Dose (mJ/cm^2) at 15 mg/L Hydrogen Peroxide		
		1,4- Dioxane	TCE	1,1-DCE
LPHO	0.5-log	594	456	445
	1-log	1188	912	891
	2-log	2377	1823	1782
2016 MP[1]	0.5-log	1051	781	581
	1-log	2102	1562	1162
	2-log	4204	3123	2324
2017 MP[1]	0.5-log	1882	994	-
	1-log	3765	1988	-
	2-log	7530	3977	-

[1] MP UV doses are weighted to hydrogen peroxide

Testing evaluated the potential formation of a range of oxidation byproducts. A summary of findings from the byproduct evaluation is provided below:

- Nitrite was formed with MP UV/peroxide at concentration up to 0.5 mg/L as N. Nitrite is a regulated contaminant with a USEPA MCL of 1 mg/L as N. Nitrite formation is a function of the delivered UV dose. Actual nitrite formation may vary in the full-scale reactor depending on the UV dose and lamp spacing. Nitrite formation was negligible with LPHO UV/peroxide.

- Both LPHO and MP UV/peroxide resulted in increased formation potential for TTHMs and HAA5. However, TTHM and HAA5 concentrations were well below the regulatory limits.
- Blended surface and groundwater TTHM testing showed similar results compared to the 2016 TTHM levels. The HAA5 concentrations were slightly higher results than the 2016 groundwater HAA5 levels. The blended water was well below regulatory limits.
- No increases in AOC concentrations were measured after AOP treatment.
- The background matrix exhibited a slight cytotoxic response for the two assays that tested for cytotoxicity, but the response was low and could be the result of other factors.
- AOP treatment with both LPHO and MP UV did not result in a significant increase in toxicity based on the three tests completed.

5 REFERENCES

Andrews, S. 2009. "Canadian AOP Research/Practice for Treatment of Taste & Odour and EDC/PPCPs." *Americana.* Montreal.

Bolton, J.R., and K.G. Linden. 2003. "Standardization of Methods for Fluence (UV Dose) Determination in Bench-Scale UV Experiments." *Journal of Environmental Engineering* 129 (3): 209-216.

Buxton, G.V., C.L. Greenstock, P.M. Helman, and A.B. Ross. 1998. "Critical Review of Rate Constants for Reactions of Hydrated Electrons, Hydrogen Atoms and Hydroxyl Radicals (•OH/•O) in Aqueous Solution." *Journal of Physical and Chemical Reference Data* 17 (2): 513-886.

Dotson, A., V. Keen, D. Metz, and K. Linden. 2010. "UV/H_2O_2 Treatment of Drinking Water Increases Post-Chlorination DBP Formation." *Water Research* 44 (12): 3703-3713.

Glaze, W.H., Y. Lay, and J. Kang. 1995. "Advanced Oxidation Processes: A kinetic Model for the Oxidation of 1,2-Dibromo-3-chloropropane in Water by the Combination of Hydrogen Peroxide and UV Radiation." *Industrial Engineering Chemistry Research* 34 (7): 2314-2323.

Kamber, M., S. Flückiger-Isler, G. Engelhardt, R. Jaeckh, and E. Zeiger. 2009. "Comparison of the Ames II and Traditional Ames Test Responses With Respect to Mutagenicity, Strain Specificities, Need for Metabolism and Correlation With Rodent Carcinogenicity." *Mutagenesis* 24 (4): 359-366.

Klassen, N.V., D. Marchington, and H.C.E. McGowan. 1994. "H_2O_2 Determination by the I_3^- Method and by $KMnO_4$ Titration." *Analytical Chemistry* 66 (18): 2921-2925.

Linden, K.G., A.M. Parker, F. Rosario-Ortiz, U. von Gunten, H. Mestankova, S. Canonica, K. Schirmer, et al. 2015. *Advanced Oxidation and Transofrmation of Organic Contaminants [Project #4241].* Denver: Water Research Foundation.

Martijn, A.J., J.C. Kruithof, M.R. Hughes, R.A. Mastan, A.R. Van Rompay, and J.P. Malley. 2015. "Induced Genotoxicity in Nitrate-Rich Water Treated with Medium-Pressure Ultraviolet Processes." *Journal AWWA* 107 (6): 301-312.

Martijn, A.J., M.G. Boersma, J.M. Vervoort, I. Rietjens, and J.C. Kruithof. 2014. "Formation of Genotoxic Compounds by Medium Pressure Ultraviolet Treatment of Nitrate-Rich Water." *Desalination and Water Treatment* 52 (34-36): 6275-6281.

Martjin, A.J., and J.C. Kruithof. 2012. "UV and UV/H_2O_2 Treatment: The Silver Bullet for By Product and Genotoxicity Formation in Water Production." *Ozone: Science & Engineering* 34 (2): 92-100.

Merlet, N., H. Thibaud, and M. Dore. 1985. "Chloropicrin formation during oxidative treatments in the preparation of drinking water." *Science of the Total Environment* 47: 223-228.

Mortelmans, K., and E. Zeiger. 2000. "The Ames Salmonella/Microsome Mutagenicity Assay." *Mutation Research/Fundamental and Molecular Mechanisms of Mutagenesis* 24 (4): 29-60.

Oppenländer, T. 2003. *Photochemical Purification of Water and Air.* Wiley-VCH.

Reckhow, D.A., K.G. Linden, J. Kim, H. Shemer, and G. Makdissy. 2015. "Effect of UV Treatment on DBP Formation." *Journal AWWA* 102 (6): 100-113.

Rosenfeldt, E.J., and K.G. Linden. 2007. "The R_OH/UV Concept to Characterize and the Model UV/H_2O_2 Process in Natural Waters." 41 (7): 2548-2553.

Routledge, E.J., and J.P. Sumpter. 1996. "Estrogenic Activity of Surfactants and Some of Their Degradation Products Assessed Using a Recombinant Yeast Screen." *Environmental Toxicology and Chemistry* 15 (3): 241-248.

Routledge, E.J., and J.P. Sumpter. 1997. "Structural Features of Alkylphenolic Chemicals Associated with Estrogenic Activity." *Journal of Biological Chemistry* 272 (6): 3280-3288.

Shemer, H., and K.G. Linden. 2007. "Photolysis, Oxidation and Subsequent Toxicity of a Mixture of Polycyclic Aromatic Hydrocarbons in Natural Water." *Journal of Photochemistry and Photobiology A: Chemistry* 187 (2-3): 186-195.

Sun, M., C. Lopez-Velandia, and D.R.U. Knappe. 2016. "Determination of 1,4-Dioxane in the Cape Fear River Watershed by Heated Purge-and-Trap Preconcentration and Gas Chromatography-Mass Spectrometry." *Environmental Science and Technology* 50 (5): 2246-2256.

Swaim, P., A. Royce, T. Smiths, T. Maloney, D.. Ehlen, and B. Carter. 2007. "Effectiveness of UV Advanced Oxidation for Destruction of Micro-Pollutants." *Fourth International Ultraviolet Association Congress.* Los Angeles.

Appendix A Nitrate Report

Testing Report

UV Advanced Oxidation Collimated Beam Testing and Subsequent Modeling to Predict Impact of Nitrate on Hydroxyl Radical Generation Efficiency in Well Water from LADWP

By Sydney Ulliman, Charles Sharpless, PhD and Karl Linden, PhD.
August 31, 2017, Revised November 20, 2017 and May 30, 2018

University of Colorado Boulder

Introduction

UV advanced oxidation process (AOP) experiments were performed at the University of Colorado Boulder for the Los Angeles Department of Water and Power (LADWP). The goal of this study was to better understand the effect of nitrate on hydroxyl radical (•OH) scavenging in medium pressure UV/H_2O_2 (MPUV) and low-pressure UV/H_2O_2 (LPUV) systems. The evaluation examined the impact on •OH production by the following parameters:

- nitrate concentration
- water depth
- hydrogen peroxide (H_2O_2) concentration
- background water matrix

Nitrate was studied due to its role as both a promoter and scavenger of OH radicals, based on its UV absorbance of some wavelengths emitted by MPUV. Water depth was evaluated to compared shallow and longer pathlengths for UV light to travel and the impacts on the OH radical generation due to UV absorbance over different pathlengths. Hydrogen peroxide was examined at a level relevant to practice, to determine how the presence of H_2O_2 with nitrate affects the OH radical generation efficiency. The background water matrix was evaluated to determine the effect of scavenging from different water matrix constituents. Following the experimental work, the data were analyzed, and a model developed to evaluate various scenarios of UV fluence and nitrate concentration on the production of hydroxyl radical under MP UV irradiation.

Part 1: Bench Scale Testing - Experimental Results

I. Analytical Methods

Water quality

Lab-grade DI water (i.e. ultrapure water, resistance = 18 MΩ cm) and well water from the North Hollywood West wellfield (labeled as NH037 in Table 1), collected and shipped by LADWP to the University of Colorado, served as test water matrices for exposures. Pertinent water quality parameters were measured (Table 1) and compared to previously used well waters (TJ and NHC) using methods presented in Table 2. Water quality parameters were measured prior to and after UV exposure (1000 mJ/cm^2) for NH037. These values are presented in Tables A1-6 in Attachment A. The absorbance spectrum of the native well water is illustrated in Figure 1 (right).

Table 1. Water Quality for well waters.

Parameter	Units	NH037	TJ	NHC
Total organic carbon	ppm as C	0.42	0.75	0.31
Alkalinity	ppm as $CaCO_3$	209	152	155
Nitrate	ppm NO_3-N	1.24	7.07	2.33
Nitrite*	ppm NO_2-N	ND	ND	ND
UVA 254 nm (UVT)	m^{-1} (%)	6.70 (98.5%)	2.07 (95.3%)	0.010 (99.7%)
LPUV ·OH scavenging rate	$\times 10^4$ s^{-1}	3.79	2.34	2.21
LPUV ·OH steady-state concentration	$\times 10^{-13}$ M	2.20	3.71	3.95

*Method reporting limit of 0.10 ppm NO_2-N

Table 2. Analytical Methods.

Analysis	**Method**
Hydrogen peroxide	Triiodide colorimetric method (Klassen 1994)[1]
TOC	UV persulfate oxidation/conductivity method - Standard Methods 5310C and EPA 415.3 compliant
Alkalinity	Hach digital titrator method, in compliance with EPA method 310.2
pH	Orion Star A211 meter
UV_{254}	Cary Bio 100 spectrophotometer (Varian Inc., Palo Alto, TX)
Nitrate	Hach TNT 835 kit. Approved by the EPA. Reference Method: 40 CFR 141
Nitrite	Hach TNT 839 kit. Equivalent to EPA method. Reference Method EPA 353.2

Solutions were spiked with para-chlorobenzoic acid (pCBA), NO_3^-, and H_2O_2 to achieve concentrations of 1 ppm, 10 ppm NO_3-N and 10 ppm, respectively. Water depths of 3 and 9 cm were tested to assess the impact of pathlength but were not selected to represent the average pathlength in a specific UV reactor. All experiments were carried out in duplicate. pCBA was selected as a chemical probe to measure the steady state ·OH production in the

UV/H_2O_2 system because it reacts with •OH at a rate that far exceeds its reaction rate with UV light. The absorption spectra of pCBA and NO_3^- can be viewed in Figure 1 (left) and H_2O_2 absorbance in Figure 2a.

Because pCBA was rapidly consumed by •OH, experiments to measure •OH were performed at UV doses up to 1000 mJ/cm^2, including 0, 250, 500, 750 and 1000 mJ/cm^2. All doses were calculated as peroxide weighted, relative to 254 nm. To determine the formation of nitrite (NO_2^-) and degradation of H_2O_2 in the MPUV system, separate experiments were performed at doses up to 4000 mJ/cm^2 and at a 9 cm sample depth. Previous bench scale testing indicated MPUV doses in excess of 5000 mJ/cm^2 would be required to achieve the full-scale treatment goals. Experimental results were also modeled (See Part II) to predict performance at high fluence levels and varying depths.

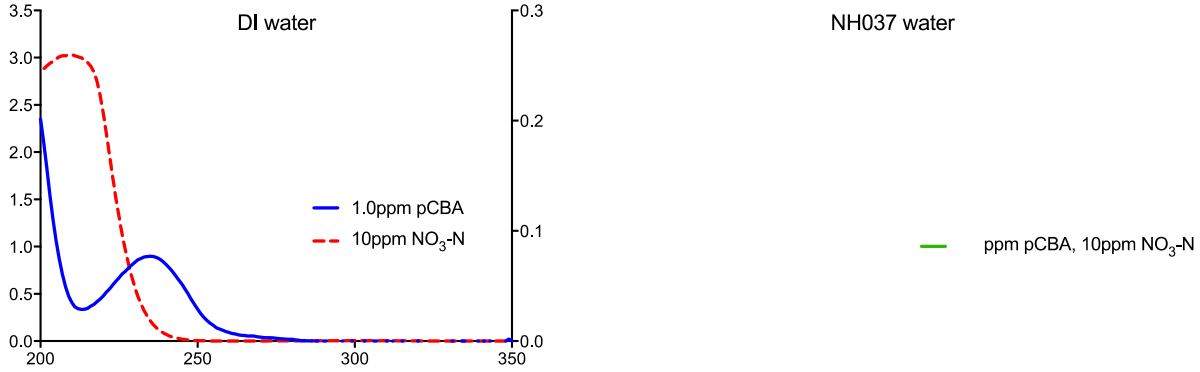

Figure 1. Absorbance spectra of NO_3-N (primary y-axis) and pCBA (secondary y-axis) in DI water (left graph) and well water with added pCBA and NO_3-N (right graph) and. Absorbance values reflect concentrations used for experimental testing.

Low pressure and medium pressure UV/H_2O_2 experiments were conducted in benchtop quasi-collimated system setups (Figure 2b) with the details of individual experiments presented in Tables A1-6 in Attachment A. For the LPUV system, four LPUV lamps (15 watt, #G15T8) were housed above two 4-inch apertures equipped with a manual shutter. For the MPUV system, a Calgon Carbon UV Technologies LLC (Pittsburg, PA) benchtop instrument was used in conjunction with a single 1 kW MP lamp (ozone-free, Calgon Carbon). The MP and LPUV lamp emission spectra are presented in Figure 2a.

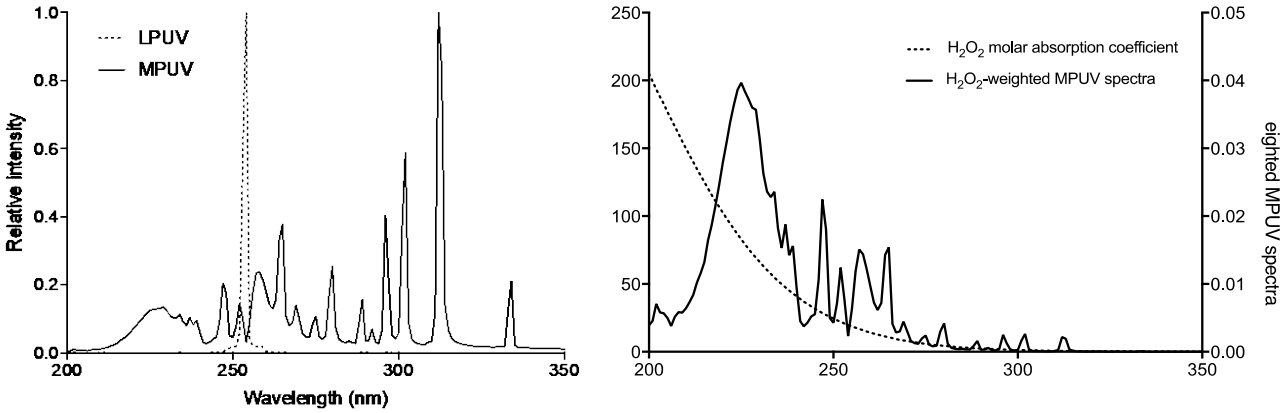

Figure 2a. Normalized MP and LPUV lamp emission spectrum (left graph) and H_2O_2 molar absorption coefficients (primary y-axis) and H_2O_2-weighted MPUV spectra (secondary axis) (right graph).

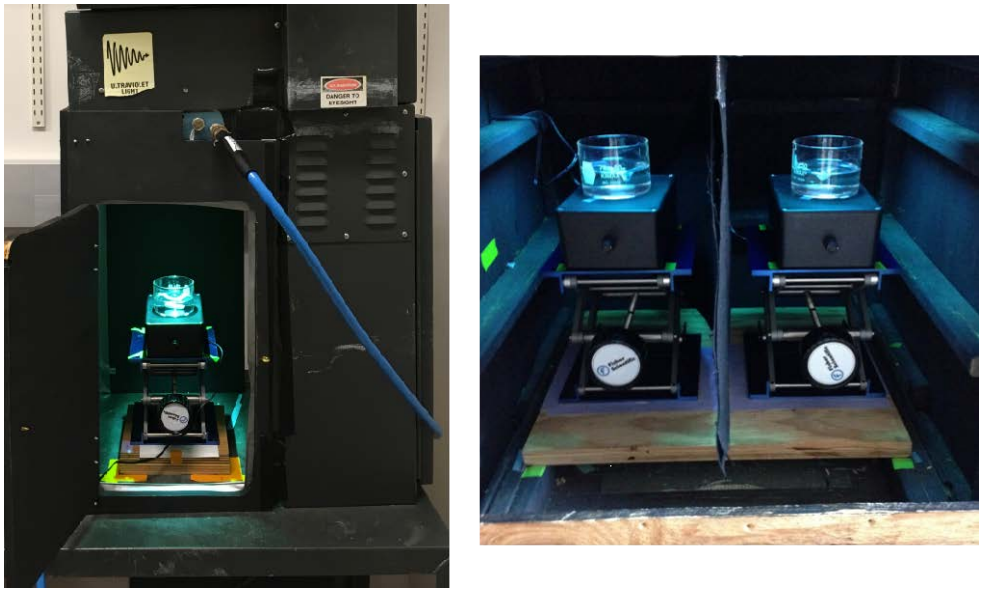

Figure 2b. MPUV (left) and LPUV (right) quasi-collimated bench-scale setups.

Incident UV irradiance was measured by a calibrated radiometer (International Light Inc., Model 1700/SED 240/W). UV dose was calculated by multiplying the average irradiance by the exposure time in seconds. The UV average irradiance was determined by correcting the incident irradiance (radiometer reading) for sample depth, absorbance, sample reflectance, and the petri factor according to Bolton and Linden, 2003.[2] Two additional corrections were required for the MPUV average irradiance calculation: sensor factor and a H_2O_2-weighting factor. The latter weights each wavelength by the H_2O_2 molar absorption coefficient relative to its value at 254 nm (H_2O_2 molar absorption shown in Figure 2a).

Hydroxyl radical determination

Samples were analyzed for the concentration of the radical probe, pCBA, using an Agilent 1100 series high performance liquid chromatograph (HPLC) and UV detector (at 235 nm for pCBA detection) equipped with a reverse phase C-18 column (HPLC method found in (Ulliman et al., 2017)).[3]

The concentration of •OH was then calculated using the following relationship:

$$\ln\frac{[pCBA]}{[pCBA]_o} = \frac{-k_{\cdot OH,pCBA}[\cdot OH]_{ss}}{E_o} \times F \qquad (1)$$

where E_0 is the average fluence rate (mW/cm^2), F is the fluence (0 to ~1000 mJ/cm^2) (i.e., UV dose) and $k_{\cdot OH,pCBA}$ is a time-based reaction rate constant between pCBA and hydroxyl radicals (M^{-1}s^{-1}).

In this equation, the quantity $\frac{-k_{\cdot OH,pCBA}[\cdot OH]_{ss}}{E_o}$ is the slope of the plot of ln([pCBA]/[pCBA]$_0$) *vs* F, and [•OH]$_{ss}$ can be calculated as:

$$[\cdot OH]_{ss} = \frac{-slope \times E_o}{k_{\cdot OH,pCBA}} \qquad (2)$$

The value for $k_{\cdot OH,pCBA}$ has been reported as 5×10^9 M^{-1}s^{-1} by Buxton *et al.*, 1988.[4]

II. Results and Discussion

The influence of NO_3^- concentration, H_2O_2 concentration, water depth, and water matrix on •OH steady state concentration was assessed using pCBA as a probe compound.

A comparison between MP and LPUV

Illustrated in Figure 3 is the measured steady-state •OH concentrations of samples with and without 10 ppm H_2O_2 and irradiated by MP and LPUV. Addition of nitrate was shown to produce radicals in the MPUV irradiated samples without H_2O_2 addition whereas negligible radical production was observed in nitrate-rich LPUV treated waters.

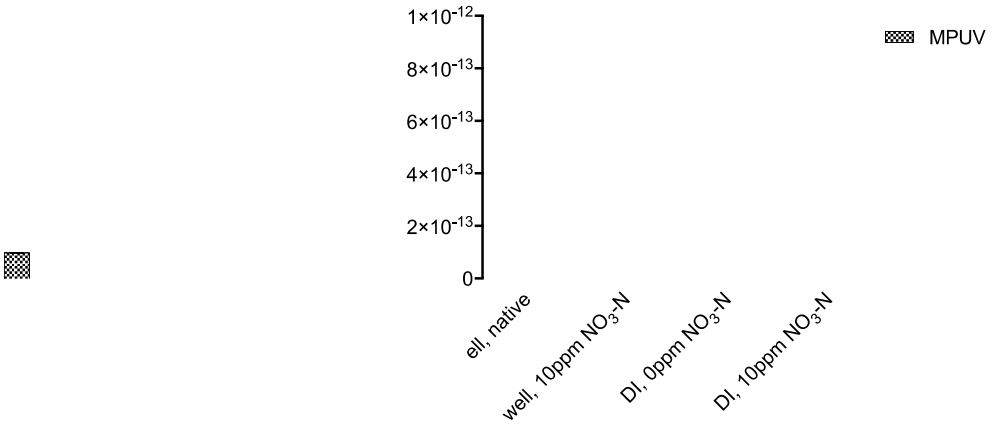

Figure 3. A comparison of MP and LPUV steady-state hydroxyl radical production determined in well and DI water at a 3 cm water depth with 0 ppm H_2O_2 (A) and 10 ppm H_2O_2 (B) with and without NO_3^- addition (displayed on x-axis). Error bars represent the standard deviations between duplicate experiments. Well water contained a native NO_3-N concentration of 1.24 ppm.

Nitrate strongly absorbs light emitted below 250 nm (Figure 1). During MPUV exposure, the resulting photochemical reactions include the reduction of nitrate to nitrite (NO_2^-) and production of •OH (Rxns 1 and 2). A more comprehensive list of major reactions involving nitrate can be viewed in Sharpless *et al.*, 2003.[5] As shown in Rxn 3, nitrite produced in Rxn 1 is also an •OH scavenger with a high second order reaction rate with •OH (k_{OH} = 10^{10} $M^{-1}s^{-1}$). These results are used in development of a model to predict the impact of nitrate on •OH radical production.

$$NO_3^- + h\nu \rightarrow NO_2^- + O \quad \text{(R1)}$$

$$NO_3^- + h\nu + H^+ \rightarrow NO_2 + \bullet OH \quad \text{(R2)}$$

$$NO_2^- + \bullet OH \rightarrow \bullet NO_2 + OH^- \quad \text{(R3)}$$

With 10 ppm H_2O_2 addition (Figure 3 B), •OH radical production under MP and LPUV irradiation for scenarios with and without nitrate addition was comparable (2 to 15%, reported as the coefficient of variation). The experiential results agree with expected results. In comparing Figures 3 A and 3 B, the addition of H_2O_2 increased radical production by several orders of magnitude in LPUV/NO_3^- scenarios while a relatively minimal increase in radical production (97% well water and 70% DI water) was observed for MPUV/NO_3^- scenarios with NO_3^- addition. Keen *et al.*[6] found similarly that in the presence of nitrate, the addition of H_2O_2 (up to 10 ppm) had a positive but

dampened effect on •OH radical production. A likely explanation is that the H_2O_2 added to MPUV/NO_3^- led to a higher •OH scavenging potential since H_2O_2 has been shown to accelerate the production of NO_2^-.[5] Increased NO_2-N concentration was observed in scenarios with added H_2O_2. For example, in well water scenarios with 10ppm NO_3-N addition and at a MPUV dose of ~800 mJ/cm^2, approximately 0.31 ppm of NO_2-N was formed with added H_2O_2 whereas 0.21 ppm NO_2-N was formed without added H_2O_2.

Water matrix and sample depth

Despite higher NO_2^- concentrations in scenarios with H_2O_2, added H_2O_2 increased radical production in all scenarios containing 10 ppm NO_3-N by 83% on average in 3 cm water depths and 177% in 9 cm water depths (Figure 4 A). Experiments performed in DI water, at both 3 cm and 9 cm water depths, were observed to have two to four times higher radical production when compared to experiments performed in well water. This may be because the well water contained higher concentrations of •OH scavengers, mainly carbonate species and dissolved organic matter (see Table 1) or be due to the production of nitrite as a scavenger, from the low levels of nitrate present.

When H_2O_2 concentration is held constant and NO_3^- is varied (Figure 4 B), added NO_3^- inhibited radical production by 30% in well water and 21 to 55% in DI water, respectively. A possible explanation is the scavenging of •OH by NO_2^- generated from NO_3^- photolysis.

Figure 4. Hydroxyl radical steady state concentration produced by MPUV exposure of well and DI water containing 10 ppm NO_3^- at varied water depths and H_2O_2 concentrations (A) and containing 10 ppm H_2O_2 at varied water depths and NO_3^- concentrations (B). Well water contained a native NO_3-N concentration of 1.24 ppm.

For scenarios with NO_3^- (added or native), NO_2^- is produced at a constant rate during MPUV exposure and accumulates in the system. As a result, NO_2^- scavenges •OH at an increasing rate (reaction 2) with increasing time or UV dose.[5] Nitrite production as a function of UV doses can be viewed in Figure 5. The linear increase of NO_2^- concentrations (Figure 5) suggests that radical scavenging may also increase with increased MPUV dose. This may result in decreased MPUV efficiency for higher UV doses applied in the presence of nitrate and H_2O_2. These points are further presented in Part II when the results are modeled.

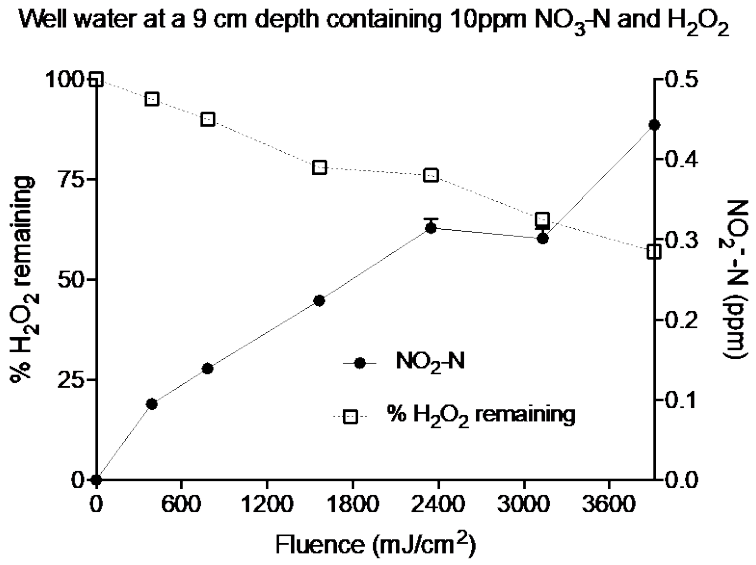

Figure 5. NO_2^- generation and H_2O_2 degradation as a function of MPUV dose. Experiments were performed in well water containing 10 ppm NO_3-N and H_2O_2 concentrations at a 9 cm depth.

Part II: Modelling Production of Hydroxyl Radical and Nitrite During Medium Pressure Irradiation of Solutions Containing Hydrogen Peroxide and Nitrate

Overview and Summary of Modeling

As noted in Part I, bench scale medium pressure (MP) UV/H_2O_2 experiments indicated that elevated nitrate (NO_3^-) could decrease •OH concentrations and that this effect was associated with the photochemical production of nitrite (NO_2^-) by NO_3^- photolysis, thus offsetting any potential gain in •OH from NO_3^- photolysis. At the highest

NO_2^- levels reached in experiments using 1000 mJ cm^{-2} fluence (H_2O_2 weighted), NO_2^- contributions to •OH scavenging are calculated to be approximately three-fold higher than the background rate in this water (details provided in Section II). To further explore the extent of this effect a kinetic model was developed to predict NO_2^- and •OH production rates and concentrations as a function of H_2O_2 and NO_3^- concentrations as well as water depth. Two key model variables, the background water •OH scavenging rate constant and an empirical efficiency of NO_2^- destruction by •OH, were parameterized by fitting NO_2^- and •OH kinetics from experimental scenario 16 in Part I. These parameters were then fixed for use in two different model applications described below. In one application, the effect of NO_3^-, H_2O_2, and water depth on NO_2^- and •OH levels was modelled for comparison to bench scale test results 9 through 16, which involved single point measurements at 1000 mJ cm^{-2} nominal H_2O_2-weighted fluence. Model results compare very favorably with experiments for •OH and generally NO_2^- as well, but a tendency was noted for the model to overpredict NO_2^- levels with added NO_3^- in the absence of H_2O_2 and to underpredict NO_2^- levels with added H_2O_2 in the absence of additional NO_3^- (see Table IV and Fig 9 in Section IV, Model Results). In the second model application, full NO_2^- and •OH kinetic profiles were modelled for varying levels of NO_3^- with fixed H_2O_2 concentration (10 mg/L) and water depth (9 cm). These results suggest that any level of NO_3^- will always detrimentally impact MPUV/H_2O_2 performance due to OH scavenging by photochemically produced NO_2^-.

I. Review of Bench Scale Testing Results

This work examined whether photochemical modeling could reproduce results from experimental scenarios 9 through 16 in the Part I Bench Scale Testing (See Tables A3 and A4 in Attachment A) and further explore the extent to which NO_2^- production interferes with MP-UV/H_2O_2 performance. Scenarios 9 to 16 tested LADWP well water, and the conditions and results are summarized in Table 3 and Figures 6 and 7. In the Table, F stands for fluence, which is H_2O_2-weighted throughout this report, with the weighting determined as per the dose calculation spreadsheets used in the bench scale tests.

Table 3. Experimental conditions and NO_2^- and •OH results for bench scale tests 9 through 16.

	Total NO_3^-	Added H_2O_2	Depth	H_2O_2 weighted F	NO_2^-	$[•OH]_{ss}$
Exp. ID	*mg-N/L*	*mg/L*	*cm*	*mJ cm $^{-2}$*	*(mg-N/L)*	*(M)*
9	1.24	0	3	1000	0.09	8.0E-14
10	11.24	0	3	1000	0.21	1.3E-13
11	1.24	10	3	1000	0.14	3.5E-13
12	11.24	10	3	1000	0.30	2.5E-13
13	1.24	0	9	1000	0.06	3.7E-14
14	11.24	0	9	720	0.09	5.8E-14
15	1.24	10	9	1000	0.10	2.3E-13
16	11.24	10	9	1000	0.19	1.6E-13

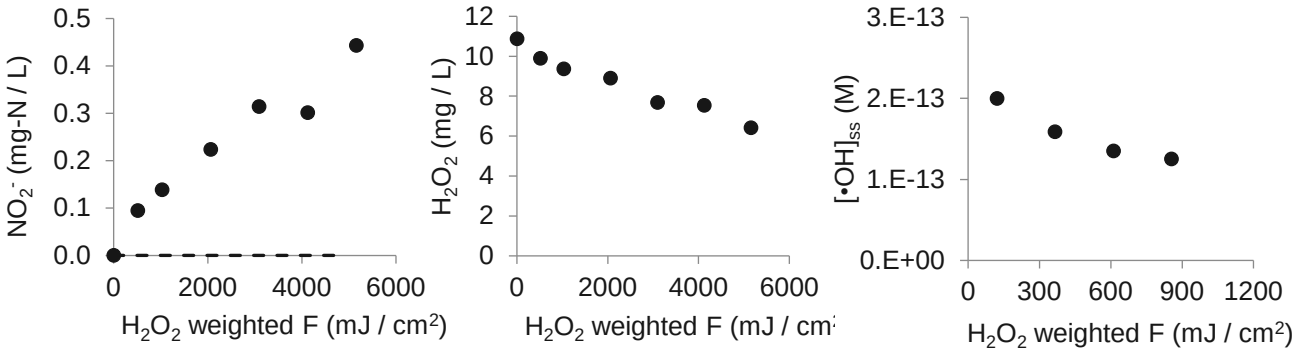

Figure 6. Experiment 16 results for NO_2^-, H_2O_2, and •OH. The fluence dependence of $[•OH]_{ss}$ was calculated from the results shown in Figure 6 as described in the text.

The second panel in Fig 6 displays the fluence dependence of steady state •OH concentrations, $[•OH]_{ss}$, which was not reported in Part I (Tables A1-A6), which instead gave average $[•OH]_{ss}$ values over the irradiation period (summarized in Table 3) determined from linear best-fits to 1st order plots of p-chlorobenzoic acid (pCBA) loss. However, when NO_3^- levels are high, the 1st order pCBA loss is not linear and slows with time as shown in Figure 7, which displays results for scenario 16. The curvature indicates a decrease in $[•OH]_{ss}$ with irradiation, which can be ascribed to scavenging by NO_2^-. To determine the fluence dependence of $[•OH]_{ss}$ shown in Fig 7, the slope between individual pairs of data in Fig 7 was used along with Eqns 1 and 2 in Part I. The fluence associated with each $[•OH]_{ss}$ value in the figure was taken as the average between the two points used in the calculation.

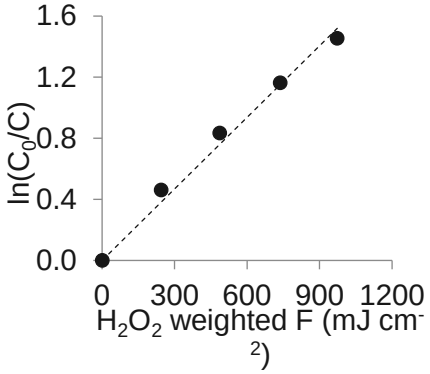

Figure 7. 1st order plot of pCBA loss during experiment 16 demonstrating non-linearity of results. Pairs of data points were used to determine the fluence dependence of $[•OH]_{ss}$ as described in the text.

II. Conclusions Concerning NO_2^- Impact From Bench Scale Results

The results in Table 3 can be used to show that NO_2^- levels reached at 1000 mJ cm^{-2} should negatively impact $[\bullet OH]_{ss}$. A key parameter controlling $[\bullet OH]_{ss}$ in any aquatic advanced oxidation process (AOP) is the rate of •OH scavenging by the water. Several water constituents can contribute to scavenging as shown in Rxns 4 to 8.

$$NOM + \bullet OH \rightarrow \text{products} \qquad k_{OH,OM} = 2.5\text{x}10^4 \text{ L mg-C}^{-1} \text{ s}^{-1} \text{ (ref 7)} \quad \text{(R4)}$$

$$HCO_3^- + \bullet OH \rightarrow \bullet CO_3^- + H_2O \qquad k_{OH,HCO3-} = 1\text{x}10^7 \text{ M}^{-1} \text{ s}^{-1} \text{ (ref 8)} \quad \text{(R5)}$$

$$CO_3^{2-} + \bullet OH \rightarrow \bullet CO_3^- + OH^- \qquad k_{OH,CO32-} = 4\text{x}10^8 \text{ M}^{-1} \text{ s}^{-1} \text{ (ref 8)} \quad \text{(R6)}$$

$$H_2O_2 + \bullet OH \rightarrow HOO\bullet + H_2O \qquad k_{OH,H2O2} = 2.7\text{x}10^8 \text{ M}^{-1} \text{ s}^{-1} \text{ (ref 8)} \quad \text{(R7)}$$

$$NO_2^- + \bullet OH \rightarrow \bullet NO_2 + H_2O \qquad k_{OH,NO2-} = 1\text{x}10^{10} \text{ M}^{-1} \text{ s}^{-1} \text{ (ref 8)} \quad \text{(R8)}$$

Additionally, pCBA, the •OH probe used in bench scale tests, scavenges •OH with $k_s = 5.0\text{x}10^9 \text{ M}^{-1} \text{ s}^{-1}$.[4] From these equations and the known water composition, total k_s values for the unirradiated and irradiated water can be calculated via Eqn 3.

$$k_{s,tot} = k_{OH,OM}C_{OM} + k_{OH,HCO3-}[HCO_3^-] + k_{OH,CO32-}[CO_3^{2-}] + k_{OH,H2O2}[H_2O_2] + k_{OH,NO2}[NO_2^-] \quad (3)$$

Here, HCO_3^- and CO_3^{2-} concentrations were determined from the known alkalinity and pH of the LADWP water, 168 ppm and 7.4, respectively. Predicted $k_{s,tot}$ values in the LADPW water before irradiation (no NO_2^-) are $7.8\text{x}10^4$ s^{-1} without H_2O_2 and $8.6\text{x}10^4$ s^{-1} with 10 mg/L H_2O_2. For comparison, the contribution to k_s from NO_2^- at the lowest and highest values reached with 1000 mJ cm^{-2} (Table 3), 0.1 and 0.3 mg-N/L, is $7.1\text{x}10^4$ s^{-1} and $2.1\text{x}10^5$ s^{-1}, respectively, the latter being almost 3-fold larger than the background scavenging. These results indicate that NO_2^- production negatively impacts $[\bullet OH]_{ss}$ and combined with experimental observations (Table 3) suggest that •OH scavenging by photochemically produced NO_2^- is substantial enough to more than cancel out any positive contribution to •OH made by NO_3^- photolysis with MP-UV under the water quality conditions of the LADWP test water.

III. Model Background

To further explore the potential interplay between NO_3^- production of •OH and NO_2^- and their effect on $[\bullet OH]_{ss}$, a photochemical kinetic model was developed as none currently exist. The calculations were carried out in Excel, and the mathematical equations involved are provided as an Attachment (B) to this document. The model involves three photochemical reactions (Rxns 9-11) and three thermal equations (reactions 12-14).

$$H_2O_2 + h\nu \rightarrow 2\bullet OH \qquad \Phi_{H2O2} = 1.11 \quad \text{(R9)}$$

$$NO_3^- + h\nu + H_2O \rightarrow {\bullet}NO_2 + {\bullet}OH + OH^- \quad \Phi^N_{OH,\lambda} \quad \text{(R10)}$$

$$NO_3^- + h\nu \rightarrow NO_2^- + O \quad \Phi_{NO2-,\lambda} \quad \text{(R11)}$$

$${\bullet}OH + H_2O_2 \rightarrow H_2O + H^+ + O_2^- \quad k_{OH,H2O2} \quad \text{(R12)}$$

$${\bullet}OH + NO_2^- \rightarrow {\bullet}NO_2 + OH^- \quad k_{OH,NO2-} \quad \text{(R13)}$$

$${\bullet}OH + \text{LA water} \rightarrow \text{products} \quad k_{s,w} \quad \text{(R14)}$$

The quantum yield, Φ_{H2O2}, represents the wavelength independent efficiency of H_2O_2 loss and ·OH production, and the value is taken from Goldstein *et al.*, 2007.[9] The quantum yield, $\Phi^N_{OH,\lambda}$, represents the wavelength dependent efficiency of ·OH production by NO_3^-. Values from 200 to 300 nm were reported by Goldstein and Rabani[10] at roughly 5 nm intervals, and to obtain 1 nm resolution for use in calculations their data were fit to an exponential decay (see model spreadsheet, "Inputs and results.xlsx" worksheet "nitrate QYs"). Similarly, the quantum yield, $\Phi_{NO2-,\lambda}$, represents the wavelength dependent efficiency of NO_2^- production by NO_3^-. Values from 200 to 300 nm were reported by Goldstein and Rabani[10] at roughly 5 nm intervals, and to obtain 1 nm resolution for use in calculations their data were fit to a Gaussian curve (see model spreadsheet, "Inputs and results.xlsx" worksheet "nitrate QYs"). Rate constants for Rxns 12 and 13 are given above (Rxns 7 and 8). For modelling, the value of $k_{s,w}$ (Rxn 14) was used as a fitting parameter to match $[{\bullet}OH]_{ss}$ concentrations from scenario 16 (Fig 6). The fitted $k_{s,w}$, 8.35×10^4 s^{-1}, agrees well with the value predicted from the water quality, 7.8×10^4 s^{-1} (see above).

The model only considers one loss pathway for NO_2^-, reaction with ·OH (Rxn 13) . It ignores NO_2^- photolysis, and preliminary model runs show that the quantum yield for NO_2^- photolysis would need to be greater than 20% to have even a small influence on the NO_2^- kinetics (data not shown). In contrast, calculated rates of NO_2^- loss via Rxn 13 are too large to be compatible with production rates in bench scale testing. This is likely due to the fact that a sequence of reactions involving ·NO_2, ·NO (from nitrite photolysis), and water regenerates NO_2^-, which decreases its apparent rate of loss.[9,10] Rather than trying to account for all of the radical intermediate chemistry, the model applies a correction factor (γ) to the efficiency of Rxn 13. The correction factor was used to fit the model to the NO_2^- results from bench scale scenario 16. The correction factor (γ) calculated to be 0.56. Preliminary sensitivity analysis indicates that the model is much more dependent on γ than on inclusion of NO_2^- photolysis. For this purpose, a less fine-grained model (lower time resolution) was run to simulate scenario 16 that included terms for the rate of light absorption by nitrite and a user-controlled photolysis quantum yield. The photolysis quantum yield and γ were varied to examine the effect of each on the model fit to the nitrite data, as indicated by the residual sum of squares. The photolysis of nitrite exclusively produces ·OH, and literature reports indicate that the quantum yield for this process at circumneutral pH is somewhere in the range of 2 to 15%.[11] Fixing γ at 0.56 and increasing the photolysis quantum yield from 0 to 15% increased the sum of squares (decreased the goodness of fit) from 1.3×10^{-10} to 2.2×10^{-10}. In contrast, the same magnitude of impact on the fits could be obtained by fixing the photolysis quantum yield at 0% and changing γ from 0.56 to either 0.53 or 0.61 (only a small percent

change in thermal NO_2^- loss). These results indicate that the primary mechanism for NO_2^- loss is reaction with •OH and that photolysis is essentially negligible in the experimental waters.

IV. Model Results

Figure 8 shows the model results for NO_2^-, •OH, and H_2O_2 in comparison to the experimental values from bench scale scenario 16. The first step was to fit the •OH concentration versus fluence (or time) using equations B10 to B12 in Attachment B along with experimental NO_2^- and H_2O_2 concentrations in order to find a value of $k_{s,w}$ that minimized the sum of squared residuals between the model and the experimental data. As noted above, the best fit was obtained with $k_{s,w} = 8.35x10^4\ s^{-1}$, and this value was used in all subsequent modelling. Next, the full model was run (see Attachment B) to fit the NO_2^- data leaving γ as a fitting parameter; the best fit value of γ was 0.56 (i.e., thermal reactions of radical intermediates appear to regenerate 44% of NO_2^- destroyed by •OH). Note that both $k_{s,w}$ and γ will be water quality dependent. While the dependence for $k_{s,w}$ is well understood, that is not the case for γ, where unknown reactions of $•NO_2$ and •NO with DOC may be important.

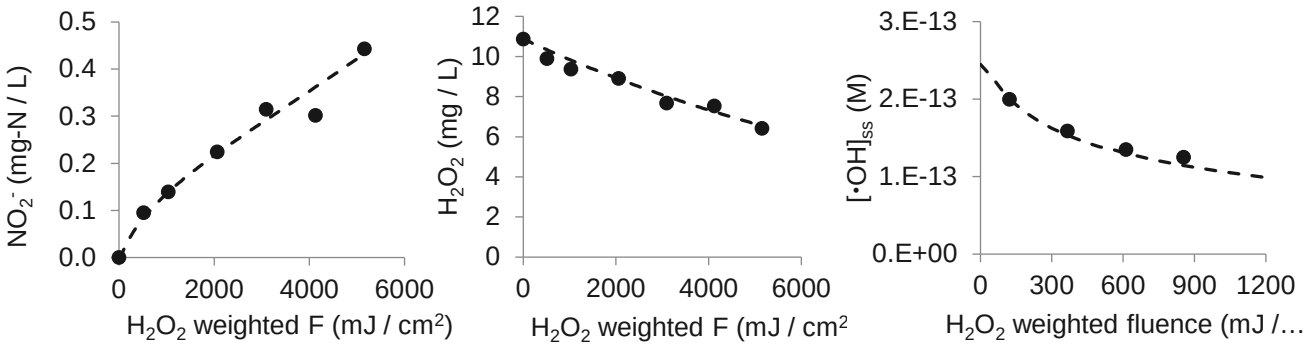

Figure 8. Experiment 16 and model results for NO_2^-, H_2O_2, and •OH. Experimental data are the symbols, model results are the dashed lines.

Using the values for $k_{s,w}$ and γ derived by fitting the data from scenario 16, the model was applied to simulate single point (1000 mJ cm^{-2}) results from bench scale experiments 9 to 16 (Table 3). In these calculations, approximately 20 time intervals were used in the model to achieve the final desired fluence, and model $[•OH]_{ss}$ values over this period were averaged for comparison to experimental values derived from the slope of 1st order pCBA loss over the same period. The model and experimental results are compared in Table 4 and Figure 9.

As noted in Section II, the levels of NO_2^- reached here account for between one half and three quarters of all the •OH scavenging in the solutions, indicating that NO_2^- could negatively impact UV/H_2O_2 AOP performance.

Table 4. Experimental and model NO_2^- and •OH results for bench scale tests 9 through 16.

	Total NO_3^-	Added H_2O_2	Depth	H_2O_2 weighted F	NO_2^- (mg-N/L)		$[OH]_{ss}$ (M)	
Exp. ID	*mg-N/L*	*mg/L*	*cm*	*mJ cm^{-2}*	*Exptl*	*Model*	*Exptl*	*Model*
9	1.24	0	3	1000	0.09	0.10	8.0E-14	4.7E-14
10	11.24	0	3	1000	0.21	0.38	1.3E-13	8.5E-14
11	1.24	10	3	1000	0.14	0.07	3.5E-13	3.1E-13
12	11.24	10	3	1000	0.30	0.29	2.5E-13	2.1E-13
13	1.24	0	9	1000	0.06	0.06	3.7E-14	1.9E-14
14	11.24	0	9	720	0.09	0.14	5.8E-14	5.7E-14
15	1.24	10	9	1000	0.10	0.04	2.3E-13	2.0E-13
16	11.24	10	9	1000	0.19	0.14	1.6E-13	1.5E-13

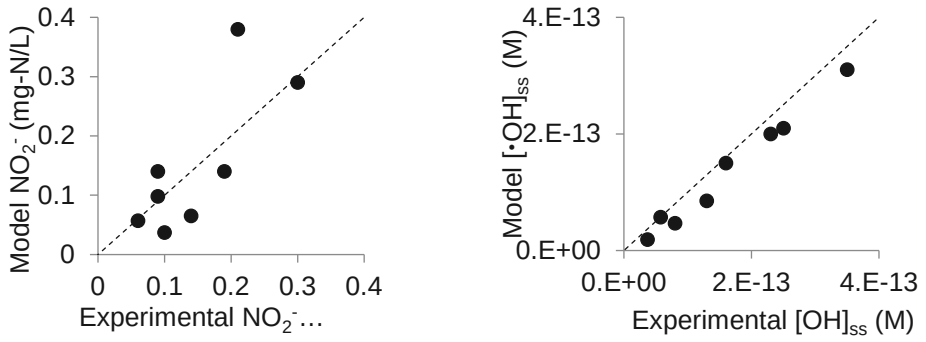

Figure 9. Model NO_2^- and •OH results plotted versus results for bench scale experiments 9 through 16 at the final fluence values indicated in Table 5. Dashes are the 1:1 lines.

On balance, the model matched the experiment quite well, particularly with regard to •OH. Consistent with the experimental results, the model predicts that in the absence of H_2O_2, elevated NO_3^- levels enhance •OH radical production, despite the scavenging effect from NO_2^-. In contrast, and also consistent with experiment, the model predicts that with 10 mg/L H_2O_2, NO_3^- at 10 mg-N/L should decrease $[•OH]_{ss}$ by roughly 30%. With regard to NO_2^-, a tendency was noted for the model to overpredict NO_2^- levels with added NO_3^- in the absence of H_2O_2 and to underpredict NO_2^- levels with added H_2O_2 in the absence of additional NO_3^-. While the cause of these discrepancies is unknown, larger than expected experimental production rates of NO_2^- in the presence of H_2O_2 was reported by Sharpless *et al.*, 2003,[5] who tentatively ascribed the phenomenon to a combination of reduced NO_2^- reaction with •OH due to •OH scavenging by H_2O_2 was present and reaction between O_2^- (from Rxn 12) and $•NO_2$ to regenerate NO_2^-. The model should be accounting for both of these things via a time dependent $k_{s,tot}$ (see Attachment B) and

the use of the γ parameter, which ostensibly includes contributions from $O_2^{\bullet-}$. However, the discrepancies between model and experiment suggest that additional factors need to be considered for more accurate modeling of NO_2^-.

The model was also run to examine the effects of increasing NO_3^- with H_2O_2 fixed at 10 mg/L and a water depth of 9 cm. The results are shown in Figure 10. The model predicts that

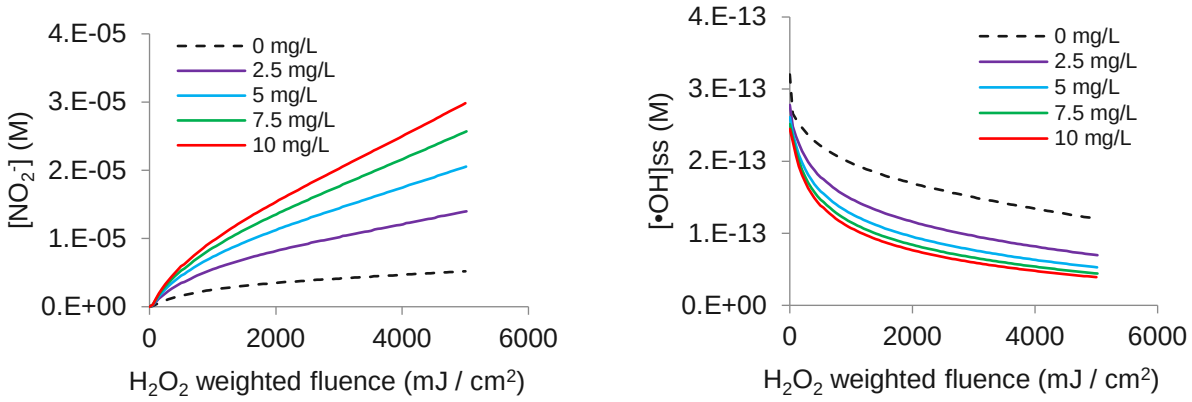

Figure 10. Model NO_2^- and •OH results for various levels of NO_3^- as indicated in the legends. H_2O_2 at 10 mg/L, water depth 9 cm.

with MP irradiation of the LA water, which has very low TOC (approx. 0.4 mg-C/L) and in which a major fraction of the light below 250 nm is absorbed by NO_3^- (10% at 250 nm and 89% at 220 nm in the raw water itself), NO_2^- quickly becomes a major •OH scavenger. This leads to continuously decreasing $[\bullet OH]_{ss}$ with increasing fluence and a negative effect of NO_3^- at all concentrations.

V. Conclusion

Experimental and model results indicate that NO_3^- detrimentally affects UV/H_2O_2 AOP performance in the LA test water when MP irradiation is used. This effect can be ascribed to the NO_2^- formed during NO_3^- photolysis, which is produced mainly at wavelengths below 250 nm, as shown in Figure 11 (right panel). This is due to the fact that both NO_3^- absorption and NO_2^- quantum yields are highest in this wavelength range (Fig 11, left panel). Elevated NO_3^- will likely be detrimental to MP-UV/H_2O_2 applications in any water, despite the additional OH that is produced, due to the production of NO_2^-. However, the data in Fig 11 indicate that LP-UV should not suffer this effect nearly as much. Indeed, the results from the bench scale experiments 23 and 24 showed a net neutral effect of NO_3^- addition with LP-UV.[1]

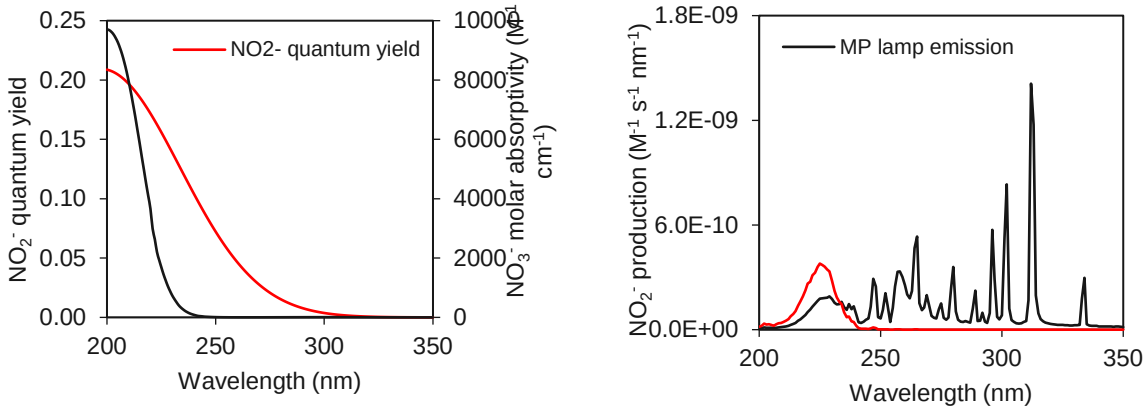

Figure 11. (left) NO_3^- molar absorptivity and NO_2^- quantum yields (left). (right) MP lamp emission spectrum and spectral production rates of NO_2^- in raw LA water with 9 cm water depth. NO_2^- quantum yields are a Gaussian fit to data from ref. 10.

Concluding remarks

Findings from this study highlight scenarios in which the presence of NO_3^- in different water matrices can enhance or inhibit radical production. Although NO_2^- and •OH are simultaneously produced (Rxns 1 and 2) when NO_3^- is irradiated with MPUV, the average •OH production was observed to be lower in samples with added NO_3^- (Figure 4) due to scavenging by NO_2^-. Additional research would need to be conducted to determine the optimum MPUV dose required to minimize NO_2^- formation and maximize •OH production in NO_3^- impacted waters.

References

1. Klassen, N. V.; Marchington, D.; McGowan, H. C. E. H2O2 determination by the I3 − method and by KMnO4 titration. Anal. Chem. **1994**, 66, 2921−2925.

2. Bolton, J. R.; Linden, K. G. Standardization of methods for fluence (UV dose) determination in bench scale UV experiments. *ASCE J. Environ. Eng.* **2003**, *129*, 209−215

3. Ulliman, S.; McKay, G.; Rosario-Ortiz, F. L.; Linden, K. Low levels of iron enhance UV/H2O2 efficiency at neutral pH. Water Res. **2017**.

4. Buxton, G.V., Greenstock, C.L., Helman, W.P., Ross, A.B., Tsang, W. Critical Review of rate constants for reactions of hydrated electrons, hydrogen atoms and hydroxyl radicals (•OH/•O^-) in aqueous solution. *J. Phys. Chem. Ref. Data* **1988**, *17*, 513-886.

5. Sharpless, C.M.; Page, M.A.; Linden, K.G. Impact of hydrogen peroxide on nitrite formation during UV disinfection. *Wat. Res.* **2003**, *37*, 4730-4736

6. Keen, O.S., Love, N.G., Linden, K.G. The role of effluent nitrate in trace organic chemical oxidation during UV disinfection. Water Res. **2012**, *46*, 5224–5234. https://doi.org/10.1016/j.watres.2012.06.052

7. Schwarzenbach, R.P.; Gschwend, P.M.; Imboden, D.M. *Environmental Organic Chemistry, 2nd Ed.* (Chapter 16). Hoboken, NJ, Wiley Interscience, 2003,

8. Notre Dame Radiation Laboratory/National Institutes of Standards and Technology (NDRL/NIST) Solution Kinetics Database, http://kinetics.nist.gov/solution/ (accessed 10/12/17). Values apply to aqueous solution and are rounded averages of results where multiple values exist.

9. Goldstein, S.; Aschengrau, D.; Diamant, Y.; Rabani, J. Photolysis of aqueous H_2O_2: quantum yield and applications for polychromatic UV actinometry in photoreactors. *Environ. Sci. Technol.* **2007**, *41*, 7486-7490.

10. Goldstein, S.; Rabani, J. Mechanism of nitrite formation by nitrate photolysis in aqueous solutions: the role of peroxynitrite, nitrogen dioxide, and hydroxyl radical. *J. Am. Chem. Soc.* **2007**, *129*, 10597-10601

11. Mack, J.; Bolton, J. Photochemistry of nitrite and nitrate in aqueous solution: a review. *J. Photochem. Photobiol. A: Chem.* **1999**, *128*, 1-13

ATTACHMENT A: Data from Experimental Work

Table A1: MPa. Water quality data. Selected water quality parameters were measured before and after UV exposure, the results are presented below. Excel copy available upon request. Max UV dose for MPUV experiments at a water depth 3 cm and 8.88 cm is ~900 mJ/cm^2 and 800 mJ/cm^2, respectively. Max UV dose for LPUV is 1000 mJ/cm^2.

	Lamp:		Medium pressure UV									
	Experiment ID:		1	1d	2	2d	3	3d	4	4d		
Experimental Parameters	Water Type		Mili-Q									
	Nitrate (mg/L NO3 as N)		0		10		0		10			
	H_2O_2 (mg/L)		0		0		10		10			
	Water Depth (cm)		3		3		3		3			
	UV Dose (mJ/cm^2)											
Measurements	UVA	0	0.0158		0.0182		0.0160		0.0182			
		max	0.0193	0.0188	0.0212	0.0159	0.0168	0.0177	0.0171	0.0156		
	TOC (mg/L)	0	614		614		614		307			
		max	398		688		579		507			
	H_2O_2 (mg/L)	0	–	–	–	--	10.31	10.31	9.83	9.54		
		max	–	–	–	--	9.28	9.41	9.38	8.60		
	nitrate (mg/L)	0	–	–	10.2		–	--	10.2			
		max	–	–	10.1	10.05	–	--	11	11		
	nitrite (mg/L)	0	–	–	DL		–	--	DL			
		max	–	–	0.1795	0.1835	–	--	0.139	0.143		
	alkalinity (mg/L as CaCO3)	0	–	–	–	--	–	--	–	–		
		max	–	–	–	--	–	--	–	–		
	pH	0	–	–	–	--	–	--	–	–		
		max	–	–	–	--	–	--	–	–		
	E_o (mW/cm^2)		1.579	1.579	0.765	0.765	1.571	1.571	0.765	0.765		
	pCBA degradation (s^{-1})		0.000E+00	1.827E-06	1.934E-03	1.963E-03	4.142E-03	4.119E-03	3.187E-03	3.337E-03		
	[OH]ss (M)		0.000E+00	3.655E-16	3.868E-13	3.927E-13	8.285E-13	8.238E-13	6.375E-13	6.674E-13		

Table A2: MPb. Water quality data. Selected water quality parameters were measured before and after UV exposure, the results are presented below. Excel copy available upon request. Max UV dose for MPUV experiments at a water depth 3 cm and 8.88 cm is ~900 mJ/cm^2 and 800 mJ/cm^2, respectively. Max UV dose for LPUV is 1000 mJ/cm^2.

	Lamp:		Medium pressure UV									
	Experiment ID:		5	5d	6	6d	7	7d	8	8d		
Experimental Parameters	Water Type		Mili-Q									
	Nitrate (mg/L NO3 as N)		0		10		0		10			
	H_2O_2 (mg/L)		0		0		10		10			
	Water Depth (cm)		8		8		8		8			
	UV Dose (mJ/cm^2)											
Measurements	UVA	0	0.0158		0.0279		0.0160		0.0182			
		max	0.0181	0.0190	0.0203	0.0212	0.0166	0.0165	0.0179	0.0188		
	TOC (mg/L)	0	307		307		307		307			
		max	769		669		613		546			
	H_2O_2 (mg/L)	0	–	–	–	--	10.40	10.87	9.69	9.33		
		max	–	–	–	--	9.02	10.62	8.99	8.99		
	nitrate (mg/L)	0	–	–	10.2		–	--	10.2	10.3		
		max	–	–	10.3	9.93	–	--	11.3	10.9		
	nitrite (mg/L)	0	–	–	DL		–	--	DL			
		max	–	–	0.1325	0.1415	–	--	0.0925	0.103		
	alkalinity (mg/L as CaCO3)	0	–	–	–	--	–	--	–	–		
		max	–	–	–	--	–	--	–	–		
	pH	0	–	–	–	--	–	--	–	–		
		max	–	–	–	--	–	--	–	–		
	E_o (mW/cm^2)		1.057	1.057	0.479	0.479	1.051	1.051	0.479	0.479		
	pCBA degradation (s^{-1})		1.651E-06	0.000E+00	7.998E-04	7.905E-04	4.303E-03	4.242E-03	2.040E-03	1.820E-03		
	[OH]ss (M)		3.302E-16	0.000E+00	1.600E-13	1.581E-13	8.607E-13	8.484E-13	4.080E-13	3.640E-13		

Table A3: MPc. Water quality data. Selected water quality parameters were measured before and after UV exposure, the results are presented below. Excel copy available upon request. Max UV dose for MPUV experiments at a water depth 3 cm and 8.88 cm is ~900 mJ/cm^2 and 800 mJ/cm^2, respectively. Max UV dose for LPUV is 1000 mJ/cm^2.

	Lamp:		Medium pressure UV									
	Experiment ID:		9	9d	10	10d	11	11d	12	12d		
Experimental Parameters	Water Type		LA Water									
	Nitrate (mg/L NO3 as N)		Native		10		Native		10			
	H_2O_2 (mg/L)		0		0		10		10			
	Water Depth (cm)		3		3		3		3			
	UV Dose (mJ/cm^2)											
Measurements	UVA	0	0.0256		0.0279		0.0256		0.0279			
		max	0.0397	0.0358	0.0405	0.0412	0.0336	0.0377	0.0549	0.0375		
	TOC (mg/L)	0	432		432		432		432			
		max	1058		4510		1152		1747			
	H_2O_2 (mg/L)	0	–	–	–	--	9.92	10.14	10.04	9.79		
		max	–	–	–	--	8.53	8.64	8.48	8.47		
	nitrate (mg/L)	0	1.24		10.2		1.24		10.4			
		max	1.175	1.165	9.72	10.05	1.47	1.46	11.45	11.2		
	nitrite (mg/L)	0	DL		DL		DL		DL			
		max	0.085	0.0875	0.2085	0.2085	0.1415	0.1365	0.294	0.3165		
	alkalinity (mg/L as CaCO3)	0	168		168		168		168			
		max	162		146	--	162	--	162	–		
	pH	0	7.40		7.40		7.40		7.40			
		max	7.7	7.93	7.8	7.96	7.98	7.23	7.3	7.26		
	E_o (mW/cm^2)		1.116	1.116	0.737	0.737	1.116	1.116	0.737	0.737		
	pCBA degradation (s^{-1})		3.957E-04	3.917E-04	6.376E-04	6.260E-04	1.734E-03	1.813E-03	1.256E-03	1.242E-03		
	[OH]ss (M)		7.914E-14	7.834E-14	1.275E-13	1.252E-13	3.468E-13	3.627E-13	2.512E-13	2.484E-13		

Table A4: MPd. Water quality data. Selected water quality parameters were measured before and after UV exposure, the results are presented below. Excel copy available upon request. Max UV dose for MPUV experiments at a water depth 3 cm and 8.88 cm is ~900 mJ/cm^2 and 800 mJ/cm^2, respectively. Max UV dose for LPUV is 1000 mJ/cm^2.

	Lamp:		Medium pressure UV											
	Experiment ID:		13		13d		14		14d		15		15d	
Experimental Parameters	Water Type		LA Water											
	Nitrate (mg/L NO3 as N)		Native				10				Native			
	H_2O_2 (mg/L)		0				0				10			
	Water Depth (cm)		8				8				8			
	UV Dose (mJ/cm^2)													
Measurements	UVA	0	0.0256				0.0279				0.0256			
		max	0.0409		0.0359		0.0421		0.0399		0.0339		0.0374	
	TOC (mg/L)	0	432				432				432			
		max	1035				1051				1048			
	H_2O_2 (mg/L)	0	–		–		–		--		8.91		9.51	
		max	–		–		–		--		8.45		8.84	
	nitrate (mg/L)	0	1.24				10.2				1.24			
		max	1.18		1.18		10.4		10.2		1.405		1.445	
	nitrite (mg/L)	0	DL				DL				DL			
		max	0.059		0.0555		0.085		0.0855		0.097		0.093	
	alkalinity (mg/L as CaCO3)	0	168				168				168			
		max	166		–		164		--		158		--	
	pH	0	7.40				7.40				7.40			
		max	6.67		7.88		7.91		7.1		7.26		7.07	
	E_o (mW/cm^2)		0.617		0.617		0.636		0.636		0.599		0.599	
	pCBA degradation (s^{-1})		1.833E-04		1.855E-04		2.574E-04		2.632E-04		1.144E-03		1.161E-03	
	[OH]ss (M)		3.667E-14		3.709E-14		5.147E-14		5.264E-14		2.289E-13		2.322E-13	

Lamp:	Medium pressure UV							
Experiment ID:	16		16d					
Water Type	LA Water							
Nitrate (mg/L NO3 as N)	10							
H_2O_2 (mg/L)	10							
Water Depth (cm)	8							
UV Dose (mJ/cm^2)								
UVA	0	0.0279						
	max	0.0413		0.0383				
TOC (mg/L)	0	432						
	max	1083						
H_2O_2 (mg/L)	0	9.75		9.78				
	max	8.69		8.63				
nitrate (mg/L)	0	10.2						
	max	11.55		11.55				
nitrite (mg/L)	0	DL						
	max	0.19		0.1875				
alkalinity (mg/L as CaCO3)	0	168						
	max	168		–				
pH	0	7.40						
	max	7.69		7.89				
E_o (mW/cm^2)		0.441		0.441				
pCBA degradation (s^{-1})		8.230E-04		8.011E-04				
[OH]ss (M)		1.646E-13		1.602E-13				

Table A5: LPa. Water quality data. Selected water quality parameters were measured before and after UV exposure, the results are presented below. Excel copy available upon request. Max UV dose for MPUV experiments at a water depth 3 cm and 8.88 cm is ~900 mJ/cm^2 and 800 mJ/cm^2, respectively. Max UV dose for LPUV is 1000 mJ/cm^2.

	Lamp:		Low Pressure UV											
	Experiment ID:		17		17d		18		18d		19		19d	
Experimental Parameters	Water Type		Mili-Q											
	Nitrate (mg/L NO3 as N)		0				10				0			
	H_2O_2 (mg/L)		0				0				10			
	Water Depth (cm)		3				3				3			
	UV Dose (mJ/cm^2)													
Measurements	UVA	0	0.0158				0.0182				0.0160			
		max	0.0193		0.0184		0.0224		0.0229		0.0115		0.0130	
	TOC (mg/L)	0	614				614				614			
		max	746				747				666			
	H_2O_2 (mg/L)	0	–		–		–		--		9.90		9.90	
		max	–		–		–		--		8.45		8.96	
	nitrate (mg/L)	0	–		–		10.3				–		--	
		max	–		–		10.5		10.5		–		--	
	nitrite (mg/L)	0	–		–		DL				–		--	
		max	–		–		0.015		0.015		–		--	
	alkalinity (mg/L as CaCO3)	0	–		–		–		--		–		--	
		max	–		–		–		--		–		--	
	pH	0	–		–		–		--		–		--	
		max	–		–		–		--		–		--	
	E_o (mW/cm^2)		0.791		0.791		0.790		0.790		0.791		0.791	
	pCBA degradation (s^{-1})		0.000E+00		4.189E-06		1.357E-04		1.432E-04		3.635E-03		3.575E-03	
	[OH]ss (M)		0.000E+00		8.377E-16		2.715E-14		2.864E-14		7.269E-13		7.150E-13	

	Lamp:		Low Pressure UV											
	Experiment ID:		20		20d									
Experimental Parameters	Water Type		Mili-Q											
	Nitrate (mg/L NO3 as N)		10											
	H_2O_2 (mg/L)		10											
	Water Depth (cm)		3											
	UV Dose (mJ/cm^2)													
Measurements	UVA	0	0.0182											
		max	0.0184		0.0184									
	TOC (mg/L)	0	614											
		max	745											
	H_2O_2 (mg/L)	0	9.87		9.88									
		max	9.74		9.20									
	nitrate (mg/L)	0	10.3											
		max	11.6		11.4									
	nitrite (mg/L)	0	DL											
		max	0.017		0.016									
	alkalinity (mg/L as CaCO3)	0	–		–									
		max	–		–									
	pH	0	–		–									
		max	–		–									
	E_o (mW/cm^2)		0.790		0.790									
	pCBA degradation (s^{-1})		3.365E-03		3.226E-03									
	[OH]ss (M)		6.730E-13		6.451E-13									

Table A6: LPb. Water quality data. Selected water quality parameters were measured before and after UV exposure, the results are presented below. Excel copy available upon request. Max UV dose for MPUV experiments at a water depth 3 cm and 8.88 cm is ~900 mJ/cm^2 and 800 mJ/cm^2, respectively. Max UV dose for LPUV is 1000 mJ/cm^2.

	Lamp:		Low Pressure UV													
	Experiment ID:		21		21d		22		22d		23		23d		24		24d	
Experimental Parameters	Water Type		LA Water													
	Nitrate (mg/L NO3 as N)		Native				10				Native				10			
	H_2O_2 (mg/L)		0				0				10				10			
	Water Depth (cm)		3				3				3				3			
	UV Dose (mJ/cm^2)																	
Measurements	UVA	0	0.0256				0.0279				0.0256				0.0279			
		max	0.0323		0.0324		0.0434		0.0362		0.0374		0.0322		0.0460		0.0394	
	TOC (mg/L)	0	432				432				432				432			
		max	1251				1221				1890				1575			
	H_2O_2 (mg/L)	0	–		–		–		--		10.02				10.43			
		max	–		–		–		--		9.17				9.5		9.18	
	nitrate (mg/L)	0	1.23				10.3				1.23				10.3			
		max	1.275		1.25		10.25		10.15		1.445		1.405		11.6		11.45	
	nitrite (mg/L)	0	DL				DL				DL				DL			
		max	DL				DL				DL				0.024		0.017	
	alkalinity (mg/L as CaCO3)	0	168				168				168				168			
		max	94		–		82		--		79		--		82		–	
	pH	0	7.40				7.40				7.40				7.40			
		max	7.73		7.86		7.73		7.96		7.84		7.98		7.78		7.94	
	E_o (mW/cm^2)		0.774		0.774		0.768		0.768		0.774		0.774		0.768		0.768	
	pCBA degradation (s^{-1})		0.000E+00		0.000E+00		4.509E-06		1.723E-05		1.303E-03		1.444E-03		1.359E-03		1.360E-03	
	[OH]ss (M)		0.000E+00		0.000E+00		9.019E-16		3.447E-15		2.607E-13		2.887E-13		2.718E-13		2.720E-13	

ATTACHMENT B: Kinetic Model Calculations

Flowchart of Main Model Calculations

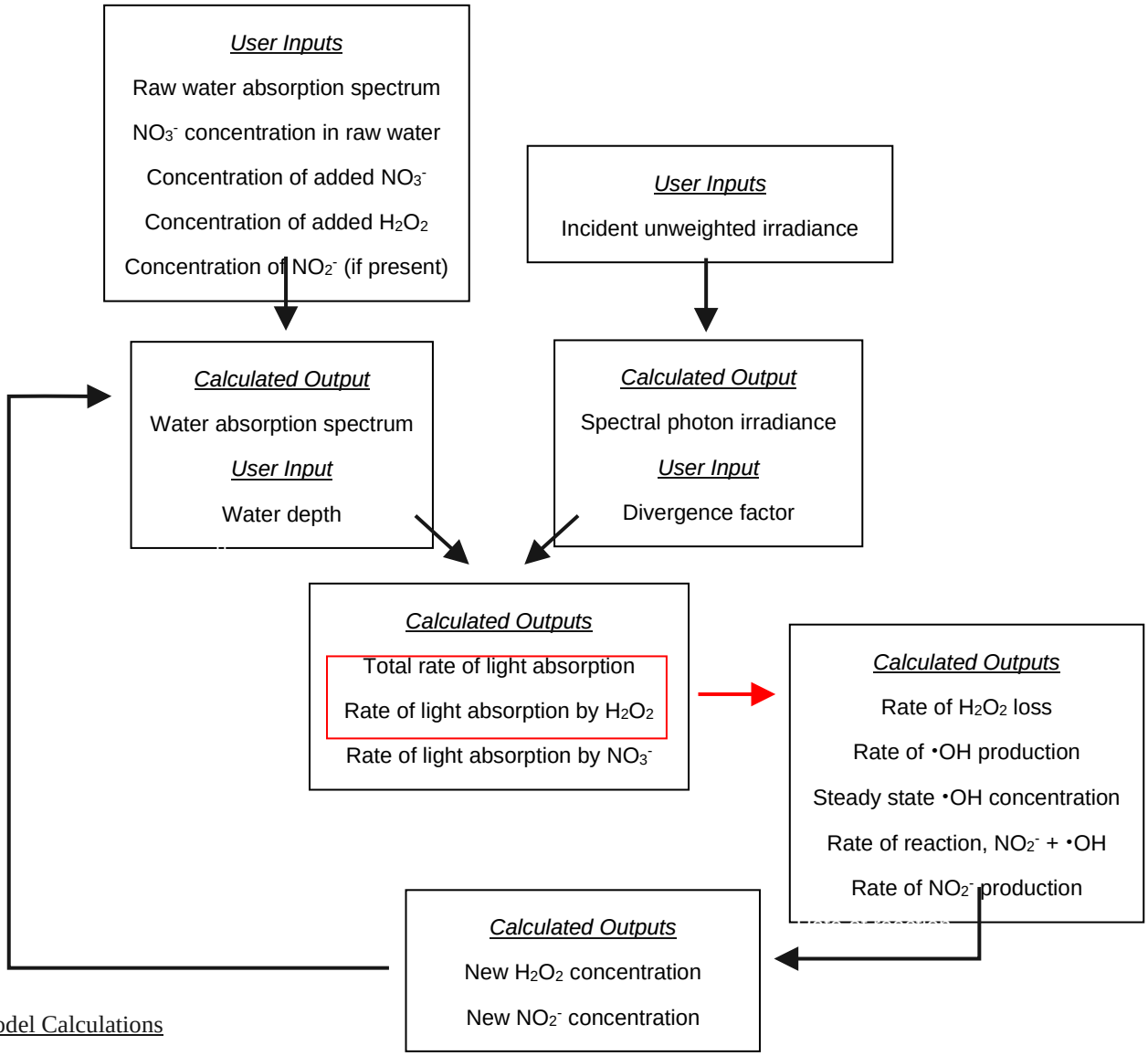

Model Calculations

The kinetic model runs in Microsoft Excel using one master spreadsheet ("Inputs and results.xlsx") and 10 "slave" spreadsheets ("Model step A.xlsx" through "Model step J.xlsx"), each of which carries out the calculations described below for 10 time intervals, where step B calls on the final results of step A, step C calls on the final results of step B, etc. Overall, the model includes 101 discrete time steps (100 time intervals) between which several values are iterated.

Several quantities in the model require summation over the relevant spectral range, and such summations were performed from 200 to 350 nm with 1 nm resolution ($\Delta\lambda$). Such spectral quantities are denoted with λ in parentheses, such as $R_{a,H2O2}(\lambda,t)$, and include units of nm^{-1}; $R_{a,H2O2}(\lambda,t)$, for example, is the spectral rate of light

absorption by H_2O_2 at time t, with units of Es L^{-1} s^{-1} nm^{-1}. As just indicated, quantities denoted with t in parentheses, such as $a_\lambda(t)$, are time dependent. Quantities denoted with a subscripted λ, such as a_λ, vary with wavelength but do not have spectral units. Details about photolysis quantum yields and values of bimolecular rate constants involving •OH can be found in Sec. II of the main report.

The model begins by calculating the absorption coefficients of the solution, $a_{\lambda,t}$ (cm^{-1}), via Eqn A1, with time set to 0. Here, $a_{\lambda,w}$ is the decadal absorption coefficient of the raw water, $\varepsilon_{\lambda,NO3-}$, $\varepsilon_{\lambda,H2O2}$, and are the molar absorptivity of NO_3^-, H_2O_2, and NO_2^-, respectively.

$$a_\lambda(t) = a_{\lambda,w} + [NO_3^-]\,\varepsilon_{\lambda,NO3-} + [H_2O_2](t)\,\varepsilon_{\lambda,H2O2} + [NO_2^-](t)\,\varepsilon_{\lambda,NO2-} \quad \text{(B1)}$$

The NO_3^- concentration is input as any supplemental NO_3^- added to the raw water. Based on experimental data from bench scale testing showing negligible change in $[NO_3^-]$ up to 5000 mJ cm^{-2} (Attachment A), it remains fixed at its initial value throughout the calculations. The initial concentration of H_2O_2 is set based on the amount added to the water; photolysis (Rxn 9 in the main report) causes it to decrease with time according to Eqn B2, where $R_{a,H2O2}$ (Es L^{-1} s^{-1}) is the rate of light absorption by H_2O_2 (Eqns B3-B5), Φ_{H2O2} is the H_2O_2 photolysis quantum yield (see main report sec. III), and Δt is the user determined time interval between time t and t-1. To compare with results from the bench scale experiments, the time interval was set to achieve total H_2O_2 weighted fluences between 1000 and 5000 mJ cm^{-2}.

$$[H_2O_2](t) = [H_2O_2](t\text{-}1) - R_{a,H2O2}(t\text{-}1)\,\Phi_{H2O2}\,\Delta t \quad \text{(B2)}$$

$$R_{a,H2O2}(t) = \sum_\lambda R_{a,H2O2}(\lambda,t)\,\Delta\lambda \quad \text{(B3)}$$

$$R_{a,H2O2}(\lambda,t) = R_{a,tot}(\lambda,t)\left(\frac{[H_2O_2](t)\,\varepsilon_{\lambda,H2O2}}{a_\lambda(t)}\right) \quad \text{(B4)}$$

$$R_{a,tot}(\lambda,t) = \frac{E_p^0(\lambda)\,DF\left(1-10^{-a_\lambda(t)\,z}\right)\text{x }1000}{z} \quad \text{(B5)}$$

In eqns B4 and B5, $R_{a,tot}$ is the rate of light absorption by the solution (Es L^{-1} s^{-1}), $E_p^0(\lambda)$ is the spectral photon irradiance (Es cm^{-2} s^{-1} nm^{-1}), DF is the divergence factor (unitless)[2], and z is the water depth (cm). Irradiance values for input to the model are not weighted in any way, and were set here to roughly match experimental values from the bench scale tests. Divergence factors depend on the water depth and were set to equal to experimental values from the bench scale tests.

In Eqn B1, the initial concentration of NO_2^- is zero. It is produced by NO_3^- photolysis (Rxn 11in main report) and thermal reactions that are not accounted for directly due to lack of detailed knowledge of the various radical concentrations needed in order to do so. Rather, those reactions are accounted for as an efficiency adjustment to the rate of removal of NO_2^- by reaction with •OH (γ, Part II, Secs. III and IV in main report). Considering this, the NO_2^- concentration over time is calculated via Eqns B6 to B9.

$$[NO_2^-](t) = [NO_2^-](t\text{-}1) + [R_{NO2\text{-}}(t\text{-}1) - \gamma R_{OH,NO2\text{-}}(t\text{-}1)]\,\Delta t \quad \text{(B6)}$$

$$R_{NO2\text{-}}(t) = \sum_\lambda R_{a,NO3\text{-}}(\lambda,t)\,\Phi_{NO2\text{-},\lambda} \quad \text{(B7)}$$

$$R_{a,NO3\text{-}}(\lambda,t) = R_{a,tot}(\lambda,t)\left(\frac{[NO_3^-]\,\varepsilon_{\lambda,NO3\text{-}}}{a_{\lambda,t}}\right) \quad \text{(B8)}$$

$$R_{OH,NO2\text{-}}(t) = k_{OH,NO2\text{-}}[NO_2^-](t)[\bullet OH]_{ss}(t) \quad \text{(B9)}$$

Here, $R_{NO2\text{-}}$ is the rate of NO_2^- production (M s^{-1}), $R_{OH,NO2\text{-}}$ is the rate of reaction between NO_2^- and •OH (M s^{-1}), $R_{a,NO3\text{-}}$ is the rate of light absorption by NO_3^- (Es L^{-1} s^{-1}), and other symbols have been previously defined (see Sec. II of the main report).

Equation B9 requires a value for $[\bullet OH]_{ss}$ at each time point. This is calculated using Eqn B10. Here, R_{OH} is the production rate of •OH (M s^{-1}), which is calculated assuming only contributions from H_2O_2 and NO_3^- photolysis (Eqn B11). The pseudo-1st order rate constant for •OH scavenging, k_s (s^{-1}), is calculated via Eqn B12, where $k_{s,w}$ was fit to 8.35×10^4 s^{-1} as discussed in Part II, Sec. III of the main report, and the time dependent H_2O_2 and NO_2^- concentrations were computed as described above.

$$[\bullet OH]_{ss}(t) = \frac{R_{OH}(t)}{k_s(t)} \quad \text{(B10)}$$

$$R_{OH}(t) = R_{a,H2O2}(t)\,\Phi_{H2O2} + \sum_\lambda R_{a,NO3\text{-}}(\lambda,t)\,\Phi^N_{OH,\lambda} \quad \text{(B11)}$$

$$k_s(t) = k_{s,w} + k_{OH,H2O2}[H_2O_2](t) + k_{OH,NO2}[NO_2^-](t) \quad \text{(B12)}$$

Appendix B Scavenging Report

Scavenging Demand Test: LADWP Waters

Linden Laboratory – University of Colorado Boulder

May 2018

Background and Methods

Water Samples

Samples collected by the Los Angeles Department of Water and Power (LADWP), were from wells NH037, TJ, and NHC. The samples were shipped on ice to the University of Colorado Boulder. Samples were stored at 4°C until water quality analysis and background scavenging testing. Pertinent water quality parameters were determined prior to Advanced Oxidation Process (AOP) treatment (Table 1). An Orion Star A211 meter was used for pH measurements. UV absorbance was measured using a 1 cm path length quartz cuvette by a Cary Bio 100 spectrophotometer (Varian Inc., Palo Alto, TX). Alkalinity was determined using a Hach Digital Titrator according to Hach method 8203. Total organic carbon (TOC) was measured by Sievers 5301 C instrument. Nitrite and nitrate were determined using Hach kits TNT 839 and 835, respectively.

Background Scavenging

Background radical scavenging experiments were carried out in duplicate (test 1 and test 2) for each well water using approximately 8 mg/L of hydrogen peroxide and 500 µg/L of para-chlorobenzoic acid (pCBA) as a probe to measure hydroxyl radical production and scavenging. pCBA reacts with hydroxyl radicals at a rate which far exceeds its reaction rate with UV light, making it an ideal probe to measure the formation and scavenging of hydroxyl radicals in UV-based AOPs. Low Pressure UV - hydrogen peroxide (LPUV/H_2O_2) scavenging experiments were performed using a quasi-collimated LPUV system setup for dual exposures. Instead of containing a single collimated hole (Figure 1), the collimated beam had two side-by-side holes separated by a light-impermeable barrier.

Four LPUV lamps (15 watt, #G15T8) were housed above two 4-inch apertures equipped with a manual shutter. Incident UV irradiance (1.014 mW/cm^2) was measured by a calibrated radiometer (International Light Inc., Model 1700/SED 240/W). UV fluence (i.e. dose) was calculated by multiplying the average irradiance by the exposure time in seconds. The average irradiance was determined by correcting the incident irradiance (radiometer reading) for sample depth, absorbance at 254 nm, sample reflectance, and petri factor (Bolton and Linden 2003).

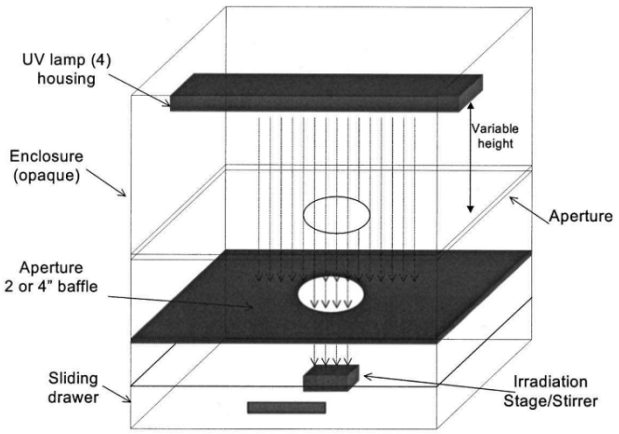

Figure 1. Labeled bench-scale quasi-collimated LP UV system (Bolton and Linden, 2003)

Samples were analyzed for the concentration of the radical probe, pCBA, using an Agilent 1100 series high performance liquid chromatograph (HPLC) and UV detector (at 235 nm) equipped with a reverse phase C-18 column.

The concentration of steady state hydroxyl radical concentration, [HO·], was then calculated using the following relationship:

$$\ln\frac{[pCBA]}{[pCBA]_o} = \frac{-k_{HO\cdot,pCBA}[HO\cdot]_{ss}}{E_o} \times F \qquad (1)$$

where E_0 is the average fluence rate (mW/cm^2), F is the fluence (mJ/cm^2) (i.e., UV dose) and $k_{HO\cdot,pCBA}$ is a time-based reaction rate constant between pCBA and hydroxyl radicals (M^{-1}s^{-1}).

In this equation, the quantity $\frac{-k_{HO\cdot,pCBA}[HO\cdot]}{E_o}$ is the slope of the plot of ln([pCBA]/[pCBA]$_0$) vs F, and [HO·] can be calculated as:

$$[HO\cdot] = \frac{-slope E_o}{k_{HO\cdot,pCBA}} \qquad (2)$$

The value for $k_{HO\cdot,pCBA}$ has been reported as 5 x 10^9 M^{-1}s^{-1} by Buxton *et al.*, 1988.

The steady state UV/H_2O_2 model by Glaze et al. (1995) can then be rearranged to calculate the total hydroxyl radical scavenging coming from the sample background:

$$\sum k_s[S] = \frac{E_o \varepsilon_{254} \Phi [H_2O_2]}{U_{254}} \times \frac{1}{[HO\cdot]} \qquad (3)$$

where k_s is the hydroxyl radical reaction rate constant for a given scavenging compound (M^{-1}s^{-1}), *[S]* is the concentration of the corresponding scavenging compound (M), ε_{254} is the molar absorption of hydrogen peroxide at 254 nm (M^{-1}cm^{-1}), Φ is the quantum yield of hydroxyl radical formation by photolysis of hydrogen peroxide at 254 nm, [H_2O_2] is the concentration of hydrogen peroxide (M), and U_{254} is the wavelength energy (J/mol). Substituting Eq. 2 into Eq. 3 yields:

$$\sum k_s[S] = \frac{E_o \varepsilon_{254} \Phi [H_2O_2]}{U_{254}} \times \frac{k_{HO\cdot,pCBA}}{-slope \times E_o} = \frac{\varepsilon_{254} \Phi [H_2O_2]}{U_{254}} \times \frac{k_{HO\cdot,pCBA}}{-slope} \qquad (3)$$

Results/Discussion

Water Quality

The pH, absorbance (at 254 nm), nitrite, alkalinity, and TOC of the samples are shown in Table 1. An example for the absorbance spectra of well NH037 is presented in Figure 2.

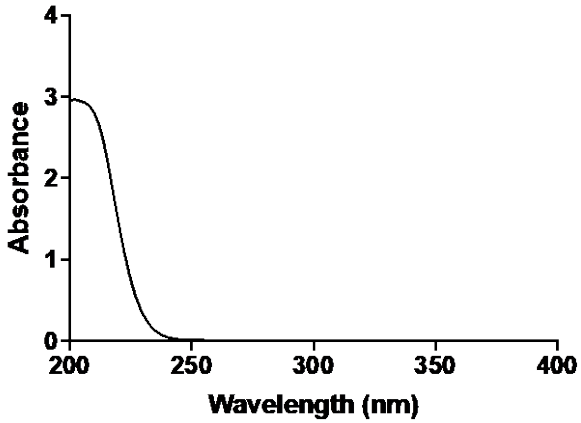

Figure 2. Absorbance spectrum of well NH037, from 200 – 400 nm

Bench-Scale Background Scavenging

In most natural waters hydroxyl radicals are scavenged mainly by two constituents: carbonates ($k_{HO,HCO3}$ = 8.5 x 10^6 L mol^{-1} s^{-1} and $k_{HO,CO3}$ = 3.9 x 10^8 L mol^{-1} s^{-1}), and TOC ($k_{HO,TOC}$ = 2.5 X 10^4 L mg^{-1} s^{-1}). While hydrogen peroxide (~8 mg/L) was added to promote formation of hydroxyl radicals, in excess it is capable of scavenging radicals ($k_{HO\cdot,H2O2}$ = 2.7 x 10^7 L mol^{-1} s^{-1}). Given their established rate constants, the relative contribution of each water quality parameter to the overall scavenging demand can be calculated (Table 1).

Hydrogen peroxide (H_2O_2) concentration was determined prior to UV exposure ([H_2O_2] initial), shown in Table 1. Since hydrogen peroxide has a relatively low molar absorption coefficient at 254 nm only a small fraction is consumed during UV exposure. Hydrogen peroxide concentrations were measured using the molybdate-activated iodide method. This method utilizes a color change that occurs when H_2O_2 reacts with potassium iodide (KI) in a buffered solution containing ammonium molybdate, forming I_3^- which can be detected spectrophotometrically at 352 nm (Klassen, 1994).

Figure 3 presents the measured degradation of pCBA in the water from wells NH037, TJ and NHC by LPUV/H_2O_2 with ~8 mg/L H_2O_2, and the theoretical decay of pCBA (term 'model'). The modeled value was calculated using the measured water quality, associated scavenging rates from Table 2, and a steady-state hydroxyl radical model previously described by Rosenfeldt and Linden (2007). This model incorporates the water quality parameters and the spectral characteristics of the LPUV setup.

Table 1. Water quality and LPUV/H_2O_2 scavenging results.

Well: NH037		Test 1	Test 2
pH		7.60	
alkalinity as $CaCO_3$		209	
TOC (mg/L)		0.450	
UV abs $_{254nm}$ (cm^{-1}) (Transmittance)		0.01874 (95.8%)	0.01874 (95.8%)
[H2O2] initial (mg/L)		8.10	7.58
Scavenger [S]	$k_{OH/S}$ (M^{-1} s^{-1} or L mg^{-1} s^{-1})	$k_{OH,S}[S]$ (s^{-1})	
TOC	2.50E+04	1.13E+04	1.13E+04
HCO_3^-	8.50E+06	1.77E+04	1.77E+04
CO_3^{-2}	3.90E+08	1.62E+03	1.62E+03
H_2O_2	2.70E+07	6.43E+03	6.02E+03
pCBA	5.00E+09	1.65E+04	1.67E+04
$\Sigma k_{OH,S}[S]$ (s^{-1})		5.35E+04	5.32E+04
$\Sigma k_{OH,S}$[S-pCBA] (s^{-1})		3.70E+04	3.66E+04
TOC (mg/L)	-	21%	21%
HCO_3^- (M)	-	33%	33%
CO_3^{-2} (M)	-	3%	3%
H_2O_2 (M)	-	12%	11%
pCBA (M)	-	31%	31%

Well: TJ		Test 1	Test 2
pH		8.01	
alkalinity as $CaCO_3$		152	
TOC (mg/L)		0.754	
UV abs $_{254nm}$ (cm^{-1}) (Transmittance)		0.0207 (95.3%)	0.0209 (95.3%)
[H2O2] initial (mg/L)		7.45	7.55
Scavenger [S]	$k_{OH/S}$ (M^{-1} s^{-1} or L mg^{-1} s^{-1})	$k_{OH,S}[S]$ (s^{-1})	
TOC	2.50E+04	1.88E+04	1.88E+04
HCO_3^-	8.50E+06	1.28E+04	1.28E+04
CO_3^{-2}	3.90E+08	3.01E+03	3.01E+03
H_2O_2	2.70E+07	5.96E+03	5.96E+03
pCBA	5.00E+09	1.58E+04	1.58E+04

$\Sigma k_{OH,S}[S]$ (s^{-1})		5.64E+04	5.64E+04
$\Sigma k_{OH,S}$[S-pCBA] (s^{-1})		4.06E+04	4.06E+04
TOC (mg/L)	-	33%	33%
HCO_3^- (M)	-	23%	23%
CO_3^{-2} (M)	-	5%	5%
H_2O_2 (M)	-	11%	11%
pCBA (M)	-	28%	28%
Well: NHC		Test 1	Test 2
pH		8.04	
alkalinity as $CaCO_3$		155	
TOC (mg/L)		0.305	
UV abs $_{254nm}$ (cm^{-1}) (Transmittance)		0.0099 (97.7%)	0.00959 (97.8%)
[H2O2] initial (mg/L)		7.46	7.13
Scavenger [S]	$k_{OH/S}$ (M^{-1} s^{-1} or L mg^{-1} s^{-1})	$k_{OH,S}[S]$ (s^{-1})	
TOC	2.50E+04	7.63E+03	7.63E+03
HCO_3^-	8.50E+06	1.30E+04	1.30E+04
CO_3^{-2}	3.90E+08	3.29E+03	3.29E+03
H_2O_2	2.70E+07	5.79E+03	5.79E+03
pCBA	5.00E+09	1.56E+04	1.56E+04
$\Sigma k_{OH,S}[S]$ (s^{-1})		4.53E+04	4.54E+04
$\Sigma k_{OH,S}$[S-pCBA] (s^{-1})		2.97E+04	2.97E+04
TOC (mg/L)	-	26%	26%
HCO_3^- (M)	-	44%	44%
CO_3^{-2} (M)	-	11%	11%
H_2O_2 (M)	-	19%	19%
pCBA (M)	-	52%	52%

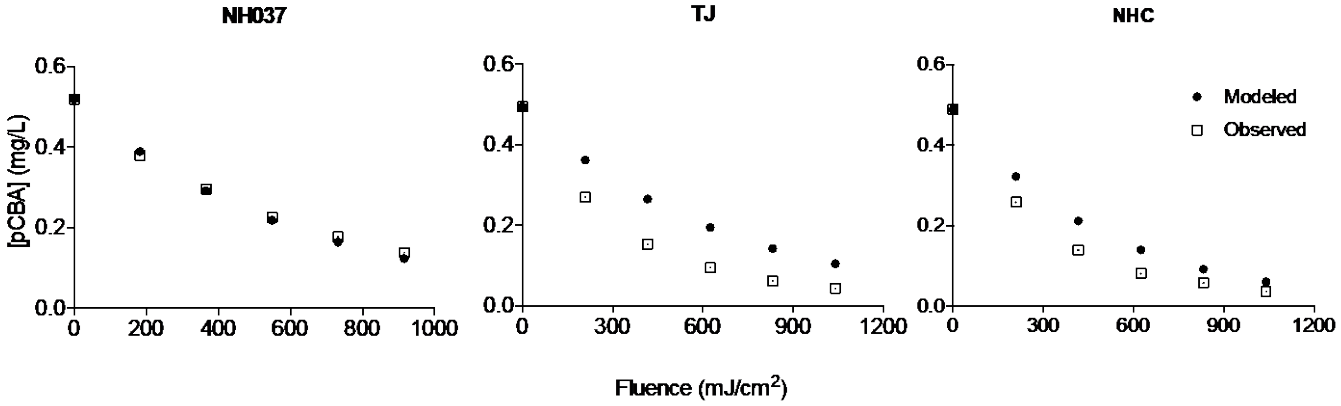

F**igure 3.** Modeled degradation of pCBA for test 1 and 2 with ~8 mg/L H_2O_2.

Table 2 summarizes the experimental and theoretical hydroxyl radical concentration and scavenging rates of the water samples.

Table 2. Comparison of modeled and experimentally determined hydroxyl radical concentration and scavenging rates for LPUV/H_2O_2.

Well: NH037	Test 1	Test 2
$[H_2O_2]$ mg/L	8.10	7.58
Scavenging Rate	$k_{OH}[S]$ (s^{-1})	
$k_{OH}[S]$, $_{TOT\text{-}Model}$	3.70E+04	3.66E+04
$k_{OH}[S]$, $_{TOT\text{-}Exp.}$	3.78E+04	3.79E+04
Steady State ·OH	$[OH]_{ss}$(M)	
$[OH]_{ss\ -\ Model}$	2.52E-13	2.38E-13
$[OH]_{ss\ –\ Exp.}$	2.21E-13	2.18E-13

Well: TJ	Test 1	Test 2
$[H_2O_2]$ mg/L	7.45	7.55
Scavenging Rate	$k_{OH}[S]$ (s^{-1})	
$k_{OH}[S]$, TOT-Model	4.06E+04	4.06E+04
$k_{OH}[S]$, TOT-Exp.	2.36E+04	2.32E+04
Steady State ·OH	$[OH]_{ss}$(M)	
$[OH]_{ss}$ - Model	2.14E-13	2.14E-13
$[OH]_{ss}$ – Exp.	3.69E-13	3.74E-13

Well: NHC	Test 1	Test 2
$[H_2O_2]$ mg/L	8.10	7.58
Scavenging Rate	$k_{OH}[S]$ (s^{-1})	
$k_{OH}[S]$, TOT-Model	2.97E+04	2.97E+04
$k_{OH}[S]$, TOT-Exp.	2.24E+04	2.19E+04
Steady State ·OH	$[OH]_{ss}$(M)	
$[OH]_{ss}$ - Model	2.94E-13	2.94E-13
$[OH]_{ss}$ – Exp.	3.90E-13	3.99E-13

Measured steady-state hydroxyl radical production (using the probe pCBA) is lower than other waters tested in this laboratory previously. The reported upper limit of achievable hydroxyl radical steady-state concentration is around 10^{-12} M (Oppenlander, 2003). Hydroxyl radical concentration results coupled with low UV absorbance (254 nm) values indicate that all three well waters are viable candidates for UV/AOP treatment, although at possible elevated doses compared to other waters.

References

Bolton, J.R., Linden, K.G. (2003) Standardization of methods for fluence (UV dose) determination in bench-scale UV experiments. ASCE J. Environ. Eng. 129(3) 209−215

Buxton, G.V., Greenstock, C.L., Helman, W.P., Ross, A.P.J. (1988) Phys. Chem. Ref. Data 1988, 17, 513.

Glaze, W.H., Lay, Y., Kang, J.W. (1995) Advanced Oxidation Processes-A kinetic model for the oxidation of 1,2-Dibromo-3-chloro- propane in water by the combination of hydrogen peroxide and UV radiation. Ind. Eng. Chem. Res. 34(7) 2314-2323.

Klassen, N. V.; Marchington, D.; McGowan, H. C. E. H2O2 determination by the I3 − method and by KMnO4 titration. Anal. Chem. 1994, 66, 2921−2925.

Watts, M.J., Hofmann, R., Rosenfeldt, E.J. (2012) "Low-pressure UV/Cl2 for advanced oxidation of taste and odor." American Water Works Association.

Oppenlander, T. (2003) Photochemical Purification of Water and Air. Wiley-VCH. 168.

Rosenfeldt, E.J., Linden, K.G., (2007) "Hydroxyl radical formation during the UV/H_2O_2 processes: The $R_{OH/UV}$ concept" *Environmental Science & Technology*. 41(7) 2548-2553

Watts, M.J., Rosenfeldt, E.J., Linden, K.G. (2007) Comparative OH radical oxidation using UV-Cl2 and UV-H2O2 processes. Aqua, 56 (8), 469-478.

Wols, B.A., Hofman-Caris, C.H.M. (2012) Review of photochemical reaction constants of organic micropollutants required for UV advanced oxidation processes in water. Water Research 46: 2815–2827.

Appendix B Toxicity Profiles

1 INTRODUCTION

This appendix presents toxicity profile summaries for the constituents of potential concern (COPCs) identified in the North Hollywood West Well Field Raw Water Quality Characterization (RWQC) report (Step 2 of 97-005 Evaluation); and, evaluated herein to assess potential risks to human health associated with failure of planned treatment (Step 5 of 97-005 Evaluation). The descriptive information presented were obtained from the United States Environmental Protection Agency's (EPA's) Integrated Risk Information System (IRIS; available online at www.epa.gov/iris) and/or Office of Environmental Health Hazard Assessment (OEHHA)'s Chemical Database (https://oehha.ca.gov/chemicals), except where noted.

The profile for each COPC (listed in Table A) includes:

- tabulated chronic cancer and non-cancer public health goals (public health goals [PHGs]; OEHHA) used in this Step 5 failure analysis, the basis for each PHG with respect to the organs or system(s) affected and any relevant notes specific to this analysis;
- industrial usage of organic COPCs;
- EPA carcinogenicity classification and Proposition 65 status in California; and
- a brief discussion of the study/studies and any uncertainty factors relevant to the development of the carcinogenic and/or non-carcinogenic PHG, whichever are applicable, used in this Step 5 analysis.

Table A: Constituents of Potential Concern (COPCs) included in the Step 5 Assessment of Risks to Human Health from Failure of Proposed Treatment (i.e.: NHWWT)

COPC
1,1-DICHLOROETHANE (1,1-DCA)
1,1-DICHLOROETHENE (1,1-DCE)
1,2,3-TRICHLOROPROPANE (1,2,3-TCP)
1,2-DICHLOROETHANE (1,2-DCA)
1,4-DIOXANE
BENZENE
CIS-1,2-DICHLOROETHENE
DI(2-ETHYLHEXYL)PHTHALATE (DEHP)
NITRATE (AS NITROGEN [N])
TETRACHLOROETHENE (PCE)
TRICHLOROETHENE (TCE)

1.1 Public Health Goals (PHGs)

The PHGs are levels of contaminants in drinking water based on human health risk assessments that are protective of public health and pose no significant health risk if consumed for a lifetime. The PHGs, which are not enforceable, have been developed by the California Environmental Protection Agency's (CalEPA's) Office of Environmental Health Hazard Assessment (OEHHA). Certain public water systems are required to use PHGs when providing information to their customers about contaminants detected in the drinking water. PHGs are used by the Division of Drinking Water (DDW) to determine the maximum contaminant levels (MCLs) for contaminants that are to be reviewed for possible revision. The California Safe Drinking Water Act of 1996 ("the Act", amended to be called Health and Safety Code, Section 116365 (h)) requires DDW to make public the list of chemicals for which an existing MCL is under review. Additionally, Section 116365 specifies that the PHG is to be based exclusively on public health considerations without regard to cost impacts.

PHGs are developed for chemical contaminants based on the best available toxicological data in the scientific literature. The PHG technical support documents and the analyses contained therein provide estimates of the levels of contaminants in drinking water that would pose no significant health risk to individuals consuming the water on a daily basis over a lifetime.

Calculations of concentrations of chemical contaminants in drinking water associated with negligible risks for carcinogenic or non-carcinogenic endpoints must consider the toxicity of the chemical and the potential exposure of individuals using the water. Tap water is used directly for drinking and for preparing food and beverages. It is also used for bathing and showering, washing, flushing toilets, and other household uses, resulting in potential dermal and inhalation exposures. Therefore, three routes of exposure, ingestion, inhalation and dermal contact with domestic water, are addressed in developing the PHG, as appropriate, which is dependent upon the physicochemical nature of the COPC (i.e., volatility, etc.).

For carcinogens, the following general equation is used to calculate the PHG for a constituent in drinking water:

$$PHG = \frac{\text{BW} * \text{R}}{q1 * or\ CSF * \ L/d} = mg/L$$

where:

BW = adult body weight (a default of 70 kg);

R = de minimis level for lifetime excess individual cancer risk (a default of 10-6);

q1* or CSF = cancer slope factor, q1* or CSF, is the upper 95 percent confidence limit on the cancer potency slope calculated by the linearized multistage (LMS) model, and CSF, is a potency derived from the lower 95 percent confidence limit on the 10 percent tumor dose (LED10). CSF = 10 percent/ LED10. Both potency estimates are converted to human equivalent [in (mg/kg-day)-1] using $BW^{3/4}$ scaling;

L/d = daily water consumption rate, liters/day

mg/L = milligrams per liter

Calculation of a public health-protective concentration in drinking water for non-carcinogenic endpoints follows this general equation:

$$PHG = \frac{\text{NOAEL * BW * RSC}}{UF(s) * Leq/d} = mg/L$$

where:

NOAEL = no-observed-adverse-effect-level, or lowest-observed-adverse effect-level modified by an uncertainty factor

BW = adult body weight (a default of 70 kg);

RSC = relative source contribution (a default of 20 percent);

UF = uncertainty factors to account for inter- and intra-species extrapolation, extrapolation of sub-chronic to chronic exposure, etc.

Leq/d = daily water consumption rate, liter equivalents/day, to account for various probable routes of exposure in addition to ingestion that would result in contamination of water supplies (a default of 4 Leq/d)

Each PHG technical support document states calculated public health-protective concentrations for a chemical in drinking water based on both carcinogenic and non-carcinogenic effects, as applicable. The more conservative of the two calculated concentrations is then adopted by OEHHA as the PHG.

Both cancer and non-cancer endpoints were evaluated in this Step 5 proposed treatment failure analysis; and, therefore, “Cancer PHG” and “Non-cancer PHG” are shown in the subsequent tables.

1.2 Toxicity Profiles

The toxicity profile for each COPC (listed in Table A) adopted in the Step 5 failure analysis are provided in the following subsections.

1.2.1 1,1-Dichloroethane (1,1-DCA)

1,1-DCA is mainly used as a feedstock in chemical synthesis, chiefly of 1,1,1-trichloroethane. It is also used as a solvent for plastics, oils and fats, as a degreaser, as a fumigant in insecticide sprays, in halon fire extinguishers, and in cementing of rubber. According to the Agency for Toxic Substances and Disease Registry (ATSDR 2015), kidney effects have been observed in cats chronically exposed to 1,1-DCA via inhalation; the results of a study in rats and mice suggest that 1,1-DCA may cause cancer, though the data were not conclusive. Although not assessed under the IRIS program, OEHHA lists 1,1-DCA under Proposition 65 as causing cancer.

OEHHA developed a cancer PHG of 3 µg/L for 1,1-DCA in drinking water (Table B). The PHG is based on an existing OEHHA cancer potency value based on mammary tumors in female Osborne-Mendel rats. The PHG to protect against non-cancer effects is 140 µg/L (Table B), based on kidney damage in cats (Hofmann et al., 1971). The PHG calculations assume an adult body weight of 70 kg and a drinking water consumption of 4 L-equivalents/day (Leq/day). The non-cancer PHG also applied a relative source contribution of 20% and an uncertainty factor of 100 (OEHHA 2003).

Table B: 1,1-DCA PHG Information Summary

PHG Type	Value µg/L	Basis of PHG
Cancer PHG	3	Mammary gland
Non-cancer PHG	140	Kidney

1.2.2 1,1-Dichloroethene (1,1-DCE)

1,1-DCE, also known as vinylidene chloride, is used in the manufacture of packaging materials, flexible films and flame-retardant coatings for fiber and carpet backing. It can also be produced as a secondary intermediate in the degradation of tetrachloroethene (PCE) and trichloroethene. The target organ is the liver, which is affected by exposure via either ingestion or inhalation (EPA 2018a; OEHHA 2018). 1,1-DCE is considered a possible human carcinogen; the evidence is suggestive of carcinogenicity but is not sufficient to assess human carcinogenic potential. 1,1-DCE is not included in Proposition 65.

No dose-response assessment for the potential carcinogenic effects of 1,1-DCE were performed by OEHHA due to the lack of appropriate data from which a quantitative estimate of the chemical's potency could be developed. OEHHA determined that there was no clear evidence that 1,1-DCE poses a carcinogenic risk to humans. Accordingly, the PHG was calculated using a non-cancer endpoint, taking into consideration uncertainty surrounding 1,1-DCE carcinogenesis in humans (OEHHA 1999). OEHHA has developed a PHG of 10 µg/L (Table C) for 1,1-DCE (also known as vinylidene chloride) in drinking water. The PHG is based on the most sensitive toxic endpoint, midzonal hepatocellular fatty changes in female rats (Quast et al., 1983). Accordingly, the Lowest Observed Adverse Effect Level (LOAEL) for this study and endpoint is 50 mg/L. Based on water consumption, the authors estimated the time-weighted average dose for females exposed to 50 mg/L 1,1-DCE in drinking water to be 9 mg/kg-day. The PHG calculation assumes an adult body weight of 70 kg, a relative source contribution of 20%, a drinking water consumption of 4 Leq/day, and applies an uncertainty factor of 3,000 (OEHHA 1999).

Table C: 1,1-DCE PHGs Information

PHG Type	Value µg/L	Basis of PHG
Cancer PHG	N/A	N/A
Non-cancer PHG	10	Liver; midzonal hepatocellular fatty changes in female rats

1.2.3 1,2,3-Trichloropropane (1,2,3-TCP)

1,2,3-TCP is an intermediate in chemical synthesis and is an industrial solvent and a degreasing agent. Under the Guidelines for Carcinogenic Risk Assessment (USEPA 2005a), 1,2,3-TCP is "likely to be carcinogenic to humans", based on a statistically significant and dose-related increase in the formation of multiple tumors (reproductive, ocular, hepatic, and gastrointestinal) in both sexes of rats and mice. Chronic non-carcinogenic effects include increased absolute liver weight in male rats via the oral route and peribronchial lymphoid hyperplasia in male rats via the inhalation route. 1,2,3-TCP is currently listed as a cancer-causing agent under Proposition 65.

OEHHA has developed a cancer PHG of 0.0007 µg/L (Table D) for 1,2,3-TCP in drinking water. The PHG is based on the most sensitive cancer endpoint for 1,2,3-TCP which caused an increase in tumors in the forestomach of the female mouse (NTP 1993). The PHG was calculated using oral data only, as no

data on the carcinogenicity of 1,2,3-TCP via the inhalation route were available. The PHG to protect against non-cancer effects is 80 µg/L (Table D), based on the effects on erythrocytes in rats (NTP 1993). The PHG calculations assume an adult body weight of 70 kg and a drinking water consumption of 4 Leq/day, a relative source contribution of 80% and an uncertainty factor of 1,000 (OEHHA 2009a).

Table D: 1,2,3-TCP PHGs Information

PHG Type	Value µg/L	Basis of PHG
Cancer PHG	0.0007	Stomach
Non-cancer PHG	80	Hematotoxin

1.2.4 1,2-Dichloroethane (1,2-DCA)

The most common use of 1,2-DCA is in the production of vinyl chloride, which is used to make polyvinyl chloride (PVC) pipes, furniture and automobile upholstery, wall coverings, housewares, and automobile parts. 1,2-DCA is also used generally as an intermediate for other organic chemical compounds and as a solvent. 1,2-DCA is a probable human carcinogen based on sufficient evidence of carcinogenicity in animals. OEHHA notes that the chronic target organ is the liver. Proposition 65 lists 1,2-DCA as a carcinogen.

OEHHA has developed a cancer PHG of 0.4 µg/L (Table E) for 1,2,3-TCP in drinking water. The PHG is based on the most sensitive cancer endpoint for 1,2-DCA from the incidence rate of hemangiosarcomas in male rats reported by NCI (1978). The PHG to protect against non-cancer effects is 480 µg/L (Table E), based on the renal lesions were observed in female rats (NTP 1991). The PHG calculations assume an adult body weight of 70 kg and a drinking water consumption of 2 L/day, a relative source contribution of 60% and an uncertainty factor of 1,000 (OEHHA 1999).

Table E: 1,2-DCA PHGs Information

PHG Type	Value µg/L	Basis of PHG
Cancer PHG	0.4	Liver, skin, testes, bile ducts, and mammary glands
Non-cancer PHG	480	Kidney

1.2.5 1,4-Dioxane

1,4-Dioxane is used as a solvent stabilizer to chlorinated compounds and as a laboratory reagent. It may be a trace contaminant in a range of chemicals used in cosmetics, detergents, and shampoos. The critical organ systems are liver, respiratory, nervous and urinary systems (EPA 2010a; OEHHA 2020). EPA characterizes 1,4-dioxane as “likely to be carcinogenic to humans”. Proposition 65 lists 1,4-dioxane as causing cancer (EPA 2018a; OEHHA 2020).

For 1,4-dioxane, OEHHA is currently developing a PHG for 1,4-dioxane. The 1E-06 lifetime cancer risk-related concentration of 0.35 ug/L was used as the PHG-like value. In 1998, the Drinking Water Program, now DDW, established an initial NL at 3.0 µg/L, based on an EPA (1990) drinking water concentration that corresponded to a 1E-06 theoretical lifetime cancer risk. Later, in 2010, EPA revised its 1,4-dioxane risk evaluation, such that a 1E-06 risk level corresponds to 0.35 µg/L (EPA 2010a, 2010b, 2013). DDW

revised its NL to 1.0 µg/L (Table F) in November 2010 (which corresponds to 3E-06) to reflect the detection limit for reporting (DLR) (cited from California State Water Resources Control Board [California Water Boards], online, 2018). EPA's tap water Regional Screening Level (RSL) Total Hazard Quotient of 0.1 (THQ = 0.1, to account for exposure to multiple constituents) of 60 µg/L (Table F) was used as a surrogate for the non-cancer PHG; this reference concentration is an estimate of the continuous lifetime inhalation exposure that the EPA believes is likely to have no appreciable risk of deleterious non-cancer effects.

Table F: 1,4-Dioxane PHGs Information

PHG Type	Value µg/L	Basis of PHG
Cancer PHG	1	See below
Non-cancer PHG	60	See below

1.2.6 Benzene

Benzene is a multiuse compound most commonly found in gasoline additives, solvents, oil extraction, photogravure printing, veterinary medicine (disinfectant); production of detergents, explosives, pharmaceuticals, and dyestuffs. Toxicological endpoints for acute and chronic effects include reproductive, aplastic anemia and acute myelogenous leukemia. Target organs for acute effects include reproductive, immune system, and hematologic system. Target organs for chronic effects include the nervous system.

Benzene is classified as a "known" carcinogen to humans by all routes of exposure. Common carcinogenic endpoints include nonlymphocytic leukemia, chronic nonlymphocytic leukemia, chronic lymphocytic leukemia, hematologic neoplasms, blood disorders such as preleukemia and aplastic anemia, Hodgkin's lymphoma, and myelodysplastic syndrome. Benzene is classified as causing cancer as well as male reproductive toxicity under Proposition 65.

OEHHA has developed a cancer PHG of 0.15 µg/L (Table G) for benzene in drinking water. The PHG is based on the upper 95 percent confidence limit benzene concentration that may result in a lifetime risk of leukemia. The PHG to protect against non-cancer effects is 26 µg/L, based on benzene-induced hematotoxicity in rats (Table G). The PHG calculations assume an adult body weight of 70 kg and a drinking water consumption of 2 L/day. The non-cancer PHG also applied a relative source contribution of 20% and an uncertainty factor of 10 (OEHHA 2001a).

Table G: Benzene PHGs Information

PHG Type	Value µg/L	Basis of PHG
Cancer PHG	0.15	Hematotoxin
Non-cancer PHG	26	Hematotoxin

1.2.7 cis-1,2-Dichloroethene (cis-1,2-DCE)

cis-1,2-DCE is a compound found as a chemical intermediate in synthesis of chlorinated solvents. It is also a common chemical in refrigerants and is the primary dichloroethene produced by anaerobic

biodegradation of PCE and TCE. Cis-1,2-DCE is a nephrotoxin, targeting the kidneys for acute and chronic effects (EPA 2018a; OEHHA 2020).

At the time of this report, there was inadequate information to assess the carcinogenic potential of this compound. It is not included in Proposition 65.

The PHG for cis-1,2-DCE is based upon the LOAEL from a 90-day oral gavage study on rats conducted by McCauley et al., 1990. Sprague-Dawley rats were dosed with cis-1,2-DCE in corn oil. Significant increases in kidney-to-body-weight ratios were observed in males at all doses, including the lowest dose tested of 32 mg/kg-day . Thus, the non-cancer PHG of 13 µg/L (Table H) is based on a LOAEL, modified with uncertainty factors (OEHHA 2011).

Table H: cis-1,2-DCE PHG Information Summary

PHG Type	Value µg/L	Basis of PHG
Cancer PHG	N/A	N/A
Non-cancer PHG	13	Kidney

1.2.8 Di(2-ethylhexyl)phthalate (DEHP)

Di(2 ethylhexyl)phthalate (DEHP) is a plasticizer for many resins and elastomers. Additionally, it is a component of tobacco smoke and a known laboratory contaminant of analytical samples. The principal and supporting studies of the oral RfD report DEHP as causing increased relative liver weight in rats and guinea pigs. Although the supporting data for carcinogenicity in humans is considered inadequate, there was a statistically significant increase in hepatocellular carcinomas in female rats and both sexes of mice fed diets containing DEHP. Except for the IUR, the TRVs used in this HHRA are from IRIS; OEHHA includes DEHP as causing cancer from both oral and inhalation routes of exposure.

OEHHA has developed a cancer PHG of 12 µg/L (Table I) for DEHP in drinking water. The cancer PHG is based on the data generated from an oncogenicity study in rats (NTP 1982). The PHG to protect against non-cancer effects is 100 µg/L (Table I), based on developmental and reproductive effects in rats. The PHG calculations assume an adult body weight of 70 kg and a drinking water consumption of 2 L/day. The non-cancer PHG also applied a relative source contribution of 20% and an uncertainty factor of 1,000 (OEHHA 1997).

Table I: DEHP PHG Information Summary

PHG Type	Value µg/L	Basis of PHG
Cancer PHG	12	Liver
Non-cancer PHG	100	Reproductive, developmental

1.2.9 Nitrate (as Nitrogen [N])

Besides natural occurrences, nitrates are mainly produced for use as fertilizers in agriculture. The second major application of nitrates is as oxidizing agents, most notably in explosives. Sodium nitrate is used to remove air bubbles from molten glass and some ceramics. Mixtures of the molten salt are used to harden some metals. Nitrate is not included in Proposition 65.

OEHHA has developed a non-cancer PHG of 12 µg/L (Table J)) for nitrate (as nitrogen) in drinking water based on several case studies of infant methemoglobinemia (Bosch et al., 1950; Walton, 1951; Sadeq et al., 2008). The PHG calculations assume an adult body weight of 70 kg and a drinking water drinking water intake rate of 0.294 L/kg-day. The non-cancer PHG also applied a relative source contribution of 100% and no uncertainty factor as the studies examined effects on human infants (OEHHA 2018).

Table J: Nitrate (as N) PHG Information Summary

PHG Type	Value µg/L	Basis of PHG
Cancer PHG	N/A	N/A
Non-cancer PHG	10,000	Hematotoxin

1.2.10 Tetrachloroethene (PCE)

PCE is used as a dry-cleaning agent and metal degreasing solvent. It is also used as a starting material for making other chemicals and is used in some consumer products (EPA 2018a; OEHHA 2018).

The EPA classifies PCE as "likely to be carcinogenic to humans" based on rodent exposure data. Proposition 65 lists PCE as "causing cancer" (EPA 2018a). A PHG of 0.06 µg/L (Table K) was established for PCE in drinking water. The PHG is based primarily on an average of CSFs for liver tumors in male and female mice exposed to PCE via the oral route (OEHHA 2001b). An estimate of the concentration of PCE in drinking water protective against chronic toxicity other than cancer was derived based on neurobehavioral endpoints (related to delayed reaction times) observed in epidemiological studies of humans with occupational or environmental exposures to inhaled PCE. The PHG is derived from a LOAEL, a 3% RSC based on data for urban areas with 0.5 µg/L PCE in drinking water, A geometric mean of estimates from three studies was used to derive an estimated health-protective concentration in drinking water of 11 µg/L (Table K) (OEHHA 2001b).

Table K: PCE PHG Information Summary

PHG Type	Value µg/L	Basis of PHG
Cancer PHG	0.06	Liver tumors in male and female mice
Non-cancer PHG	11	Geometric mean of occupational studies in humans

1.2.11 Trichloroethene (TCE)

The two major uses of TCE are as a degreaser for metal parts and as a precursor chemical, especially in the manufacture of the refrigerant, HFC-134a. TCE has also been used as an extraction solvent for greases, oils, fats, waxes, and tars; by the textile processing industry to scour cotton, wool, and other fabrics; in dry cleaning operations; and as a component of adhesives, lubricants, paints, varnishes, paint strippers, pesticides, and cold metal cleaners. TCE also occurs in the environment as a breakdown product of PCE via anaerobic reductive dechlorination (EPA 2018a; OEHHA 2018).

Using the geometric mean cancer slope factor (CSF) from two studies (Maltoni et al., 1986; NCI 1976) and a value of 7.1 Leq/day for water consumption (Bogen et al., 1988), the water concentration corresponding to a negligible cancer risk, C, was calculated as follows (OEHHA 2009b):

C = 70 kg * 10-6/0.0059 mg/kg-day-1 * 7.1 Leq/day = 0.00167 mg/L = 1.7 µg/L (Table L)

Where:

70 kg =body weight

10-6 = de minimis target cancer risk

A health-protective value for non-cancer toxicity of 1,000 µg/L (Table L) was also calculated, based on the benchmark dose (BMD10) for kidney nephropathy in an oral chronic study in rats and a 100-fold uncertainty factor (OEHHA 2009b).

Table L: TCE PHG Information Summary

PHG Type	Value µg/L	Basis of PHG
Cancer PHG	1.7	Mouse liver tumors
Non-cancer PHG	1000	Kidney nephropathy in rats

2 REFERENCES

Omg, ATSDR (Agency for Toxic Substances and Disease Registry), 2015. Toxicological Profile for 1,1-Dichloroethane. US Department of Health and Human Services, Public Health Service.

California Water Boards, online. 2018. 1,4-Dioxane. California Water Resources Control Board. Accessed October 2018. https://www.waterboards.ca.gov/drinking_water/certlic/drinkingwater/14-Dioxane.html

Chieco, P., M.T Moslen and E.S. Reynolds. 1981. Effect of administrative vehicle on oral 1,1-dichloroethylene toxicity. Toxicol Appl Pharmacol., 57: 146-155.

DTSC (Department of Toxic Substances Control) 1994. CalTOX, A Multimedia Total Exposure Model for Hazardous Waste Sites. Spreadsheet User's Guide. Version 1.5. Prepared by the University of California, Davis, in cooperation with Lawrence Livermore National Laboratory for the Department of Toxic Substances Control, California Environmental Protection Agency, Sacramento, California.

EPA (United States Environmental Protection Agency). 1990. 1,4-Dioxane. Integrated Risk Information System (IRIS), US Environmental Protection Agency, September 1 (cited by California Water Boards, online (2018).

EPA (United States Environmental Protection Agency). 2010a. 1,4-Dioxane, IRIS, US EPA, Accessed August 11, 2010 (cited by California Water Boards, online (2018).

EPA (United States Environmental Protection Agency). 2010b. Toxicological Review of 1,4-Dioxane, in support of summary information on IRIS. Accessed August 11, 2010 (cited by California Water Boards, online (2018).

EPA (United States Environmental Protection Agency), 2018a. Integrated Risk Information System (IRIS), last accessed March 2018. http://www.epa.gov/iris. Last accessed July 2018.

EPA (United States Protection Agency) 2018b. 2018 Edition of the Drinking Water Standards and Health Advisories Tables. EPA 822-F-18-001. Office of Water. March.

EPA (Environmental Protection Agency). 2018c. Regional Screening Level (RSL) Summary Table (TR = 1E-06, HQ = 0.1 https://semspub.epa.gov/work/HQ/197253.pdf

EPA (United States Environmental Protection Agency). 2005. Guidelines for Carcinogen Risk Assessment. Risk Assessment Forum, Washington, DC; EPA/630/P-03/001B. Available from: http://www.epa.gov/iris/backgrd.html.

EPA (Environmental Protection Agency). 1987a. 1,1-Dichloroethylene. Health Advisory. Office of Drinking Water. March.

EPA (Environmental Protection Agency). 1987b. Cis-1,2-Dichloroethylene. Health Advisory. Office of Drinking Water. March.

EPA (Environmental Protection Agency). 1987c. p-Dioxane. Health Advisory. Office of Drinking Water. March.

EPA (Environmental Protection Agency). 1987d. Tetrachloroethylene. Health Advisory. Office of Drinking Water. March.

Hofmann HT, Birnstiel H, Jobst P. 1971. Zur inhalationstoxicität von 1,1- and 1,2dichloräthan. Arch Toxikol 27:248-265.

Jenkins, L.J., Jr., M.J. Trabulus and S.D. Murphy. 1972. Biochemical effects of 1,1-dichloroethylene in rats: Comparison with carbon tetrachloride and 1,2-dichloroethylene. Toxicol Appl Pharmacol., 23: 501-510.

Keating, GA, McKone, TE. 1993. Measurements and evaluation of water-to-air transfer and air concentration of trichloroethylene in a shower chamber, modeling of indoor air quality and exposure. ASTM STP 1205. Niren, L., Nagada, ed., American Society for Testing and Materials, Philadelphia, PA. pp 14-24.

Maltoni C, Lefemine G, Cotti G. 1986. Experimental research on trichloroethylene carcinogenesis. In: Archives of Research on Industrial Carcinogenesis, Vol. V. Princeton Scientific Publishing Co., Inc., Princeton, NJ, p. 393.

McKone TE. 1987. Human exposure to volatile organic compounds in household tap water - the indoor inhalation pathway. Environ Sci Technol 21:1194-1201.

McCauley PT, Robinson M, Condie LW, et al. 1990. The effect of subacute and subchronic oral exposure to cis-1,2-dichloroethylene in rats. U.S. Environmental Protection Agency, Health Effects Research Laboratory, and Air Force Aerospace Medical Research Laboratory, Wright-Patterson AFB, Cincinnati OH.

NCI (National Cancer Institute). 1976. Carcinogenesis bioassay of trichloroethylene. NCI-CG-TR-2. National Cancer Institute, Washington, DC, DHEW. No. (NIH)75-802.

Nomiyama, K, Nomiyama, H. 1974a. Respiratory retention, uptake and excretion of organic solvents in man. Benzene, toluene, n-hexane, trichloroethylene, acetone, ethyl acetate, and ethyl alcohol. Int Arch Arbeitsmed., 32: 75-83.

Nomiyama, K, Nomiyama, H. 1974b. Respiratory elimination of organic solvents in man. Benzene, toluene, n-hexane, trichloroethylene, acetone, ethyl acetate and ethyl alcohol. Int Arch Arbeitsmed., 32: 85-91.

National Toxicology Program (NTP). 1982. Carcinogenesis bioassay of di(2-ethylhexyl)-phthalate (CAS No. 117-81-7) in F344 rats and B6C3F1 mice (feed study). National Toxicology Program NTP-80-37, NIH Publication 82-1773, Research Triangle Park, N.C.

National Toxicology Program (NTP). 2008. Technical Report on the Toxicology and Carcinogenesis Studies of Sodium Dichromate Dihydrate in F344/N Rats and B6C3F1 Mice. NTP TR 546. NIH Publication No. 07-5887, National Toxicology Program, Research Triangle Park, North Carolina, Accessed at: http://ntp.niehs.nih.gov/ntp/htdocs/LT_rpts/tr546.pdf

National Toxicology Program (NTP). 1993. Toxicology and carcinogenesis of 1,2,3-trichloropropane (CAS No. 96-18-4) in F344/N Rats and B6C3F1 Mice (gavage studies). Technical Report Series No 384. NIH publication No. 94-2839. Research Triangle Park, NC: National Toxicology Program. 348 pp.

OEHHA (California Environmental Protection Agency, Office of Environmental Health Hazard Assessment). 1997. Public Health Goal for Di(2-Ethylhexyl)Phthalate (DEHP) in Drinking Water. December. https://oehha.ca.gov/chemicals/11-dichloroethylene

OEHHA (California Environmental Protection Agency, Office of Environmental Health Hazard Assessment). 1999. Public Health Goal for 1,1-Dichloroethylene in Drinking Water. February. https://oehha.ca.gov/chemicals/11-dichloroethylene

OEHHA (California Environmental Protection Agency, Office of Environmental Health Hazard Assessment). 2001a. Public Health Goal for Benzene in Drinking Water. June. https://oehha.ca.gov/chemicals/benzene

OEHHA (California Environmental Protection Agency, Office of Environmental Health Hazard Assessment). 2001b. Public Health Goal for Tetrachloroethylene in Drinking Water. August. https://oehha.ca.gov/chemicals/tetrachloroethylene

OEHHA (California Environmental Protection Agency, Office of Environmental Health Hazard Assessment). 2003. Public Health Goal for 1,1-Dichloroethane in Drinking Water. September. https://oehha.ca.gov/chemicals/1,1-Dichloroethane

OEHHA (California Environmental Protection Agency, Office of Environmental Health Hazard Assessment). 2009a. Public Health Goal for 1,2,3-Trichloropropane in Drinking Water. August. https://oehha.ca.gov/chemicals/1,2,3-Trichloropropane

OEHHA (California Environmental Protection Agency, Office of Environmental Health Hazard Assessment). 2009b. Public Health Goal for Trichloroethylene in Drinking Water. July. https://oehha.ca.gov/chemicals/trichloroethylene

OEHHA (California Environmental Protection Agency, Office of Environmental Health Hazard Assessment). 2006. Public Health Goal for cis- and trans-1,2-Dichloroethylene in Drinking Water. March. https://oehha.ca.gov/chemicals/12-dichloroethylene-cis

OEHHA (California Environmental Protection Agency, Office of Environmental Health Hazard Assessment). 2006. Public Health Goal for cis- and trans-1,2-Dichloroethylene in Drinking Water. March. https://oehha.ca.gov/chemicals/12-dichloroethylene-cis

OEHHA (California Environmental Protection Agency, Office of Environmental Health Hazard Assessment), 2020. OEHHA Chemicals Database. Last accessed March 2020. https://oehha.ca.gov/chemicals

Quast JF, Humiston CG, Schwetz RW, Balmer MF, Rampy LW, Norris JM, Gehring PJ. 1977. Results of 90-day toxicity study in rats given vinylidene chloride in their drinking water or exposed to VDC vapor by inhalation. Toxicol Appl Pharmacol 4:187.

Appendix C 1-Day Exposure Scenario - Human Health Risk Assessment Calculations and Results

COPCs	Cancer	Non-cancer	PHG or NL (µg/L)				3 Well Scenario Combined Flow					5 Well Scenario Combined Flow				
							Maximum Concentrations					Maximum Concentrations				
			Cancer		Non-Cancer		Concentration (µg/L)	Cancer Risk at 10^{-6}	% Contribution	Non-cancer Hazard	% Contribution	Concentration (µg/L)	Cancer Risk at 10^{-6}	% Contribution	Non-cancer Hazard	% Contribution
			Guideline	Mode of Action / System	Guideline	Mode of Action / System										
1,1-DICHLOROETHANE (1,1-DCA)	x	x	3	Mammary gland	140	Kidney	Non-Detect	--	--	--	--	Non-Detect	--	--	--	--
1,1-DICHLOROETHENE (1,1-DCE)	NA	x	--	--	10	Liver	1.3	--	--	0.13	18.6%	1.30	--	--	0.13	15.2%
1,2,3-TRICHLOROPROPANE (1,2,3-TCP)	x	x	0.0007	Stomach	80	Hematotoxic	Non-Detect	--	--	--	--	Non-Detect	--	--	--	--
1,2-DICHLOROETHANE (1,2-DCA)	x	x	0.40	Liver, skin, testes, bile ducts, and mammary glands	480	Kidney	Non-Detect	--	--	--	--	Non-Detect	--	--	--	--
1,4-DIOXANE	x	x	0.35	Nervous system, respiratory system, liver and gall bladder	210	Liver, urinary	4.0	4.5E-10	24.9%	0.02	2.9%	3.4	3.8E-10	14.5%	0.02	1.9%
BENZENE	x	x	0.15	Hematotoxic	26	Hematotoxic	Non-Detect	--	--	--	--	Non-Detect	--	--	--	--
CIS-1,2-DICHLOROETHYLENE (CIS-1,2-DCE)	NA	x	--	--	13	Kidney	Non-Detect	--	--	--	--	Non-Detect	--	--	--	--
DI(2-ETHYLHEXYL) PHTHALATE (DEHP)	x	x	12	Liver	100	Reproductive and developmental	Non-Detect	--	--	--	--	Non-Detect	--	--	--	--
NITRATE (AS NITROGEN [N])	NA	x	--	--	10,000	Hematotoxic	3,806	--	--	0.38	54.3%	4,103	--	--	0.41	48.0%
TETRACHLOROETHENE (PCE)	x	x	0.06	Liver	11	Cognitive and visual effects	1.9	1.2E-09	68.9%	0.17	24.3%	3.2	2.1E-09	79.4%	0.29	34.0%
TRICHLOROETHENE (TCE)	x	x	1.7	Liver	1,000	Kidney	4.9	1.1E-10	6.3%	0.00	0.0%	7.0	1.6E-10	6.1%	0.01	0.8%
							TOTALS	**1.8E-09**	**100%**	**0.70**	**100%**	**TOTALS**	**2.6E-09**	**100%**	**0.85**	**100%**

Notes: COPCs = Constituents of Potential Concern; PHG = Public Health Goal; NL = Notification Level; µg/L = micrograms per liter; NA= Not Applicable - COPC is not a carcinogen; “--" indicates not applicable

Appendix D 10-Day Exposure Scenario - Human Health Risk Assessment Calculations and Results Table

COPCs	Cancer	PHG or NL (µg/L)		3 Well Scenario Combined Flow						5 Well Scenario Combined Flow					
				Normal Anticipated Concentrations			Maximum Concentrations			Normal Anticipated Concentrations			Maximum Concentrations		
		Cancer	Mode of Action / System	Concentration (µg/L)	Cancer Risk at 10^{-6}	% Contribution	Concentration (µg/L)	Cancer Risk at 10^{-6}	% Contribution	Concentration (µg/L)	Cancer Risk at 10^{-6}	% Contribution	Concentration (µg/L)	Cancer Risk at 10^{-6}	% Contribution
1,1-DICHLOROETHANE (1,1-DCA)	x	3	Mammary gland	Non-Detect	--	--	Non-Detect	--	--	Non-Detect	--	--	Non-Detect	--	--
1,1-DICHLOROETHENE (1,1-DCE)	NA	--	--	Non-Detect	--	--	1.30	--	--	Non-Detect	--	--	1.30	--	--
1,2,3-TRICHLOROPROPANE (1,2,3-TCP)	x	0.0007	Stomach	Non-Detect	--	--	Non-Detect	--	--	Non-Detect	--	--	Non-Detect	--	--
1,2-DICHLOROETHANE (1,2-DCA)	x	0.40	Liver, skin, testes, bile ducts, and mammary glands	Non-Detect	--	--	Non-Detect	--	--	Non-Detect	--	--	Non-Detect	--	--
1,4-DIOXANE	x	0.35	Nervous system, respiratory system, liver and gall bladder	1.79	2.0E-09	30.1%	4.00	4.5E-09	24.9%	3.36	3.8E-09	35.7%	3.40	3.8E-09	14.5%
BENZENE	x	0.15	Hematotoxic	Non-Detect	--	--	Non-Detect	--	--	Non-Detect	--	--	Non-Detect	--	--
DI(2-ETHYLHEXYL) PHTHALATE (DEHP)	NA	--	--	Non-Detect	--	--	Non-Detect	--	--	Non-Detect	--	--	Non-Detect	--	--
NITRATE (AS NITROGEN [N])	x	12	Liver	Non-Detect	--	--	Non-Detect	--	--	Non-Detect	--	--	Non-Detect	--	--
TETRACHLOROETHENE (PCE)	NA	--	--	2,808	--	--	3,806	--	--	2,961	--	--	4,103	--	--
TRICHLOROETHENE (TCE)	x	0.06	Liver	0.66	4.3E-09	65.0%	1.90	1.2E-08	68.9%	0.97	6.3E-09	59.9%	3.20	2.1E-08	79.4%
1,1-DICHLOROETHANE (1,1-DCA)	x	1.7	Liver	1.41	3.3E-10	4.9%	4.90	1.1E-09	6.3%	2.00	4.6E-10	4.4%	7.00	1.6E-09	6.1%
				TOTALS	**6.7E-09**	**100%**	**TOTALS**	**1.8E-08**	**100%**	**TOTALS**	**1.1E-08**	**100.0%**	**TOTALS**	**2.6E-08**	**100%**

Notes: COPCs = Constituents of Potential Concern; PHG = Public Health Goal; NL = Notification Level; µg/L = micrograms per liter; NA= Not Applicable - COPC is not a carcinogen; “--" indicates not applicable